

IRREGULARITIES AND MOVEMENTS IN THE UPPER ATMOSPHERE

A THESIS

SUBMITTED FOR THE DEGREE OF

DOCTOR OF PHILOSOPHY

OF THE

GUJARAT UNIVERSITY

AHMEDABAD

BY

VINODKUMAR PURSHOTTAMDAS PATEL

MAY 1982

043



B11672

THE LIBRARY
PHYSICAL RESEARCH LABORATORY
NAVRANGPURA
AHMEDABAD-380 009

PHYSICAL RESEARCH LABORATORY

AHMEDABAD 380009

INDIA

DEDICATED TO

:

My Grandmother - Smt. Ambaben
and
My Family Members


C E R T I F I C A T E

I hereby declare that the work presented in this thesis is original and has not formed the basis for award of any degree of any university or institution.



(V.P. Patel)
Author

Certified by:

 Harish Chandra
(M.R. Deshpande) (H. Chandra)
Thesis Advisers

Horizontal movement of the ionospheric irregularities following the spaced receiver fading method of Mitra has been the most common method to study the dynamics in the E and F regions of ionosphere. Ionospheric drift work at the Physical Research Laboratory started in 1954 when an experiment based on Mitra's technique was built and operated at Ahmedabad. The measurements were also continued at Ahmedabad during IGY-IGC and IQSY periods and showed variability in drift direction. However, when similar experimental set-up was installed at Thumba close to the centre of equatorial electrojet in 1964 the observations revealed a very consistent picture with westward drift during daytime and eastward drift during nighttime. The observations showed that the drift measurement in the electrojet region is highly correlated with the electrojet. Encouraged by the results at Thumba it was felt to have a coordinated chain of drift stations and examine circulation pattern at low latitudes in India. With this aim the drift measurements were restarted at Ahmedabad in 1970 using new improved instrumentation. Additional stations were set-up at Madras and Tiruchirapalli close to the equator also. To examine the validity of the technique at tropical latitudes simultaneous measurements were made at Ahmedabad and Udaipur separated by about 200 km during the year 1973-74, and the comparison showed an excellent agreement. The drift measurements at Ahmedabad during daytime hours of E-region for the period 1970-75 constitute

the longest continuous spell of observations made at this station and this has allowed to study the behaviour of the drift pattern at this latitude zone in some detail. It has been possible to examine the effects like of seasons, changes due to lunar tidal effects, of magnetic activity, of the solar activity and of the interplanetary magnetic field. The thesis is primarily based on the results obtained from the measurements of drifts in E-region at Ahmedabad during the period 1970-75 and from the published data of E-region drifts at Yamagawa and Sibizmir analysed to study the global circulation pattern. In addition a study of the quiet day geomagnetic field variations in the electrojet latitudes, of counter electrojet effects in the geomagnetic field variations at different latitudes and on the E-region drifts at Ahmedabad was undertaken. A spaced receiver scintillation experiment was conducted during the period February 1978 - July 1979 at Tiruchirapalli and preliminary results of the dynamics and nature of irregularities causing VHF scintillations are also included in the thesis.

The thesis has been divided into six chapters.

The first chapter is an introductory one and briefs of ionosphere, geomagnetism, dynamo theory, electrical conductivities in the upper atmosphere, motions in the ionosphere and techniques to measure them.

The second chapter describes methods of data reduction, experimental set up and the results at Ahmedabad during the

period 1970-75. This includes the basic morphology i.e. daily, seasonal and solar cycle variations. Dependence on magnetic activity, on interplanetary magnetic field and on lunar age are also shown to be significant.

The third chapter describes the results of the morphology of drifts at a middle latitude station at Yamagawa and at a high latitude station Sibizmir. The chapter also includes discussions on the results at electrojet latitude stations for a comparison of drifts on a world-wide scale.


The fourth chapter is on the geomagnetic studies. The quiet day daily variation of H component at electrojet stations Huancayo and Trivandrum are studied from a large set of data and the seasonal and solar cycle effects are discussed. The phenomenon of counter electrojet is studied in detail and the associated effects in geomagnetic components at low, middle and high latitudes are described. One major finding has been the changes in the drifts observed at Ahmedabad during counter electrojet events of winter months.

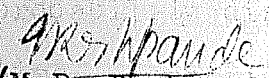
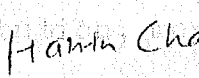
The fifth chapter is on the spaced receiver scintillation experiment conducted for about one and half years at Tiruchirapalli. The preliminary results on the occurrence frequency of scintillation daily variations of the scintillation index and of the velocity of irregularities causing scintillation on a few typical nights are presented. Scale size of the irregularities estimated using

correlation method, the results of the cross-spectral analysis of some typical records are shown here. Examples on application of these to communication are presented which include the probability distribution, message reliability, and auto-correlation time. Comparison with simultaneous HF drifts by Mitra's technique is also presented.

The last chapter gives the summary of the main results in the thesis and the suggestions for future work.

It is sincerely hoped that the present investigations have contributed to the better understanding of the dynamical behaviour of the E-region of the ionosphere.


(V.P. Patel)
Author

 
(M.R. Deshpande) (H. Chandra)
Thesis Advisers

The last chapter gives the summary of the main results in the thesis and the suggestions for future work.

It is sincerely hoped that the present investigations have contributed to the better understanding of the dynamical behaviour of the E-region of the ionosphere.

ACKNOWLEDGEMENTS

The author expresses his deep sense of gratitude and indebtedness to Prof.M.R. Deshpande for introducing the author to the subject of this thesis and for his invaluable guidance, advice and encouragement throughout this study.

The author is sincerely grateful to Dr.H. Chandra for his active guidance, countless discussions and a number of constructive suggestions in the course of this work. The author owes him a special debt of thanks for his zeal in supervising the preparation of the thesis.

The author is thankful to Prof.R.G. Rastogi for encouragement, suggestions and many fruitful discussions during the course of this work. His willing encouragement helped the author a lot in getting through many critical moments.

The author is thankful to the Principal of Jamal Mohamed College, Tiruchirapalli and members of the management committee of the college for providing facilities for the ETS-2 project (Spaced Receiver Experiment).

Thanks are also due to Mr.Banshidhar, Mr.N.M. Vadher, Mr.M.B. Dadhanian and Mr.V.D. Patel for development, installation and operation of the Spaced Receiver Experiment at Tiruchirapalli.

Sincere thanks are due to Mr.F de Castillo for supplying some of the unpublished data of geomagnetic field at Huancayo.

The author had wide ranging discussions on many scientific aspects related to the present work with Prof.R.P. Kane. The author renders his sincere thanks to him.

The scientific discussions with Prof.R. Raghavarao, Prof.R. Pratap, Dr.G. Subramaniam, Dr.V.B. Gohel, Dr.G.D. Vyas, Dr.Rajesh Pande, Dr.Shyamlal, Dr.B.G. Anandrao and Mr.Avinash Khare are also thankfully acknowledged.

Thanks are due to Profs. K.R. Ramanathan, D. Lal, S.P. Pandya, Satyaprakash and R.V. Bhonsle for the encouragement.

Thanks are also due to Drs! (Mrs.) Girija Rajaram, K.N.Iyer, A.V. Janve and M. Singh for the fruitful discussions which the author had with them during their stay in PRL.

Thanks are also due to Miss Chhaya R. Shah, Mr.K.C. Patel, Mr.M.V. Bhavsar, Mrs. Bharati K. Bhatt and Mrs.Suchita D. Desai for the excellent computational assistance provided to the author.

It is a pleasure to thank Mr.P.S. Shah and his colleagues at PRL Computer Centre for their kind cooperation in data processing and analysis.

Thanks are also due to Mrs.R.R. Bharucha and other library staff for providing excellent facilities during the course of this work.

The painstaking job of elegantly typing the thesis was most efficiently done by Mr.P. Raghavan. The author records his sincere thanks and appreciation to him. The author also acknowledges the willing assistance of Mr.D. Stephen and Mr.Philip C. Samuel at all times of need.

The author greatly appreciates the assistance of the following people at various stages of the preparation of the thesis: Mr.H.S. Panchal of Drafting Section for drafting and photo-stenciling the diagrams; Mr.C.B. Khopkar of Photography Section for printing the diagrams and Mr.Babulal for the efficient cyclostyling of the thesis. The author also appreciates the excellent xerox work done by Mr.J.G. Vora, Mr.D.H. Gandhi and Mrs.Bhatt on many occasions.

Thanks are due to the Physical Research Laboratory administration for providing the author all possible help for the completion of this work.

It is my great pleasure to appreciate the friendly encouragement provided by my friends Dr.H.O. Vats, Dr.K.P.Singhal and Dr.G. Sethia.

I am deeply indebted to all the members of my family for their affection and encouragement.

I am most grateful to my wife, Inaxi whose profound understanding and the moral support during my excruciating moments of anxiety and despair, proved to be invaluable. Finally it would be unjustified not to appreciate the refreshing moments provided by my little daughter Shruti, at many moments of need.

--- V. P. PATEL

List of Author's PublicationsPapers published in Journals

1. Chandra H., V.P. Patel and R.G. Rastogi,
Ionospheric E region drift pattern at low-latitudes,
Curr. Sci., 46(24), 835-836 (1977).
2. Patel V.P., H. Chandra and R.G. Rastogi,
Ionospheric E-region drift measurements over Ahmedabad
during 1970-75,
Ind. J. Rad. & Space Phys., 7(1), 22-25 (1978).
3. Patel V.P. and R.G. Rastogi,
On the solar control of the quiet-day geomagnetic
variations near the magnetic equator,
Curr. Sci., 47(10), 325-327 (1978).
- *4. Chandra H. and V.P. Patel,
Ionospheric E-region drifts and geomagnetic field
variations,
Ind. J. Rad. & Space Phys., 7, 139-141 (1978).
5. Patel V.P. and Chandra H.,
Magnetic activity effects in the E-region drifts at
Ahmedabad,
Ind. J. Rad. & Space Phys., 7, 63 (1978).
- *6. Kane R.P., V.P. Patel and A.V. Janve,
Storm-time variations of foE at low latitude,
J. Atmos. Terr. Phys., 41, 163-168 (1979).
7. Patel V.P., G.D. Vyas, H. Chandra, H.O. Vats, R.G. Rastogi and
M.R. Deshpande
Ionospheric irregularity studies by spaced fading and
spaced scintillation records,
Ind. J. Rad. & Space Phys., 8, 198-200 (1979).
8. Patel V.P., H. Chandra and R.G. Rastogi
Lunar tides in the E-region drifts over Ahmedabad,
Curr. Sci., 49, 348-348 (1980).
9. Patel V.P. and H. Chandra,
Ionospheric E-region drifts at Yamagawa during IQSY,
J. Geomag. Geoelectr., 32, 129-136 (1980).

*These publications do not form a part of the thesis.

10. Kane R.P. and V.P. Patel,
Association of equatorial counter-electrojet with
geomagnetic changes in the low and middle latitudes
in the Indian region,
J. Geomag. Geoelectr., 32, 137-144 (1980).
- *11. Patel V.P. and H. Chandra
A test of dispersion in the spaced receiver fading
observation near magnetic equator,
Ind. J. Rad. & Space Phys., 9, 64-65 (1980).
12. Chandra H., G.D. Vyas and V.P. Patel,
Changes in the low latitude drifts associated with
counter-electrojet,
Ind. J. Rad. & Space Phys., 10, 164-166 (1981).
13. Patel V.P. and H. Chandra,
Ionospheric E-region drifts at Sibizmir during 1970-75,
Ind. J. Rad. & Space Phys., (1982) (in press).

Symposium Papers

14. Deshpande M.R., H.O. Vats and V.P. Patel,
A method to estimate temporal variation of ionization
irregularities in the ionosphere,
Presented at the 5th annual radio and space science
symposium held at NPL, New Delhi, Jan. 22-25. (1979).
15. Patel V.P., H.O. Vats and M.R. Deshpande,
On the amplitude distribution of VHF waves and message
reliability,
Presented at the National Space Sciences Symposium
held at Banaras Hindu University, Varanasi, India,
Jan. 22-25 (1980).
16. Patel V.P., M.R. Deshpande, A. Sengupta, H.O. Vats and
H. Chandra,
Velocity and direction of different periodicities in a
diffraction pattern,
Presented at the National Space Sciences Symposium
held at Banaras Hindu University, Varanasi, India,
Jan. 22-25 (1980).
17. Patel V.P., H. Chandra, R.G. Rastogi and R.P. Kane,
Changes in the declination (D) in low and middle
latitudes during counter-electrojet days,
Presented at the National Space Sciences Symposium
held at Banaras Hindu University, Varanasi, India,
Jan. 22-25 (1980).

C O N T E N T SPage

Dedications

Certificate

Preface

i

Acknowledgements

v

List of Author's Publications

ix

Contents

xi

Chapter - I : Introduction

1

1.1 Introduction to Ionosphere

1

1.2 Geomagnetism

4

1.2.1 Dynamo Theory

8

1.2.2 Conductivity of the Ionosphere

11

1.2.3 Equatorial Electrojet

14

1.2.4 Counter-Electrojet

17

1.3 Motion of Neutral Atmosphere

18

1.3.1 Prevailing Winds

20

1.3.2 Planetary Waves

20

1.3.3 Tidal Oscillations

20

1.3.4 Internal Gravity Waves

21

1.3.5 Turbulence

21

1.4	Motion of the Ionisation in the Upper Atmosphere	22
1.4.1	Closely Spaced Receiver Technique (D ₁ Method)	24
1.4.2	Radio Star and Satellite Scintillation Technique	25
Chapter - II : Drift Measurements at Ahmedabad during the Period 1970-75		27
2.1	Introduction	27
2.2	Methods of Data Reduction	31
2.2.1	Time Delay Method	31
2.2.2	Full Correlation Method	34
2.2.2.1	Fading Velocity V'_c	34
2.2.2.2	True Drift Velocity V	35
2.2.2.3	Characteristic Velocity V_c	35
2.2.2.4	Apparent Drift Velocity V'	36
2.2.3	Cross Spectral Analysis	36
2.3	Experimental Set-up	38
2.3.1	Aerial System	39
2.3.2	Transmitting Unit	39
2.3.3	Receiving and Recording Unit	39
2.4	Results	41
2.4.1	Annual Variation of Drift Speed and Drift Direction	43
2.4.2	Daily Variation of Drift Speed	45

2.4.3	Seasonal Variation of the Midday Drift Velocity	48
2.4.4	Solar Cycle Variation	48
2.4.5	Magnetic Activity Effects in the E-region Drifts	49
2.4.6	Interplanetary Magnetic Field Effects in the E-region Drift	49
2.4.7	Lunar Tides in the E-region Drifts	51
2.4.8	Drifts at times of Sporadic E	53
Chapter - III : E-region Drifts at Other Latitudes - Circulation Pattern		54
3.1	Introduction	54
3.2	Circulation Pattern	56
3.3	Solar Activity Dependence of Drifts at Equatorial, Low and High Latitudes	56
3.4	Magnetic Activity and Drifts at Different Latitudes	57
3.5	Lunar Tidal Effects in Drifts at Different Latitudes	57
Reprint/Preprint		
Chapter - IV : Some Aspects of Geomagnetic Variations at Low Latitudes		58
4.1	Quiet Day Variation of Geomagnetic H-field at Low-Latitudes - Solar and Seasonal Effects	58
4.1.1	Introduction	58
4.1.2	Data Analysis and Results	59
4.2	Counter-electrojet - Geomagnetic Effects at Different Latitudes	63
4.2.1	Introduction	63

4.2.2	Counter-Electrojet Effects in Geomagnetic Field Components at Different Latitudes	68
4.2.3	Changes in the Low Latitude E-region Drifts on Counter-electrojet Days	76
Chapter - V : Spaced Receiver Experiment		78
5.1	Introduction	78
5.2	Radio Star Scintillation	78
5.3	Satellite Scintillation	89
5.4	Experimental Set-up	83
5.4.1	Receiving Antenna	84
5.4.2	Preamplifier	84
5.4.3	First Converter	85
5.4.4	Second Converter	85
5.4.5	Detector	86
5.5	Scintillation Index	87
5.6	Scintillation Observations at Tiruchirapalli	90
5.7	Comparison of Drift Speeds and Directions as Obtained by Spaced Fading Experiment and Spaced Scintillation Experiment	91
5.8	Determination of the Parameters of the Irregularities by Correlation Analysis Method	92
5.9	Velocity Spectrum and Power Spectrum by Cross Spectral Method	93
5.10	Probability Distribution of Amplitudes	94
5.11	Message Reliability	95

5.12 Auto-correlation of the Received Signal	97
Chapter-- VI : Conclusions and Suggestions	98
Suggestions for Future Work	101
References	102

CHAPTER - 1

INTRODUCTION

1.1 Introduction to Ionosphere

The neutral constituents of the upper atmosphere are acted upon by the shorter wave ultraviolet solar radiation extending into X-ray region. They produce molecular or atomic (positive) ion by detaching one of the electrons from neutral molecular or atom. Some of the electrons will attach themselves to an atom or molecule of oxygen to form a negative ion. These actions lead to several others - particularly charge transfer and three body or radiative recombinations. The region in which these processes takes place is called the 'ionosphere'. It extends from about 60 km to 1000 km and above. The electron density distribution in the ionosphere is shown in Fig.1.1. (Fig.1.1 also indicates height of different ionospheric regions (left portion) and temperature at different altitudes along with processes (right portion)).

The existence of the ionosphere as an electrically conducting region was first proposed in 1883 by Balfour and Stewart. They inferred it from a study of the small daily geomagnetic variation observed at the earth's surface. In the early ninteens, after Marconi had transmitted radiowaves across the Atalantic the presence of an ionized region in the upper atmosphere was invoked as an explanation to this effect by Kennelly and Heaviside independently. It was shown that radiowaves (of certain frequency) get reflected by the ionosphere and they play a key role in the long distance radio wave propagation.

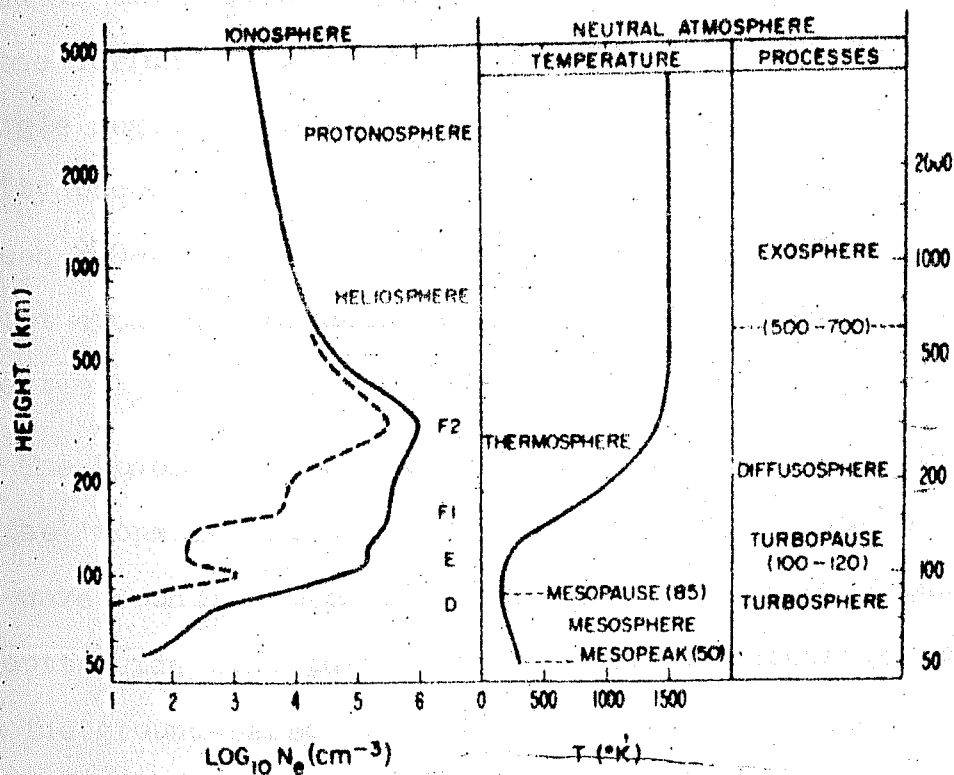


Fig.1.1 - On the left, height of different ionospheric regions and electron density at that height. On the right temperature at different altitudes and processes at different altitudes are shown.

Since then the research of the ionosphere was actively pursued by several scientists like Barnett, Breit, Tuve etc. Appleton recognized the presence of more than one ionized layers in the ionosphere and named them as E and F (F is subdivided into F_1 and F_2 during daytime); later electrons were detected in the D-region extending below the E layer into the mesosphere. The D-region lies between 60-90 km altitude. The altitude region between 90-140 km is termed as the E-region and above 140 km it is termed as the F-region. The F-region usually splits into two regions during daytime, the F_1 and the F_2 region which merge into a single region during the night-time. The maximum ionization density occurs at the F_2 peak, the height of which varies between 250-450 km depending on the location, time of day, sunspot cycle and magnetic activity. The ionisation decreases above the F_2 peak altitude.

The ionosphere is broadly classified into the 'bottomside' and the 'topside' ionosphere. This division is based on the radiowave sounding technique for studying various ionized layers. The bottomside ionosphere upto F_2 peak, is amenable to exploration from the ground-based ionosonde and hence the name. The 'topside' ionosphere cannot be investigated from the ground-based ionosonde because the underlying 'bottomside' ionosphere shields the 'topside' ionosphere.

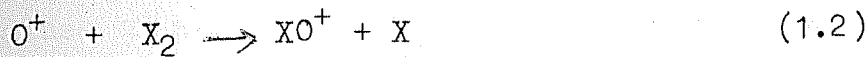
The D-region ionisation is produced mainly due to the photoionisation of molecular oxygen and molecular nitrogen by solar X-rays in the wavelength range $1-10\text{\AA}$ and also due to the photoionisation of nitric oxide by solar Lyman-alpha radiation (1216\AA). The free electrons and ions thus produced are lost through the dissociative recombination,



where XY^+ is the ionised molecule and X^* and Y^* are atoms in excited state. In the E-region (90-140 km) the ionisation is mainly produced by the photoionisation of molecular oxygen and molecular nitrogen by EUV in the range $911-1027\text{\AA}$. A small contribution comes from the X-rays in the wavelength range $10-170\text{\AA}$. The loss of ionisation in E-region is also through the dissociative recombination scheme as shown in the equation (1.1).

The lower boundary of the F-region is usually taken to be around 140 km altitude. The chief neutral constituents in the altitude range 150-600 km are atomic oxygen (O) and molecular nitrogen (N_2). The source of ionisation is solar UV radiation in the wavelength range $200-911\text{\AA}$, (the latter wavelength being the ionisation limit of atomic oxygen). The production of the F-region ionisation results mainly through the photoionisation of atomic oxygen. The free electrons are lost through a two stage processes viz. (a) formation of molecular ions by ion-atom interchange and (b) dissociative recombination. If X_2 denotes

either O_2 or N_2 the loss scheme may be written as :



These regions of the ionosphere influence the radio waves ranging from about 100 kHz to 25 MHz and hence the ionosphere can be studied using the radio waves. Early investigations were made mainly by using sounding the ionosphere by radio waves (Breit and Tuve 1926, Appleton and Barnett 1925). A detailed description of various techniques of probing the ionosphere is given in the April issue of J. Atmos. Terr. Phys. (1970).

1.2 Geomagnetism

The geomagnetic field is predominantly dipolar. It is specified in the following way:

X the northward component

Y the eastward component

Z the vertical component

or by

$$\text{the horizontal component } H = (X^2 + Y^2)^{\frac{1}{2}} \quad (1.4)$$

$$\text{the declination } D = \tan^{-1}(Y/X) \quad (1.5)$$

and

$$\text{the inclination } I = \tan^{-1}(Z/H) \quad (1.6)$$

$$\text{The total field } B \text{ (or } F \text{ or } T) = (X^2 + Y^2 + Z^2)^{\frac{1}{2}} \quad (1.7)$$

These components X, Y, Z, H are measured in Gauss (G) and have values of a fraction of a gauss on the surface of the earth. For expressing small changes a smaller unit called gamma is used (one gamma $\gamma = 10^{-5}$ G). The components D and I are in ratio and are usually converted into degrees, minutes and seconds of arc. The locus of the point I = 0 is called the magnetic dip equator where Z = 0, and the total field is completely represented by horizontal component H. In contrast with this there are points (poles) in high latitudes where H=0 and I=90° and field is represented by vertical component Z only. The arctic and antarctic magnetic dip poles were at about 76°N, 101°W and 66°S, 141°E in 1965. These positions change slightly with time. If no electric currents are flowing across the earth's surface, the geomagnetic potential V satisfies Laplace's equation and can be represented by a series of spherical harmonics in spherical polar coordinates as:

$$V = a \sum_{n=0}^{\infty} \sum_{m=0}^{\infty} P_n^m(\cos \theta) \left[\left\{ (1-C_n^m) (a/r) \right\}^{n+1} + C_n^m (r/a)^n \right] A_n^m \cos m\phi + \left\{ (1-S_n^m) (a/r)^{n+1} + S_n^m (a/r)^n \right\} B_n^m \sin m\phi \quad (1.8)$$

Here C_n^m and S_n^m are positive numbers representing fractions of the harmonic terms of external origin. Actually, V is not observed directly but the world wide distribution of components X, Y, Z can be used for determining various coefficients in the equation (1.8) by the relations:

$$X = \frac{1}{r} \frac{\partial V}{\partial \theta}, \quad Y = -\frac{1}{r \sin \theta} \frac{\partial V}{\partial \phi} \quad \text{and} \quad Z = \frac{\partial V}{\partial r} \quad (1.9)$$

Though V consists of component V^e of external origin and V^i of internal origin. The external component V^e is very small and contributes to field of the order of 100 gamma on the surface of the earth while field due to V^i is of several thousand gammas.

The geomagnetic, geographic and magnetic dip equator differ from each other in varying degrees ($0 \pm 10^\circ$) at different locations on the earth. A better matching between observed dip configuration and the calculated geomagnetic coordinates is obtained. If it is assumed that the dipole is an eccentric with the centre shifted to about 450 km (in 1965) from the centre of the earth and its axis intersecting the surface of the earth at about 81°N , 85°W and 75°S , 120°E it produces satisfactorily the very low values of about 25000 γ for the total field at south American equator and about 40000 γ at the Australasian equator.

The various components do not remain constant with time. All the components of geomagnetic field show distinct periodicities ranging from a few seconds to several thousands years. Periods upto 22 years are generally connected with solar phenomena while larger periodicities are mostly related to the internal structure of the earth and its core dynamics, though some periods of a few years could also be of internal origin.

One of the most spectacular variation exhibited by all geomagnetic components is daily variation (24 hourly) with fairly constant values at night, the field increasing shortly after sunrise reaching maximum value around noon and falling thereafter to obtain the night-time level after sunset. Such a smooth pattern is known as solar daily quiet variation (Sq). However, this quiet day pattern varies largely from day to day and season to season. The pattern of daily maximum reverses at a latitude $30-40^\circ$ and this latitude is called Sq focus. The exact latitude is different for different longitudes and seasons. The range of variation in course of a day, day-time maximum value minus the night-time minimum value is known as the daily range in the respective component. This daily range is seasonal and solar activity dependent and exhibits day to day variability also depending upon the position of the focus. The daily range is normally expected to fall off from a broad maximum value around the equator to zero value at the Sq focus. World-wide averages of solar quiet daily variations of geomagnetic components for different latitudes are shown in Fig.1.2. These variations are attributed to the motion of the upper atmosphere which produces electromotive force and electric currents by dynamo action (Elsasser, 1958).

Instruments for measuring magnetic field components, essentially based on the rotation of a carefully balanced magnet are in use all over the world for several decades. In the recent

years space measurements have used analog devices like flux-gate saturable core and spinning coil magnetometers or resonant frequency device like the proton precession or rubidium vapour optical pumping magnetometers (Matsushita and Campbell, 1967).

1.2.1 Dynamo Theory

The existence of electric currents in the upper atmosphere was first proposed by Stewart in an attempt to explain daily fluctuations in the earth's magnetic field. Stewart's proposal was put on more mathematical footing by Schuster (1889). By spherical harmonic analysis of the magnetic field, Schuster showed that the presence of the varying field could only be accounted for by currents which are external to the earth. He later (Schuster, 1908) developed a quantitative theory which accounted for these variations. In essence the Stewart-Schuster theory is the application of the dynamo principle (Elsasser, 1958) to conditions existing in the ionosphere. In this case conducting region in the ionosphere is treated as a thin spherical conducting layer which in the absence of the magnetic field, moves in a similar manner to that of the neutral atmosphere. Due to the presence of earth's magnetic field, however, the force exerted on the charged particles is at right angle to both the magnetic field and the neutral particle velocity.

The wind(velocity \underline{W}), flowing across the magnetic field B , includes the Lorentz force $e(\underline{W} \times \underline{B})$, e is the charge of electron.

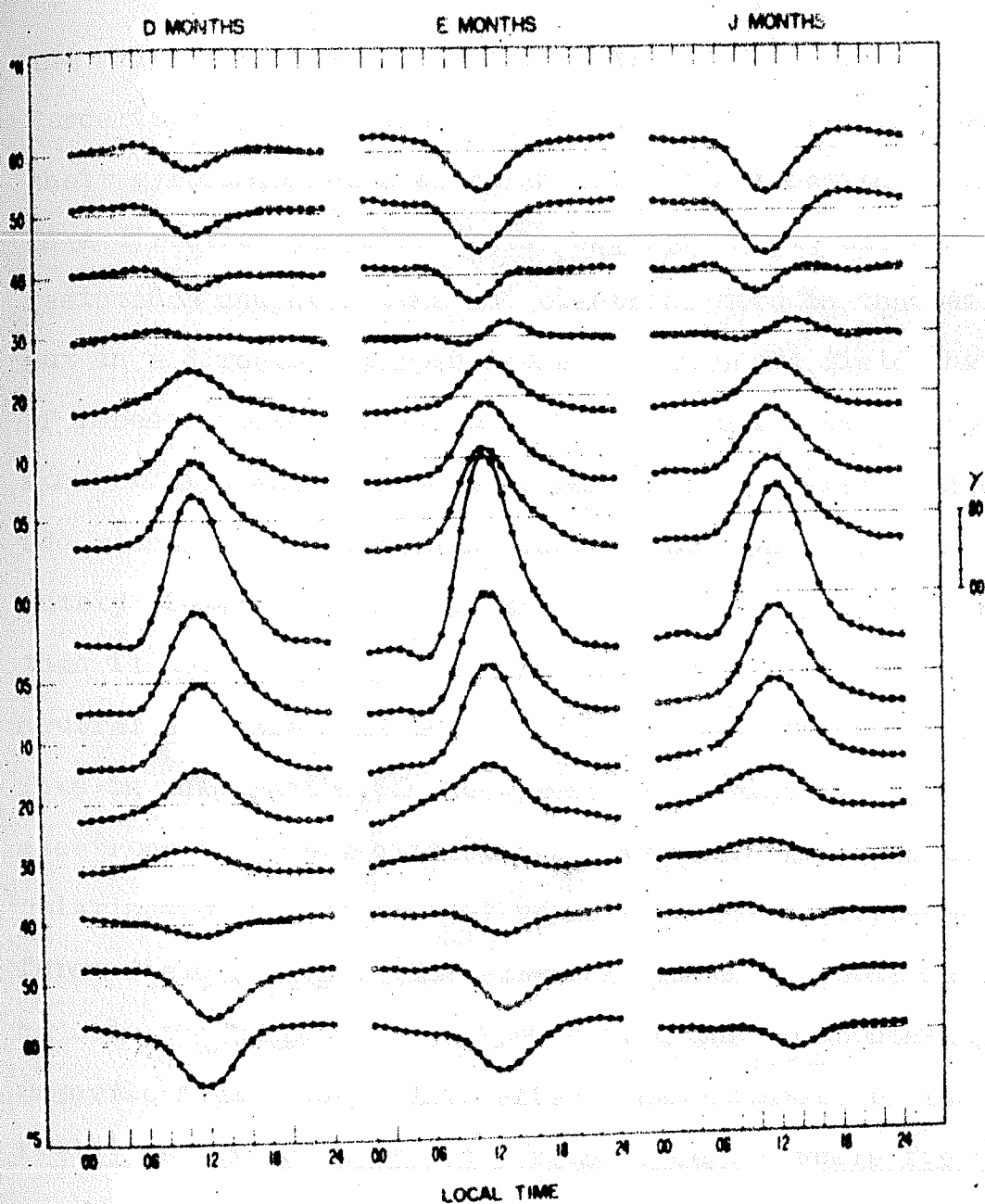


Fig.1,2 - World-wide average daily variations of the horizontal component at different latitudes for three seasons.

The extent to which ions and electrons get affected by this force depends upon the ratio of their collision frequencies to their gyrofrequencies which in turn is a function of altitude. In a direction parallel to the magnetic field the wind has no resistance and both ions and electrons move in that direction. But in a direction perpendicular to magnetic field the effect of Lorentz force depends upon how frequently the electrons or ions collide with the neutral particles compared to their (ions and electrons) gyrofrequencies. In the dynamo region (approximately 90-140 km), the electron gyrofrequency is much higher than its collision frequency with neutral particles, whereas ion-neutral collision frequency is higher than the ion gyrofrequency. Thus in this region, in the presence of wind, the ions and electrons will have differential motions. As a result the polarisation fields are set up in a direction opposite to Lorentz force field ($\underline{W} \times \underline{B}$). The extent to which the polarisation field cancels the ($\underline{W} \times \underline{B}$) field, depends upon the horizontality of the magnetic field lines. This effect (cancellation of the ($\underline{W} \times \underline{B}$) field) is maximum in the dip equator region where field lines are horizontal. However, in mid latitude region where the magnetic field lines are fairly vertical the Lorentz field will be quite effective. The polarisation field set up will modify the currents generated initially by the differential motion. The currents produced by dynamo action can be expressed as follows:-

$$\underline{J} = (\underline{\epsilon}') \cdot \underline{E}' \quad (1.10)$$

where \underline{J} is the current density

$$\underline{E}' = \underline{E} + (\underline{W} \times \underline{B}) \quad (1.11)$$

\underline{B} is the earth's magnetic field taken along Z axis

\underline{E} is the polarisation field assumed to be electrostatic which can be expressed as:

$$\underline{E} = - \nabla \phi \quad (1.12)$$

where ϕ is the secular potential and $(\underline{\epsilon}')$ is the conductivity tensor.

In these calculations it is considered that under the action of earth's magnetic field the ionosphere is nonisotropic conductor with tensor conductivity $(\underline{\epsilon}')$.

The currents thus generated are assumed to be non-divergent implying that there is no accumulation of charges. The electrostatic field set up by the charge separation is considered to be irrotational.

Thus we have

$$\nabla \cdot \underline{J} = 0 \quad (1.13)$$

$$\nabla \times \underline{E} = 0 \quad (1.14)$$

Equations (1.10), (1.13) and (1.14) alongwith the equation of motion of the neutral particle (as given below - equation (1.15) form the adequate set of equations for the formulation of the dynamo theory.

The equation of the motion of the neutral particles can be written as:

$$\frac{d\mathbf{w}}{dt} = 2\boldsymbol{\Omega} \times \mathbf{w} = \mathbf{g} - \frac{1}{\rho} \nabla p + \nabla \Psi + \frac{\mu}{\rho} \nabla^2 \mathbf{w} - \nu_{ni} (\mathbf{w} - \mathbf{v}_i) \quad (1.15)$$

is earth's angular velocity; \mathbf{g} is acceleration due to gravity; ρ is gas density; p is pressure of the atmosphere; Ψ is a scalar potential due to tide raising force like solar thermal and lunar gravitational; μ is coefficient of molecular viscosity; ν_{ni} is the neutral collision frequency and \mathbf{v}_i is the ion drift velocity.

The dynamo calculations are based on the assumed wind and conductivity models. Any uncertainties in these parameters would naturally lead to uncertainties in the estimated S_q field and currents.

The yearly average S_q current system deduced from magnetic variations recorded at the observatories situated at various latitudes during IGY (1957-58) is shown in Fig.1.3.

1.2.2 Conductivity of the Ionosphere

Tensor conductivity ($\hat{\sigma}$) is originally 3 x 3 tensor conductivity which is denoted by $\hat{\sigma}$. Taking cartesian co-ordinate system with its axis along the magnetic field direction \mathbf{B} , can be written as:

$$(\hat{\sigma}) = \begin{pmatrix} \sigma_1 & -\sigma_2 & 0 \\ \sigma_2 & \sigma_1 & 0 \\ 0 & 0 & \sigma_0 \end{pmatrix} \quad (1.16)$$

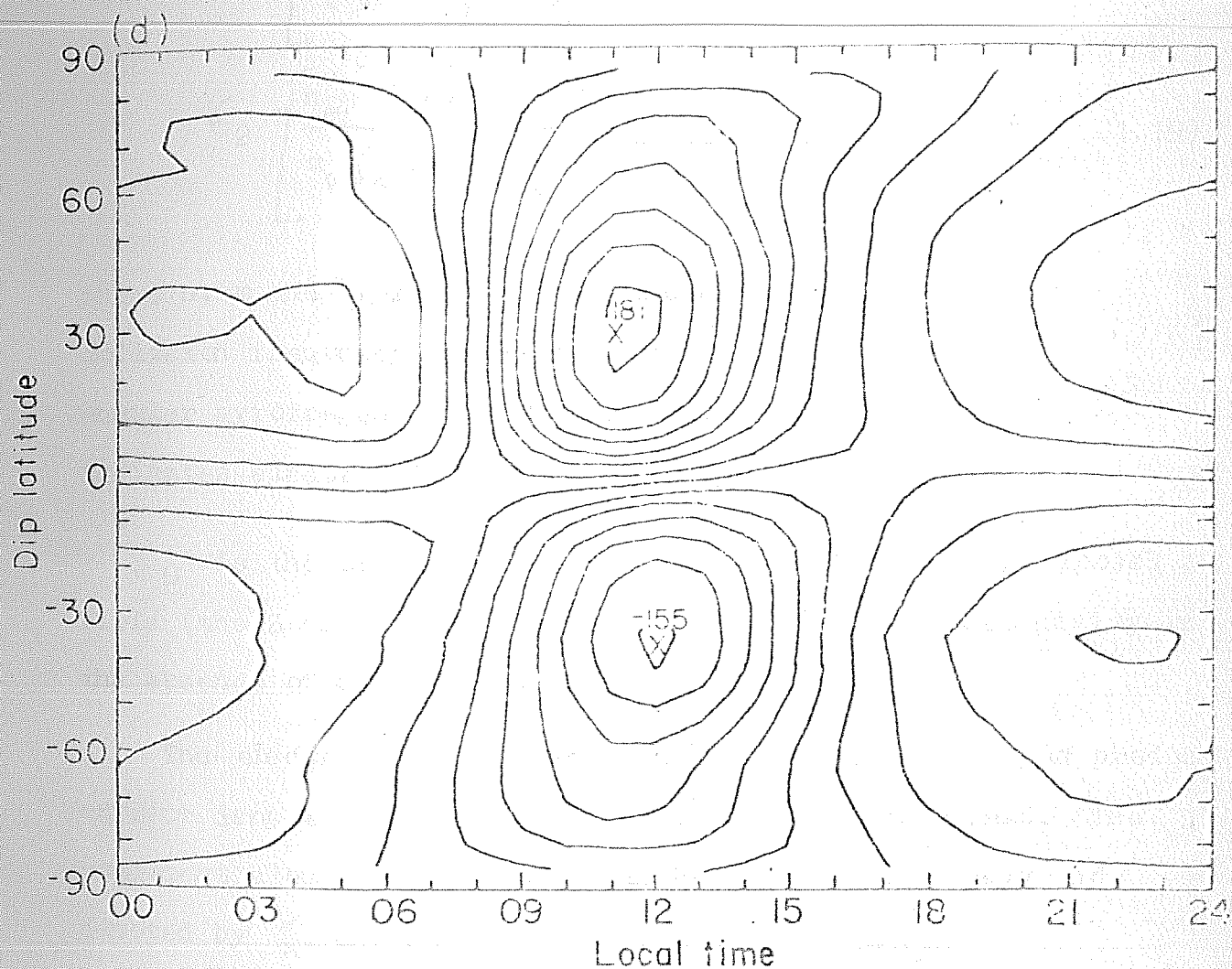


Fig.1.3 - The yearly average Sq current system deduced from magnetic variations recorded at the observatories situated at various latitudes during IGY (1957-58) (after Matsushita, 1968).

$$\text{where } \sigma_0 = \left(\frac{n_e}{m_e \nu_e} + \frac{n_i}{m_i \nu_i} \right) e^2 \quad (1.17)$$

$$\sigma_1 = \left[\frac{n_e}{m_e \nu_e} \frac{w_e \nu_e}{\nu_e^2 + w_e^2} + \frac{n_i}{m_i \nu_i} \left(\frac{\nu_i^2}{\nu_i^2 + w_i^2} \right) \right] e^2 \quad (1.18)$$

$$\sigma_2 = \left[\frac{n_e}{m_e \nu_e} \left(\frac{w_e \nu_e}{\nu_e^2 + w_e^2} \right) + \frac{n_i}{m_i \nu_i} \left(\frac{w_i \nu_i}{\nu_i^2 + w_i^2} \right) \right] e^2 \quad (1.19)$$

where n , m and ν represent the number density, mass and collision frequency of charged particles, $w = \frac{eB}{m}$ the angular gyrofrequency of the particle and subscript e or i indicates electrons or massive ions.

σ_0 is the conductivity along the direction of the imposed field (the Z direction which would have been the conductivity in the absence of magnetic field).

The electric field \underline{E} perpendicular to magnetic field produces current density \underline{j} which is not along the electric field. The component along the \underline{E} is known as Pederson conductivity and denoted by σ_1 and can be given as mentioned above.

When electric field E is perpendicular to the imposed magnetic field it also produces component of current perpendicular to electric field \underline{E} and also perpendicular to magnetic field which is denoted by σ_2 . This current is called Hall current and conductivity is termed as Hall conductivity (σ_2).

As ionosphere is inhomogeneous complications arise. To illustrate these let us suppose that it consists of two separate slab-like layers E and F, each uniform throughout, and a region between which the ionisation is comparatively weak. Let us also suppose that the E layer is moved by gravitational or thermal forces, so that it acts like dynamo. Then if the tensor (ϵ) is used to calculate currents flowing, it will in general be found that there is a component perpendicular to the top and bottom boundaries of the layers. Since, however in the simple picture no current can flow vertically, perpendicular to the boundaries, charges must appear on those boundaries, just sufficient to stop the flow. The electric field of these will also alter the components of currents in the horizontal direction. If the Z-axis is now taken upward and the earth's magnetic field in the ZX plane making angle I with OX, then it can be shown that resulting current density:

$$J = (\epsilon') \cdot E \quad (1.20)$$

$$\text{where } (\epsilon') = \begin{pmatrix} \epsilon_{xx} & \epsilon_{xy} \\ -\epsilon_{xy} & \epsilon_{yy} \end{pmatrix} \quad (1.21)$$

$$\text{and } \epsilon_{xx} = \frac{\epsilon_0 \epsilon_1}{\epsilon_0 \sin^2 I + \epsilon_1 \cos^2 I} \quad (1.22)$$

$$\epsilon_{yy} = \epsilon_1 + \frac{\epsilon_2^2 \cos^2 I}{\epsilon_0 \sin^2 I + \epsilon_1 \cos^2 I} \quad (1.23)$$

$$\epsilon_{xy} = \frac{\epsilon_0 \sin^2 I}{\epsilon_0 \sin^2 I + \epsilon_1 \cos^2 I} \quad (1.24)$$

(ϵ') is called layer conductivity (Baker and Martyn 1953) which must be used in calculating dynamo current flowing.

At the geomagnetic equator $I = 0$ hence

$$\epsilon_x \epsilon_x = \epsilon_0 \quad (1.25)$$

$$\epsilon_{yy} = \epsilon_1 + \frac{\epsilon_2^2}{\epsilon_1} \quad (1.26)$$

$$\epsilon_{xy} = 0 \quad (1.27)$$

A new component ϵ_3 which is defined as:

$$\epsilon_3 = \epsilon_1 + \frac{\epsilon_2^2}{\epsilon_1} \quad (1.28)$$

is termed as Cowling conductivity. In Fig. 1.4 the conductivities ϵ_1 , ϵ_2 and ϵ_3 are plotted as a function of height. It should be noted that the scale for ϵ_3 is smaller than that for ϵ_1 and ϵ_2 by a factor of 10.

1.2.3 Equatorial Electrojet

In 1922 when a geomagnetic observatory at Huancaayo near the dip equator was established a new feature of the daily variation of earth's magnetic field came into light. The daily range in the declination and vertical intensity Z at Huancaayo are comparable to those at the stations in similar geographic latitudes, the diurnal range in the horizontal component H

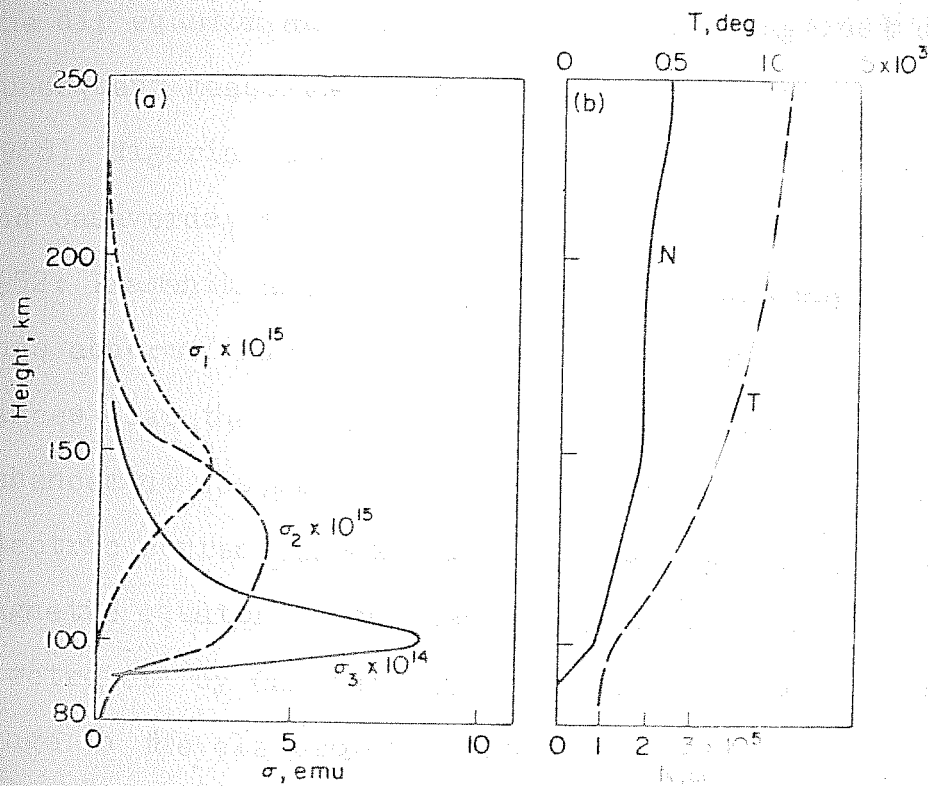


Fig.1.4 -- Conductivities σ_1 , σ_2 and σ_3 as function of height.

is abnormally large being often more than double the expected value. This abnormal range in H was interpreted by McNish (1937) as being due to locally concentrated eastward currents. Egedal (1947, 1948) reported that the diurnal range of H at six stations near the equator showed sharply peaked curves symmetrical about the dip equator and smoother than a plot against dipole latitudes. Subsequent measurements at other places viz. in Uganda (Chapman, 1948), Nigeria (Onwumechilli and Alexander, 1959), Peru (Forbush and Casaverde, 1961) and in India (Pramanik and Yegananarayana, 1952; Pramanik and Hariharan, 1953; Thiruvengadhan, 1954) showed this abnormal increase in the diurnal range in H happens at all places near the dip equator. It now became clear that the enhancement was due to overhead currents. This enhancement of electric current flowing in a narrow zone of $\pm 3^\circ$ over the magnetic equator on the sunlit hemisphere was named "Equatorial electrojet" by Chapman (1951). Fig.1.5 shows the abnormal diurnal range in the electrojet region.

The cause of equatorial electrojet lies in the special feature of electrical conductivity of the ionosphere. For a location at a dip angle I where I is very small, the vertical Hall currents are greatly inhibited and a vertical polarisation field is formed which when crossed with the predominantly horizontal north-south magnetic field produces an additional east-west motion causing the strong electrojet. Several workers notably Baker and Martyn (1953) evolved the mathematical treatment of this problem and

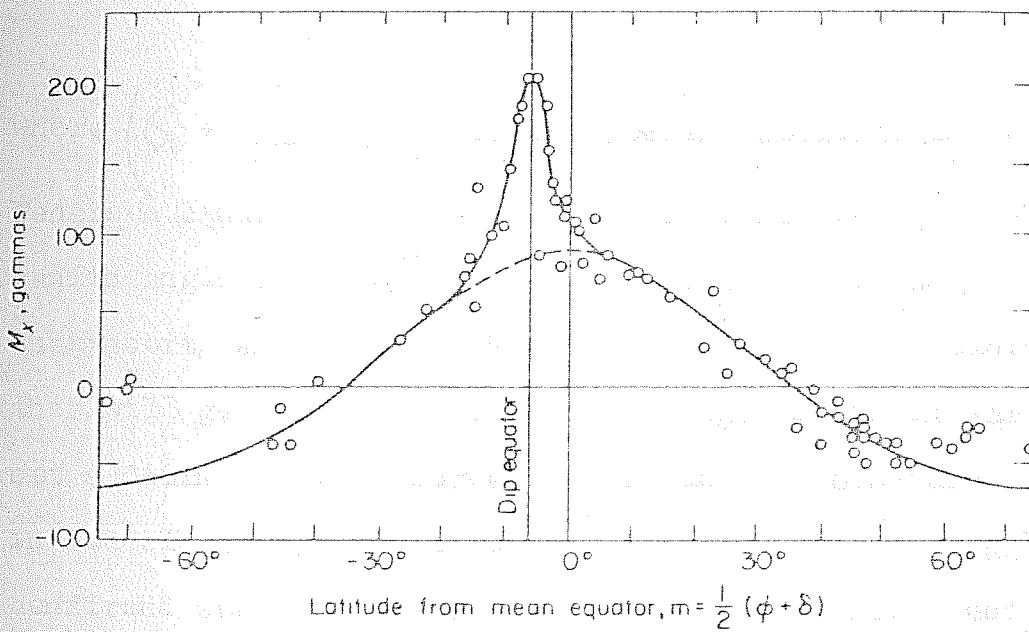


Fig.1.5 - Variation of diurnal range as function of latitude.

estimated that the width of this strip of enhanced conductivity would be about 3° in latitude and also predicted that the electrojet would lead the mid-latitude Sq by about one hour.

The electrojet current was given by:

$$\underline{J} = \underline{G}_3 \cdot E \quad (1.29)$$

$$\underline{J} = E \left(\underline{G}_1 + \frac{\underline{G}_2^2}{\underline{G}_1} \right) \quad (1.30)$$

where $\left(\underline{G}_1 + \frac{\underline{G}_2^2}{\underline{G}_1} \right) = \underline{G}_3$ is the Cowling conductivity which exceeds Pederson conductivity \underline{G}_1 in the equatorial E-region. Here again zenith angle dependence of the conductivity is neglected and Chakraborty and Pratap (1954) and Pratap (1957) pointed out that this will give only a semi-diurnal magnetic field variation and not a diurnal Sq. A survey by Forbush and Casavade (1961) in the electrojet region of the American zone during IGY (1957-58) confirmed some of the features predicted by Baker and Martyn (1953). The longitudinal difference between electrojet strengths at Huancayo and Trivandrum (about 190° and 140° respectively in 1958) is another interesting aspect (Chapman and Raja Rao, 1965). The first attempt to explain this was made by Sugiura and Guin (1966) by formulating a model for electrojet region wherein they used a set of 48G (guass) coefficient for geomagnetic field and found that Cowling conductivity was indeed highly longitude dependent. A new and very fascinating aspect of the equatorial electrojet is the phenomenon of counter-electrojet.

1.2.4 Counter-Electrojet

On some quiet days H value in equatorial region during daytime hours seem to drop below the night time level. This phenomenon was first observed by Gouin and Mayaud (1967, 1969) and was named "counter-electrojet" implying there by that during these intervals, the overhead electrojet current reversed its direction of flow temporarily. Hutton and Oyinloye (1970) studied further details. The phenomenon occurs predominantly around 0630, 1200 and 1500 LT more frequently during quiet sun years and has no relation with either solar flares or lunar age though the later may cause some modifications in magnitudes of the effect. Onwumechilli and Akasofu (1972) reported the days when counter-electrojet has strong lunar influence, but some time in phase and some times antiphase. In the equatorial region, the ionospheric E-region is characterised by the presence of irregularities giving rise to equatorial sporadic E (Es-q) almost throughout the day time (0600-1800 hr LT) so that foEs is several MHz. ~~But~~ However, the occurrence of counter-electrojets is strongly associated with disappearance of equatorial sporadic-E.

The temporary reversal of an electrojet could be, to say the least, baffling as the associated dynamics would be quite confusing. Balsley and Woodman (1971) who reported measurement of E-region drift reduced to zero when H values showed counter-electrojets; but reversal of E-region drifts was not observed

by them. Their data was obtained by determining the mean Doppler shift of oblique radar returns from a certain types of electron density irregularities. On the other hand, using the three closely spaced receiver method, Rastogi et al. (1971^a) measured E and F region drifts at Thumba (magnetic dip equator, India) and found a clear reversal during counter-electrojets; from usual westward flow to a temporary east-ward flow. The counter-electrojet phenomenon is restricted to a narrow longitude zone though it may persist in that zone for several days continuously or intermittently (Kane 1973, Rastogi 1971, 1974 ,d).

Fambitakoye et al. (1973) suggested as a possible cause of counter-electrojet an additional belt of current underlying the normal electrojet and flowing in the opposite direction.

Various other mechanisms are proposed to cause the counter-electrojet (Rastogi 1975, Richmond 1973, Fambitakoye et al. 1976, Raghavarao 1976). Phenomena of counter-electrojet reported at various equatorial station have been reviewed by Rastogi (1974) and more recently by Mayaud (1977).

1.3 Motion of Neutral Atmosphere

Winds in upper atmosphere exist. Visual observation of noctilucent clouds provides direct evidence of the existence of winds in upper atmosphere. Noctilucent clouds are considered to be assemblies of small dust and ice particles and are observed around an altitude of 80 km in high latitudes.

Movement of these clouds is naturally the neutral wind velocity at these heights. By photographing these clouds from widely spaced locations, one can determine the height as well as drift velocity of the clouds. Stormer (1932, 1933, 1935) studied horizontal drifts of such clouds and found the average speeds of the order of 80 m/s. The occurrence of such clouds is very rare and restricted to high latitudes only.

Another evidence of winds in the heights around 100 km was given by the drift of visible meteor trails. Meteor entering the earth's atmosphere with very high velocity collide with neutral particles and get heated up resulting in its vapourization and thermal ionisation of the medium. The hot meteoric particles therefore produce trail in the atmosphere which is some times even visible and is able to reflect the radiowaves incident on it. Both photographic and radio methods have been used to study the winds in the upper atmosphere.

Upper atmospheric motion is mainly characterised as (a) motion of the neutral atmosphere and (b) motion of the ionisation in the upper atmosphere.

(a) Motion of the neutral atmosphere

Motion of the upper atmosphere is governed by the hydrodynamic forces. Various types of the motion of neutral atmosphere are summarised as follows:-

1.3.1 Prevailing Winds

Prevailing winds are of global scale in mesosphere and lower thermosphere. These winds are long period winds (vary with season) whose associated coriolis forces will just balance the local north-south pressure gradient and this gradient is produced in turn by meridional variations in the temperature-height profile.

1.3.2 Planetary Waves

Planetary waves are in the lower atmosphere with periods of days. These waves are almost entirely trapped in the lower atmosphere as a result of mesospheric winds. However at some seasons a small fraction of their energy may penetrate the mesosphere and contribute to observed motions near 100 km (Hines, 1963).

1.3.3 Tidal Oscillations

Tidal oscillations are global in scale with periods related to solar and lunar days. They can also be treated as a special case of atmospheric gravity waves. The sun and moon produce tidal forces in the atmosphere. These forces set up tidal waves in the atmosphere which result in horizontal air motions. The atmosphere responds differently to forces of different periods. The motion of air across the geomagnetic field induces electromotive force, which drives currents at the levels in the ionosphere where the air is electrically conducting which cause

the periodic solar and lunar magnetic variations. The system of electric field, currents and charges produced by this process has an important influence on the ionosphere itself.

1.3.4 Internal Gravity Waves

Internal gravity waves are of periods of a few minutes to several hours having vertical wave length of a few kilometers and horizontal wave length upto thousands of km. Hines (1960, 1965) discussed the general problem of wave motions in the upper atmosphere and in particular the class of "internal gravity waves". The energy of these waves is generally derived from large-scale motions. They can be produced in the upper atmosphere by the breakdown of tidal motions, which attain large amplitudes at these heights that non-linear processes occur and cause dissipation of energy. Alternatively, wind system in the lower atmosphere can generate gravity waves, though the penetration of waves to the upper atmosphere then depends on the transmission and reflecting properties of mesosphere.

1.3.5 Turbulence

The turbulence is characterised by the random oscillations of velocity which produce irregularities in the path of a particle. The kinetic energy of the fluid due to the fluctuations in the velocity will subsequently be dissipated as heat. The fluctuations as manifested in **velocity** are different from the regular wave motions and turbulence grows at the expense of the

energy in waves either by breaking them or by extracting energy from the strain rates produced by waves. Turbulence serves as a "sink" of energy.

The methods used for the measurement of the motion of neutral atmosphere are given in the following table:-

Methods	Range
<u>Ground-based methods</u>	
(i) Meteor trail method	80-100 km.
(ii) Satellite Drag analysis	180-300 km.
<u>Rocket-borne methods</u>	
(i) Point release or 'blob' release	80-upto the apogee (can be used for predetermined level).
(ii) Trial release	80-upto the apogee.

1.4 Motion of the Ionisation in the Upper Atmosphere

At D-region height the neutral gas is sufficiently dense so that it can carry with it in its motion any ionisation that happens to be present. This is not necessarily the case in the E-region and above, however, the ions and electrons present in the E-region and above are subject to force that can exceed by a large factor, the collisional interaction with the neutral constituents.

The importance of charged particles' movement is twofold. Firstly they lead to ionospheric currents if the mean drift velocities of positive ions and electrons are unequal. Such currents, concentrated mainly in the E-region are thought to be responsible for most of short term variations in the earth's geomagnetic field. Secondly particles movements redistribute the free electrons produced by solar ionizing radiation, before they are removed by recombination or attachment. The effect of such redistribution on the shape of the layers is particularly great in the F-region where the lifetime of free electrons is measured in hours. The effect on E-region is smaller but is nevertheless thought to be appreciable.

The large-scale distribution of ionization superimposed by small scale irregularities of ionization seem to exist at every level in the ionosphere. The basic properties to be measured are their size and shape, intensity (i.e. fractional deviation of electron density) and their speed and direction of motion. Techniques for measuring motion of ionospheric irregularities are listed in the following table:-

Technique	Range
<u>Methods for measuring bulk plasma motion</u>	
(i) Thomson incoherent scatter technique	E and F region (90-450 km).
(ii) Rocket vapour release technique (Barium cloud)	80 km to the apogee.
<u>Techniques for measuring motion of irregularities</u>	
(i) Closely spaced receiver (D ₁ method)	60 - 400 km.
(ii) Radio star and satellite scintillation technique (D ₃ method)	100 - 500 km.
(iii) HF and VHF radar scatter technique (Doppler shift)	60 - 500 km.

1.4.1 Closely Spaced Receiver Technique (D₁ Method)

The pulse reflection method of Mitra (1949) generally uses a transmitter working at frequency of a few megahertz and three receivers arranged in a triangle about a wave length apart record the fluctuations in amplitude of the signal reflected from the ionosphere. This fading is usually attributed to irregularities situated near or somewhat below the height of reflection. By choosing appropriate radio frequencies it is possible to study the movement of irregularities in D, E and F

layers. The time delay between similar fades of the different receiver give the magnitude of drift velocity of the ground diffraction pattern. This simple method is useful over a large height range and gives both spacial and temporal variation of the pattern of irregularities.

Simultaneous observation of D_1 method with rocket technique, meteor radar technique, backscatter radar and incoherent radar technique has indicated that D_1 method gives a reliable estimate of average drift velocity in the ionospheric D, E and F regions (Kent and Wright 1968, Lysenko et al. 1972, Stubbs 1973, Felgate et al. 1975, Oyinloye and Akinrimisi 1976, Wright et al. 1976, Crochet et al. 1977, Tabbagh et al. 1977, Vincent et al. 1977).

Analysis of the fading record to obtain different parameters of the irregularities can be done by (i) using time delay method, (ii) cross-correlation method and (iii) cross-spectral method.

1.4.2 Radio Star and Satellite Scintillation Technique

When high frequency radio waves are passed through the ionospheric layers they are found to fluctuate rapidly in amplitude. Such high frequency radio waves might be received from radio stars or radio beacon satellites. It is believed that variations in the electron density cause the variations in phase across the wave front, these develop into diffraction pattern containing both amplitude and phase variations by the

time that the wave reaches ground. Consequently, the intensity of the radiowave changes with time and space and scintillations are produced.

If the source is an artificial satellite then it can be shown (James 1962) that velocity of the diffraction **pattern** on the ground and the changes within are related to the height and thickness of the region of irregularities, provided the velocity and position of the satellite are accurately known, these parameters of the layer can be deduced.

Recently geostationary satellites having modulated beacons at different frequencies covering high frequency (HF), very high frequency (VHF) and ultra-high frequency (UHF) are used to study the scintillation and irregularities in the ionosphere. Using spaced scintillation technique one can find different parameters like velocity, direction, size etc. of the irregularities. Paulson and Hopkins (1973) used UHF for finding above mentioned **parameters** of the ionospheric irregularities. Drift parameters obtained by this method have integrated effect of entire region.

CHAPTER - II

DRIFT MEASUREMENTS AT AHMEDABAD DURING THE PERIOD 1970-75

2.1 Introduction

The drift of ionization in the ionosphere was first noticed indirectly by Ratcliffe and Pawsey (1933) and Pawsey (1935) while studying the amplitude fluctuation (fading) of radio echo returned from the ionosphere. They concluded from the study of fading records at two spaced receivers, that the cause of fading was the interference of radiowaves reflected from scattering centres in the ionosphere. Pawsey (1935) was also first to notice a consistent time delay of record at two receivers. He attributed this to the horizontal movement in ionosphere. The measurements of horizontal movements in the ionosphere by this technique were first made by Mitra (1949) and Krautkramer (1950). Mitra used a pulsed transmitter at vertical incidence and reflected signal fluctuations were recorded at three spaced receivers situated at the vertices of a triangle of sides 100 meters each. From the time shifts between the maxima of similar fades the drift speed was determined. Radio stars and beacons from satellites have also been used as a source of radio waves instead of using ground-based pulse transmitter.

Drifts have been measured for E and F regions using Mitra's technique at a number of high latitude stations since 1949 and were reviewed by Briggs and Spencer (1954). The measurement of

E and F region drift at low latitude station Ahmedabad by Mitra's method had been carried out during different periods since 1956 by the Physical Research Laboratory. The equipment consisted of a pulse transmitter of about 1.5 KW peak ~~power~~ operated at 2.6 MHz. Receiving aerials were situated at the corners of an isocetes right angled triangle of sides equal to 120 metres along north-south and east-west directions and consisted of horizontal dipoles oriented in north-south directions. A single receiver was used with the help of the electronic switch to avoid any error due to drifts in the receiving equipment. The records were taken on 35 mm photographic film moving at a speed of 100 cms per minute.

Regular observations of E-region drifts were taken at 2.6 MHz between September 1956 to Feb. 1959, between November 1959 to Feb. 1962 and between Nov. 1964 to Jan. 1967. The results of E-region for the period 1956-66 have been summarised by Rastogi (1969). The drift speeds were found to be slightly greater during night than during daytime for any of the epochs. No significant solar cycle variation of drift speed was noticed. The most probable directions of drift were either north-west or towards south-east. During any epoch the probability of north-west direction of drift for the daytime was maximum during winter and minimum during summer. Further with the ~~decreasing~~ solar activity the direction for any of the seasons had progressively changed from the north-west to the south-east.

The solar diurnal component of the drift speed was generally greater than the corresponding solar semidiurnal component except during the winter and the equinoxes at the maximum sunspot years 1956-59.

When similar measurements were started at Thumba near the magnetic equator by Physical Research Laboratory, a very consistent picture emerged with drift direction towards west by day and towards east by night (Rastogi et al. 1966). The average day time drift speed was found to be 132 m/sec for E-region and 161 m/sec for F-region being much higher than by mid-latitude station (Deshpande et al. 1966). The elongation of irregularities in the F-region at Thumba were found to be very high along the north-south direction (Rastogi et al. 1968). It was suggested that abnormally large value of the drift speed, consistent westward direction during the daytime and extreme elongation of the irregularities are characteristics of the magnetic equatorial zone (Chandra and Rastogi, 1969). It has been shown that the daily, seasonal and latitudinal variations of drift near the magnetic equatorial zone are associated with equatorial electrojet (Chandra et al. 1971).

From the data collected at a number of locations and operated during IGY Kazimirovsky (1962, 63) noted the systematic pattern of drift suggesting a kind of large scale circulation in the E-region with different pattern during winter and summer,

while for F-region there was a single pattern with a large change over occurring between latitudes 20 and 30 degree in both hemispheres. However, the stations at low-latitude were only a few and it was felt to operate a chain of drift stations at low latitudes to understand the large scale circulation of E-region altitudes and its relationship to the Sq current system.

The observations at Ahmedabad were restarted in October 1970 as a part of a program to establish a chain of drift stations in India and map out the circulation pattern at low latitudes. The equipment was modified slightly. It was felt to test the validity of the Mitra's method to detect the movements at E-region altitude particularly in view of large scatter (large day to day variability in drift speed and direction). For this purpose simultaneous measurements of the ionospheric E-region drift were carried out by Mitra's method at Ahmedabad (geog. lat. 23°N , long. 72.6°E) and at Udaipur (geog. lat. 24°N , long. 73.7°E) with almost similar sets of equipments during 1973-75. The results of these two stations separated by 200 km showed very good similarity both on the average statistical basis as well as on the individual days (Rastogi et al. 1978). On occasions, sudden changes occur in drift velocity almost at the same time at the two places suggesting the presence of large scale atmospheric circulation pattern in the E-region of the ionosphere. High degree of correlation in the data on individual days gives strong confidence in the application of spaced receiver technique

at these latitudes. Large scatter of drift direction at tropical latitudes station is suggested due to genuine variation in the ionosphere rather than in the method of ionospheric drift measurement. Fig.2.1 shows the mass plot of the drift speed at Ahmedabad and drift speed at Udaipur during 1973-74. Correlation co-efficient is 0.75 ± 0.03 and the Fig.2.2 shows mass plot of the drift direction at Ahmedabad and drift direction at Udaipur, indicating correlation coefficient 0.89 ± 0.01 .

2.2 Methods of Data Reduction

Fading records obtained by closely spaced receiver technique are analysed to yield drifts velocities and other characteristics of the ground diffraction pattern. The analysis can be done using the following three different approaches:-

- (1) the time delay method
- (2) the correlation method and
- (3) the cross-spectral method

2.2.1 Time delay method

In this method the drifts of the ionospheric irregularities are calculated using the time delays between similar fades obtained at three closely spaced receivers as explained in the following paragraphs.

Assuming that the diffraction pattern produced by the ionospheric irregularities drifts across the ground with constant

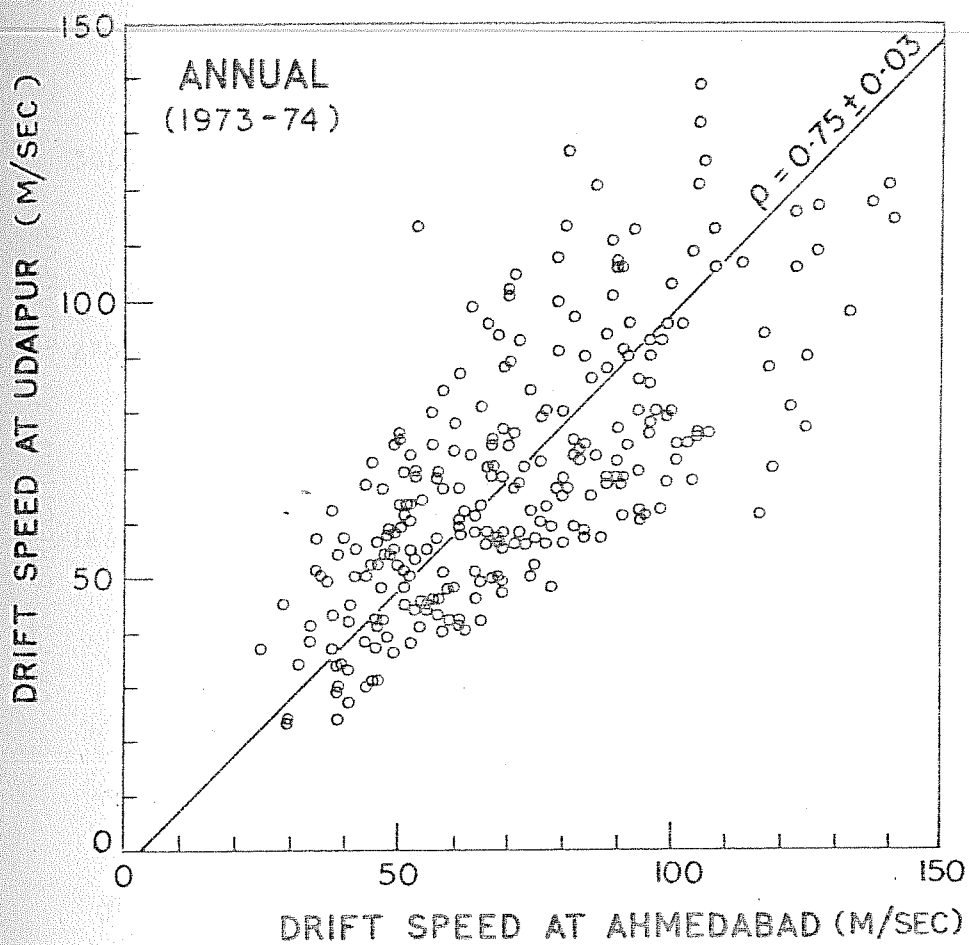


Fig.2.1 - Comparison of E-region drift speed at Ahmedabad and E-region drift speed at Udaipur.

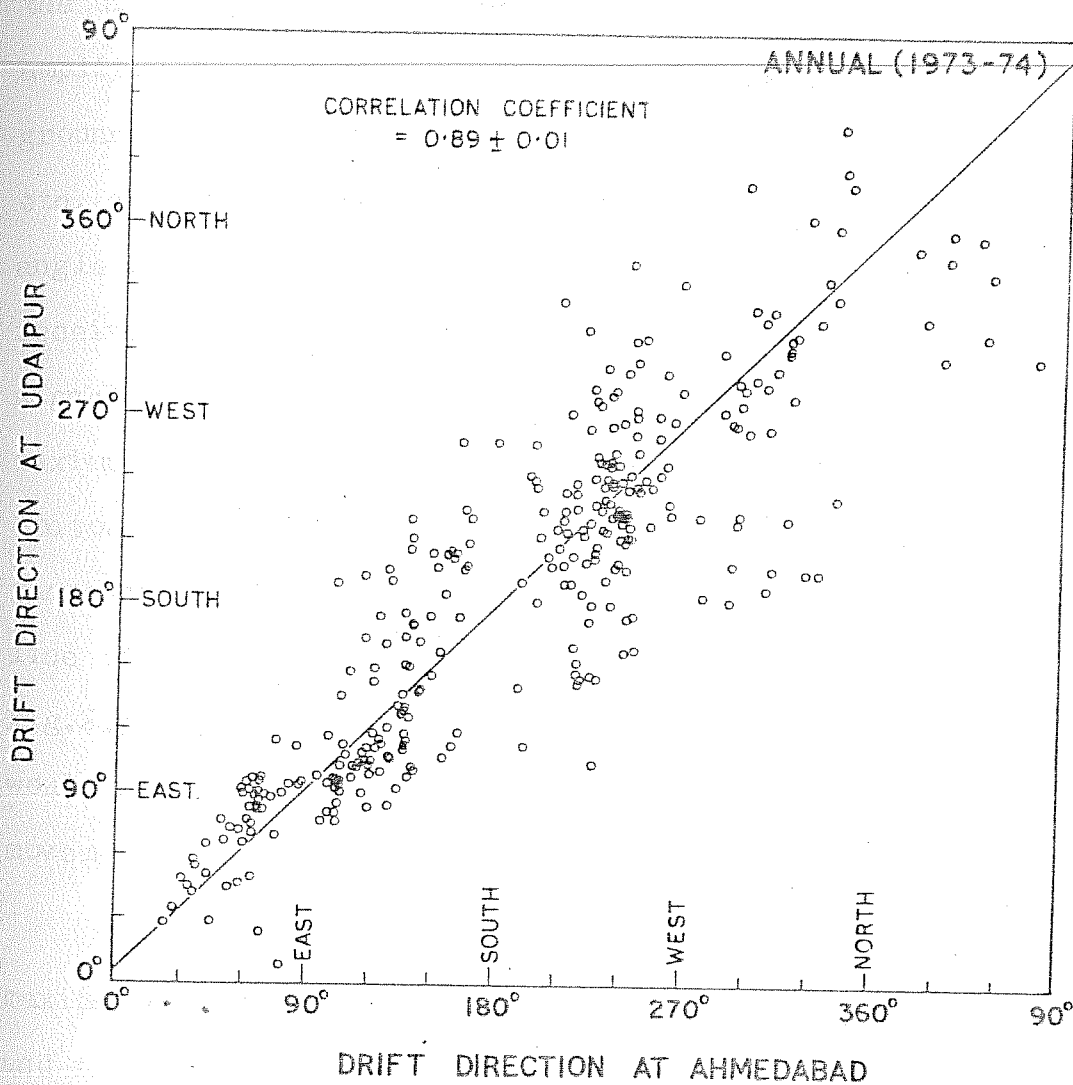


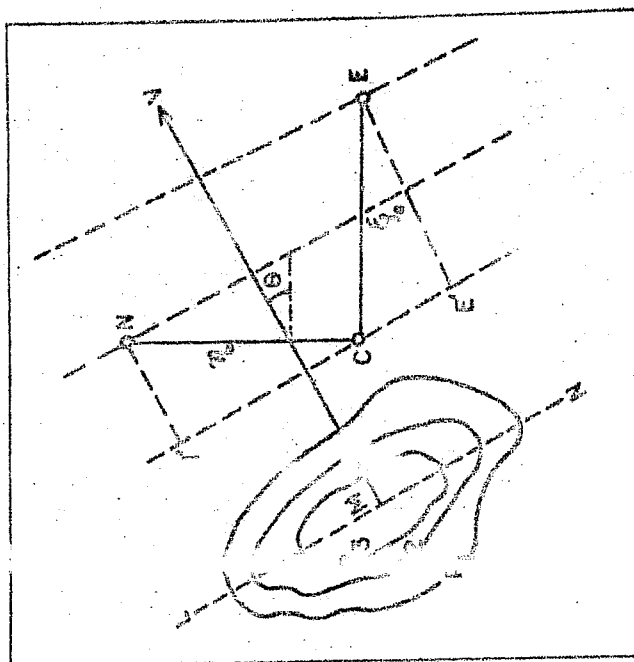
Fig.2.2 - Comparison of drift direction at Ahmedabad and drift direction at Udaipur.

velocity and without any change in the form as it moves and that the diffraction pattern on the ground is isometric in nature, the diffraction pattern can be represented by contours of constant amplitudes. Let us represent the diffraction pattern on the ground by means of contours of constant amplitudes $R_1, R_2, R_3 \dots$ etc. moving with uniform speed V' in a direction which makes an angle θ with X-axis (Fig.2.3). Let N, C and E be the three receiving sites. As different contours pass over these sites the signal strength at these sites will fluctuate with time. A maximum of signal strength will be recorded at any aerial when a contour passes over the receiver tangentially. The locus of the tangential points along the direction of drift is called the line of maximum amplitude (Ratcliffe, 1954) and it is shown in Fig.2.3 by dotted line. Under the above assumptions, this line would be a straight line, perpendicular to the direction of movement.

The contours of constant amplitudes can be in the case of maxima of amplitudes, replaced by the line of maximum amplitude and following relations can be written from the simple trigonometrical considerations:-

If T_x and T_y are the time lags between the similar fades of aerials C and E and the aerials C and N respectively then:

$$T_x = \frac{2}{V'} \frac{\cos \theta}{1} \quad (2.1)$$



g.2.5 - Contours of constant amplitudes of diffraction pattern on the ground. N, C and E are antenna positions.

$$T_y = \eta_0 \frac{\sin \theta}{V'} \quad (2.2)$$

where ξ_0 and η_0 are the distances CE and CN.

$$\text{Writing } V'_x = \frac{\xi_0}{T_x} \text{ and } V'_y = \frac{\eta_0}{T_y}$$

we have

$$\frac{\cos \theta}{V'} = \frac{1}{V'_x} \quad (2.3)$$

$$\frac{\sin \theta}{V'} = \frac{1}{V'_y} \quad (2.4)$$

$$\text{Hence } \frac{1}{V'^2} = \frac{1}{V_x'^2} + \frac{1}{V_y'^2} \quad (2.5)$$

$$\text{and } \theta = \tan^{-1} \left(\frac{V'_x}{V'_y} \right) \quad (2.6)$$

$$\text{If } \xi_0 = \eta_0 = a$$

$$V' = \frac{a}{(T_x^2 + T_y^2)^{\frac{1}{2}}} \quad (2.7)$$

$$\text{and } \theta = \tan^{-1} \left(\frac{T_y}{T_x} \right) \quad (2.8)$$

The speed V' thus obtained is the **speed** with which ground diffraction pattern moves and it must be divided by a factor of two to get the drift of irregularities of the ionization at the level of reflection. These velocities are uncorrected for the anisotropy and turbulence of diffraction pattern and are called apparent drift velocities (V'). The direction (θ) is generally measured from north.

2.2.2 Full correlation method

In the correlation method of analysis, auto and cross-correlation coefficients of the amplitude records are used to deduce the apparent drift speed, the true drift speed, the direction of drift speed and the size of the ground diffraction pattern.

Briggs et al. (1950) developed a method for separating steady and random components of the drift. The term 'random drift' means the rate at which the pattern changes its shape. In this method it was assumed that (i) the diffraction pattern is isotropic, (ii) the space and time variations are identical, and (iii) drift speeds remain the same during the course of the record. Briggs et al. (1950) have defined four velocities to describe the movement of ground diffraction pattern in terms of correlation coefficient.

2.2.2.1 Fading velocity V'_c

This is the velocity with which diffraction pattern would move in the absence of random changes to produce total observed fading. In terms of the correlation function, it is the ratio of space shift to time shift that would produce the same change in correlation.

If this time shift is T_1 for the observation made at distance r_1 apart we have

$$\rho(\xi_1, 0) = \rho(0, T_1) \quad (2.9)$$

$$\text{and } V'_c = \frac{\xi_{11}}{T_1} \quad (2.10)$$

where ξ is the correlation function. V'_c depends on the true drift velocity as well as on the random changes of the pattern for an isotropic pattern it is independent of direction but will vary with direction if the pattern is anisotropic.

2.2.2.2 True drift velocity V

V is the velocity of an observer who experiences slowest fading in the received signal. This is called steady drift speed as whatever slow fading is now experienced is on account of the random changes in the diffraction pattern.

If distance ξ_{11} is moved in the time T_1 by an observer to experience the least fading then:

$$V = \xi_{11}/T_1 \quad (2.11)$$

2.2.2.3 Characteristic velocity V_c

This represents a measure of the random changes in the pattern. V_c is the value of V'_c found by an observer moving with velocity V. By definition V_c is the ratio space shift to time shift need to produce same change in R (amplitude of the reflected wave):

$$\text{i.e. } V_c = \xi_{10}/T_1 \quad (2.12)$$

$$\text{where } \xi(\xi_{10}, 0) = \xi(0, T_1) \quad (2.13)$$

2.2.2.4 Apparent drift velocity V'

This is the velocity of the diffraction pattern experienced by a fixed receiver on the whole, without taking into account only random changes in the pattern. If T_0 is the time delay for the cross-correlation peak between two receivers at $X = 0$ and $X = \sum_1 0$

$$\text{Then } V' = \sum_1 0 / T_0 \quad (2.14)$$

Briggs et al. (1950) have shown that for an isotropic pattern:

$$V(V'_c)^2 = V_c^2 + V^2 \quad (2.15)$$

$$(V'_c)^2 = VV' \quad (2.16)$$

$$\text{Hence } V' = V \left(1 + \frac{V_c}{V} \right)^2 \quad (2.17)$$

Thus $V' > V$ and the contribution to random variation within the pattern is equivalent to (V_c^2/V) , which has a direction same as that of V , as V_c^2 has no particular direction.

2.2.3 Cross-spectral Analysis

Given finite amplitude records $X(t)$, $Y(t)$ and $Z(t)$ for the three closely spaced receivers of the D_1 method, the cross-spectral analysis involves following steps:-

- (1) Calculation of co-variance functions
- (2) Correction of co-variance function for the means and trends
- (3) Calculation of 'raw' spectral estimates
- (4) Smoothing to give the final spectral estimates
- (5) Computation of estimated gain and phase of frequency response function
- (6) Calculation of velocity and direction from the phase differences.

The three fading records are read at particular interval of time $t=h$, say, so that the corresponding "Nyquist frequency" is $f_0 = h/2$. Goodman et al. (1961) have shown that t should not be chosen so small that the whole spectral weight is crowded down to the bottom of one or two points. Further to minimise distortion due to aliasing, h must be small enough to ensure that the continuous data have no appreciable power above f_0 .

The cross-spectral estimates at a given frequency ' f ' are given by:

$$S_{jk}(f) = C_{jk}(f) - iQ_{jk}(f) \quad (2.18)$$

$$\text{and the phase } P(f) = -Q_{jk}(f)/C_{jk}(f) \quad (2.19)$$

Phase difference can be converted into time shift as

$$T_{jk} = P_{jk}/2\pi f \quad (2.20)$$

Any pair of time shifts for one spectral frequency may be used to calculate velocity and direction similar to simple Mitra's method (1949).

In a plane, wave-numbers add **vectorially**, so that the wave number along the line between J and K separated by a distance X_{jk} will be $K_{jk} = P_{jk}/X_{jk}$ and the vector addition of two such values will give the vector wave number K in the direction of the motion which has a velocity $V = 2\pi f/K$. If X_{12} and X_{13} are at right angles to each other this simplifies to:

$$2\pi f / \left[\frac{P_{12}^2}{X_{12}^2} + \frac{P_{13}^2}{X_{13}^2} \right]^{\frac{1}{2}} \quad (2.21)$$

and the angle ϕ with respect to X_{12} given by

$$\phi = \tan^{-1} \left(\frac{P_{12}}{X_{12}} \cdot \frac{X_{13}}{P_{13}} \right) \quad (2.22)$$

V should be divided by factor of two in order to get the velocity of ionization in the ionosphere.

2.3 Experimental Set-up

The experimental set up used at Ahmedabad for ionospheric drift measurements was the spaced receiver method (Mitra 1949). In this method radio pulses at a fixed frequency are transmitted vertically upwards and reflected echoes recorded at different antennae with suitable separation.

The experimental set-up consists of (1) aerial system (2) transmitting unit and (3) receiving and recording units.

2.3.1 Aerial System

The transmitting aerials were half-wave centerfed dipoles designed for the operation at 2.45 MHz. The receiving aerials were half-wave centerfed dipoles designed for 2.45 MHz and were oriented in the north-south and east-west direction. The aerials were separated by a distance of 120 meters along E-W and N-S direction.

2.3.2 Transmitting Unit

The transmitter consists of a pulse generator, a pulse modulator, an oscillator and a power amplifier. Pulse width is 100 to 300 μ sec. A schematic block diagram of the transmitter is shown in the Fig.2.4. The details of the transmitter are as follows:-

Peak power output = 3 KW

Pulse duration = 100 - 300 μ sec.

Pulse repetition frequency = 50 Hz

Output impedance = 600 ohms

Operating frequency = 2.45 MHz.

2.3.3 Receiving and Recording Unit

The receiving and recording unit incorporates an assembly of:-

- (1) Receiver
- (2) Triggering unit
- (3) Delayed pulse generator

BLOCK DIAGRAM OF THE TRANSMITTER

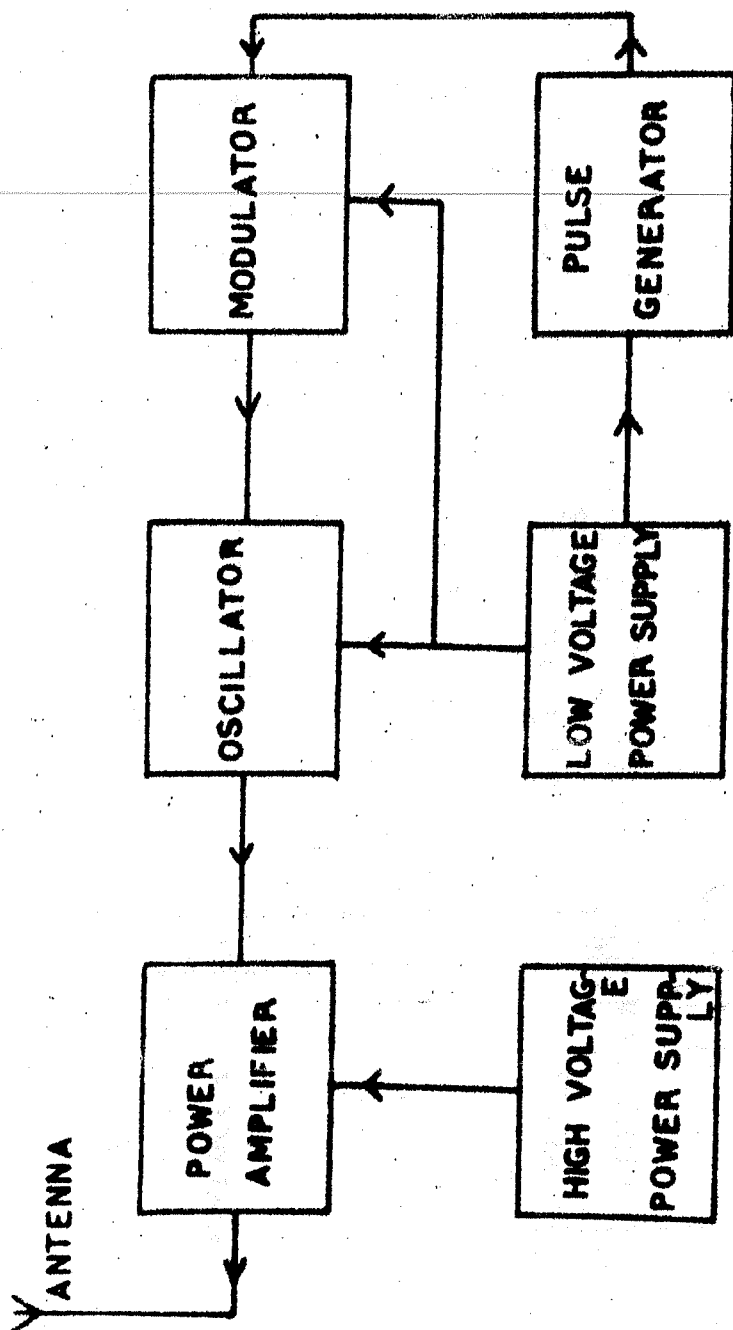


Fig.2.4 - Block diagram of transmitter

BLOCK DIAGRAM OF RECEIVING & RECORDING SYSTEM

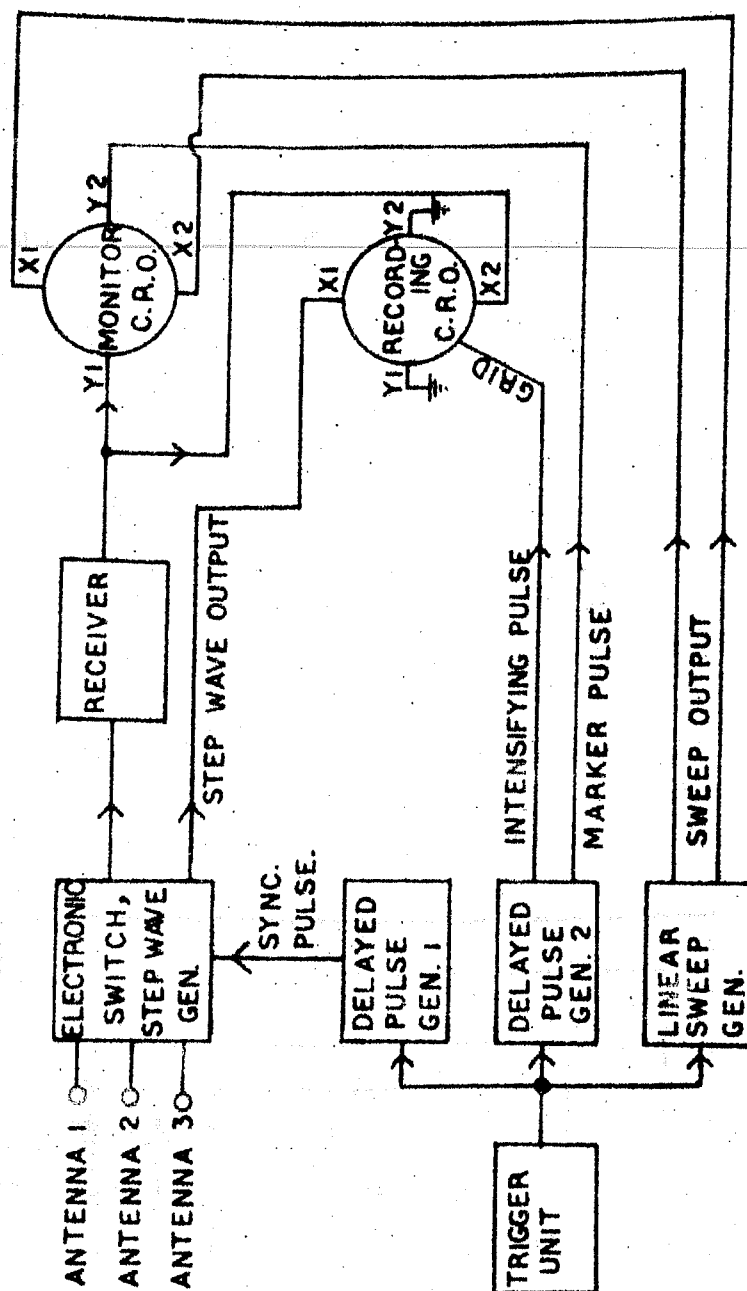


Fig.2.5 - Block diagram of receiving and recording system.

- (4) Switching circuit and step wave generator
- (5) Sweep circuits
- (6) Display units
- (7) Camera unit and time marker

A schematic block diagram of the receiving unit is shown in Fig.2.5. The pulses returned from the ionosphere are received at three spaced antennae and are brought to the receiving and recording unit by means of R.F. cables of 75 ohms impedance. The pulses from each of the three antennae are fed in sequence to the receiver through an electronic switch operating at 50 Hz. The output of the receiver is applied to the vertical deflection plates of the monitor cathode ray tube and to the horizontal deflection plates of the recording cathode ray tube.

Delayed pulse generator 1 and 2 produces D.C. pulse delayed by fixed time with respect to the start of the transmitted pulse. One of this is used to synchronise the electronic switch so that change over from one antenna to another takes place midway in the interval between two consecutive transmitted pulses. The other pulse is used as a gate pulse to select the desired echo; a pulse is applied to the grid of recording cathode ray tube generally beyond cut-off so that the spot appears on the screen only during the presence of the gate pulse. A part of same pulse is fed to the Y-plates of the monitor tube for visual adjustment of the position of the gate pulse. The fading of the echo at the output of the receiver is applied to the vertical deflection plates of the monitor cathode ray tube and to horizontal deflection plates of the recording cathode ray tube.

three antennae which is displayed on the receiving cathod ray tube is photographed on 35 mm film moving at a speed of 5 cms/mi.

Characteristics of the receiver are given below:-

- | | |
|-------------------------------|--|
| (i) RF frequencies | = Tunable from 2 MHz to 6 MH |
| (ii) Noise figure | = 3 dB maximum |
| (iii) Band width (IF) | = 3 kHz |
| (iv) Manual gain control | = Sufficient to adjust from
input variation over the
range of 1.0 micro-volt to
1.0 milli-volt. |
| (v) Overall receiver gain | = 100 dB |
| (vi) Long term gain variation | = ± 3 dB maximum |
| (vii) RF input impedance | = 75 ohms |
| (viii) Output impedance | = 10000 ohms maximum. |

2.4 Results

Hourly observations were conducted from 0800 hr LT (75° EMT) to 1600 hrs LT during 1970-75. Some of the fading records were selected from the data collected during 1971 for full correlation analysis to determine apparent drift velocity (V'), true velocity (V), characteristic velocity (V_c), apparent drift direction (ϕ), axial ratio and major and minor axis of the characteristics ellipse.

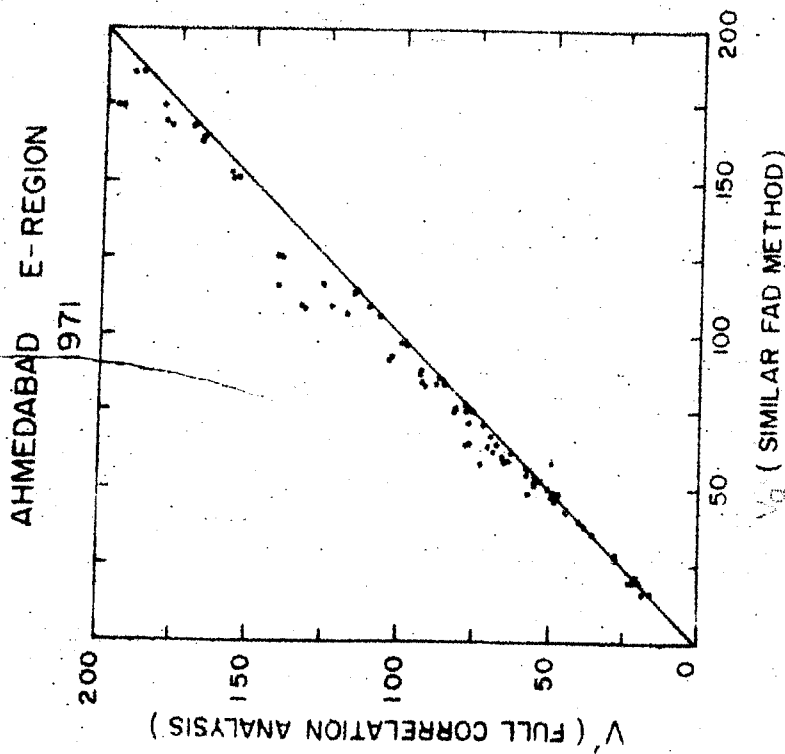
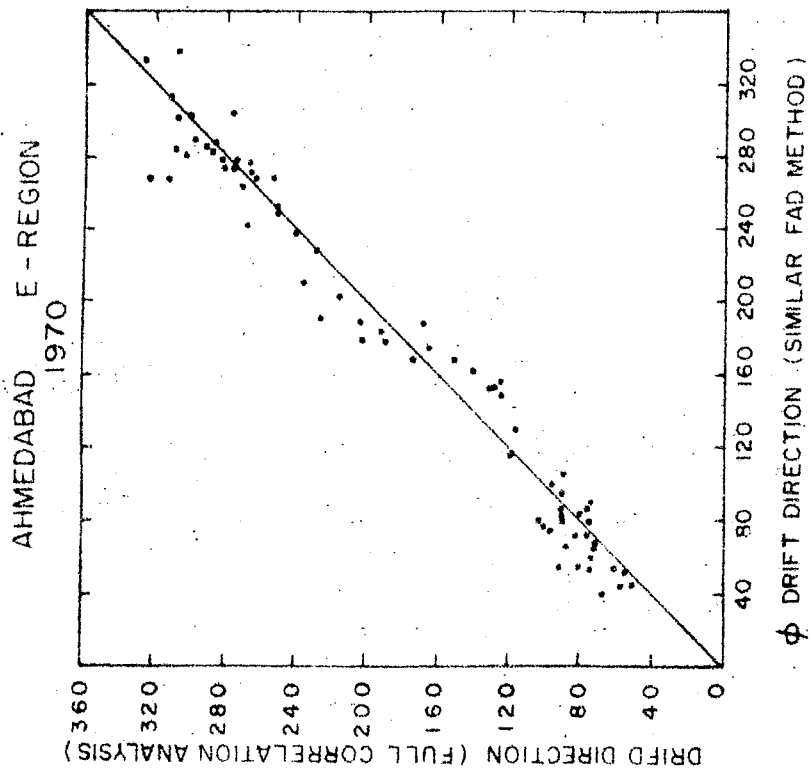


Fig.2.6 - Comparison of E-region drift speed calculated by similar fade method and full-correlation analysis.



g.2.7 - Comparison of E-region drift direction calculated by similar fade method and full-correlation analysis.

The apparent drift velocity determined by similar fade method (V_a) for the same records were compared with the apparent drift velocity determined using full correlation analysis method (Fig.2.6). It is clear from the plot that there is no significant change in the drift velocity measured by either of the methods. Hence it can be said that at these latitude anisotropy corrections for irregularities are not significant. Fig.2.7 shows the plot of apparent drift directions determined by the similar fade method (ϕ) and full correlation analysis. The directions obtained by either of the methods are similar. Hence it is concluded that the similar fade method can be used to calculate apparent velocity and direction. This saves laborious computations involved in the ~~full~~-correlation method.

Fig.2.8 shows mass plot of apparent drift velocity (V_a) determined by similar method and true velocity (V) by full correlation analysis. Fig.2.9 shows the histogram of the ratio of the apparent drift velocity (V_a) to true velocity (V). The median value of the ratio turns out to be 1.9. Hence the apparent drift velocity on the average is nearly double of the true velocity.

For a detailed study all the records were analysed by the Mitra's similar fade method as this is the quickest method to reduce data from such records and the drift velocity calculated from full correlation method is not much different. The time

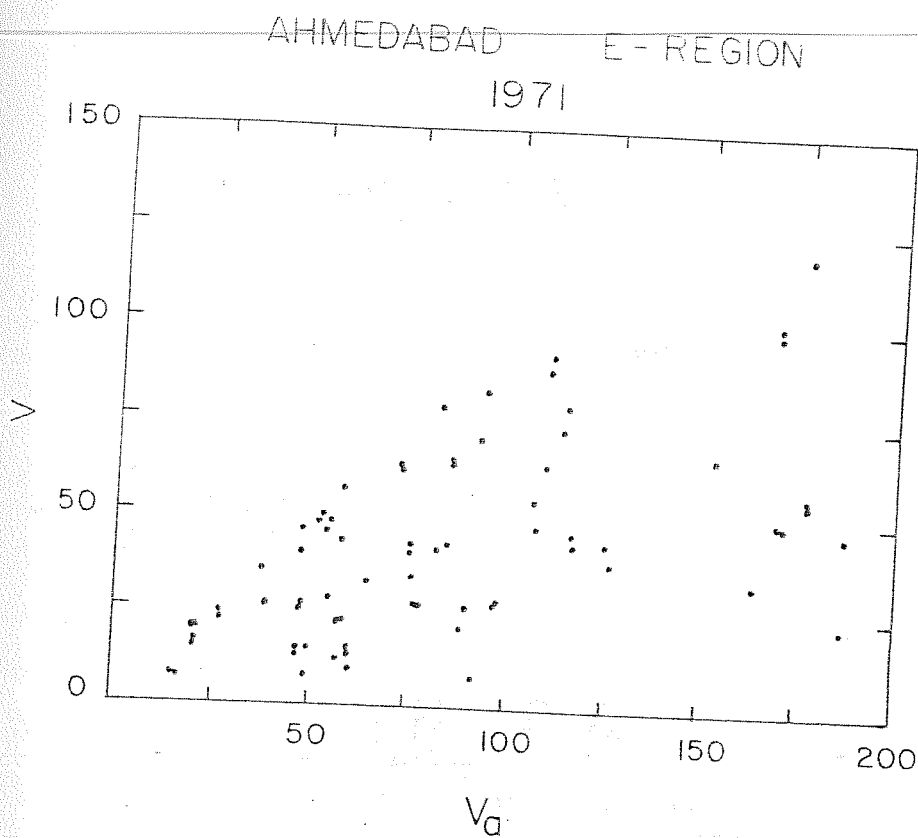


Fig.2.8 - Comparison of apparent E-region drift velocity (V_a) and true drift velocity (V).

AHMEDABAD E-REGION
1971

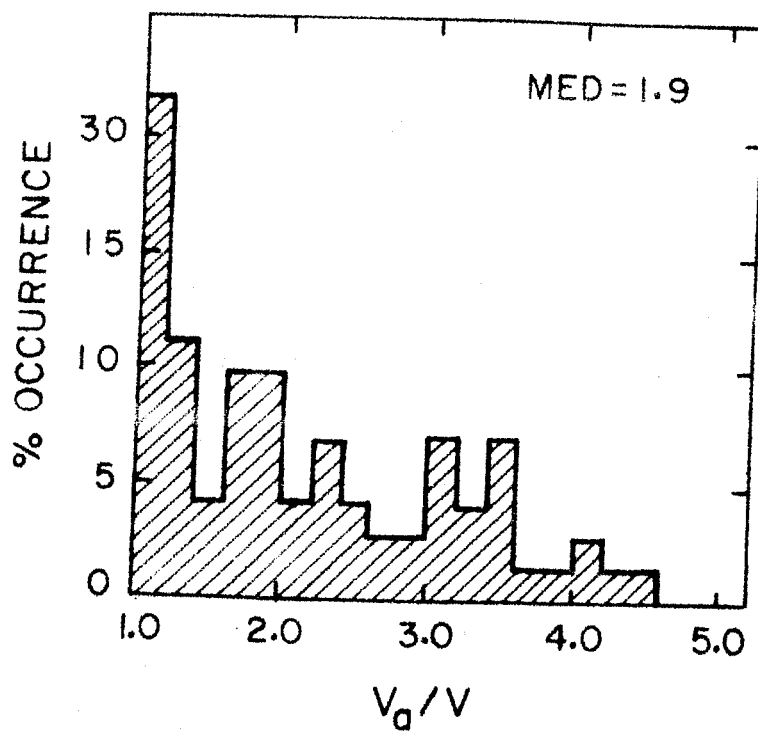


Fig.2.9 - Histogram of the ratio of apparent drift velocity and true drift velocity

shifts between pairs of aerals were fed to IBM-360 computer to compute mean time delays and then converted into different velocity components. For seasonal comparisons, the following months have been grouped together:-

- (i) Winter - This consists of the months of Nov. and Dec. of a year and Jan. and Feb. of the following year.
- (ii) Equinoxes - This consists of the months of March, April, Sept. and Oct. of a year.
- (iii) Summer - The months of May to August of a year are included in this group.

2.4.1 Annual variation of drift speed and drift direction

The annual mean histogram of the percentage occurrence of drift direction for the period 0800-1600 hrs local time (75° EMT) for the year 1974 is shown in Fig. 2.10. There is no single drift direction at this latitude, although two broad peaks are evident at SE(south-east) and SW(south-west).

Results of drift direction during all seasons during 1970-75 are shown in Fig. 2.11 as polar histograms of percentage occurrence. During winter, predominant direction is towards south-west except for the year 1971-72 when it is predominantly towards north-west. During equinoxes the direction is uniformly distributed with major peaks towards south-west and south-east except for the year 1972 when major peaks are towards north-west

AHMEDABAD E-REGION

1974

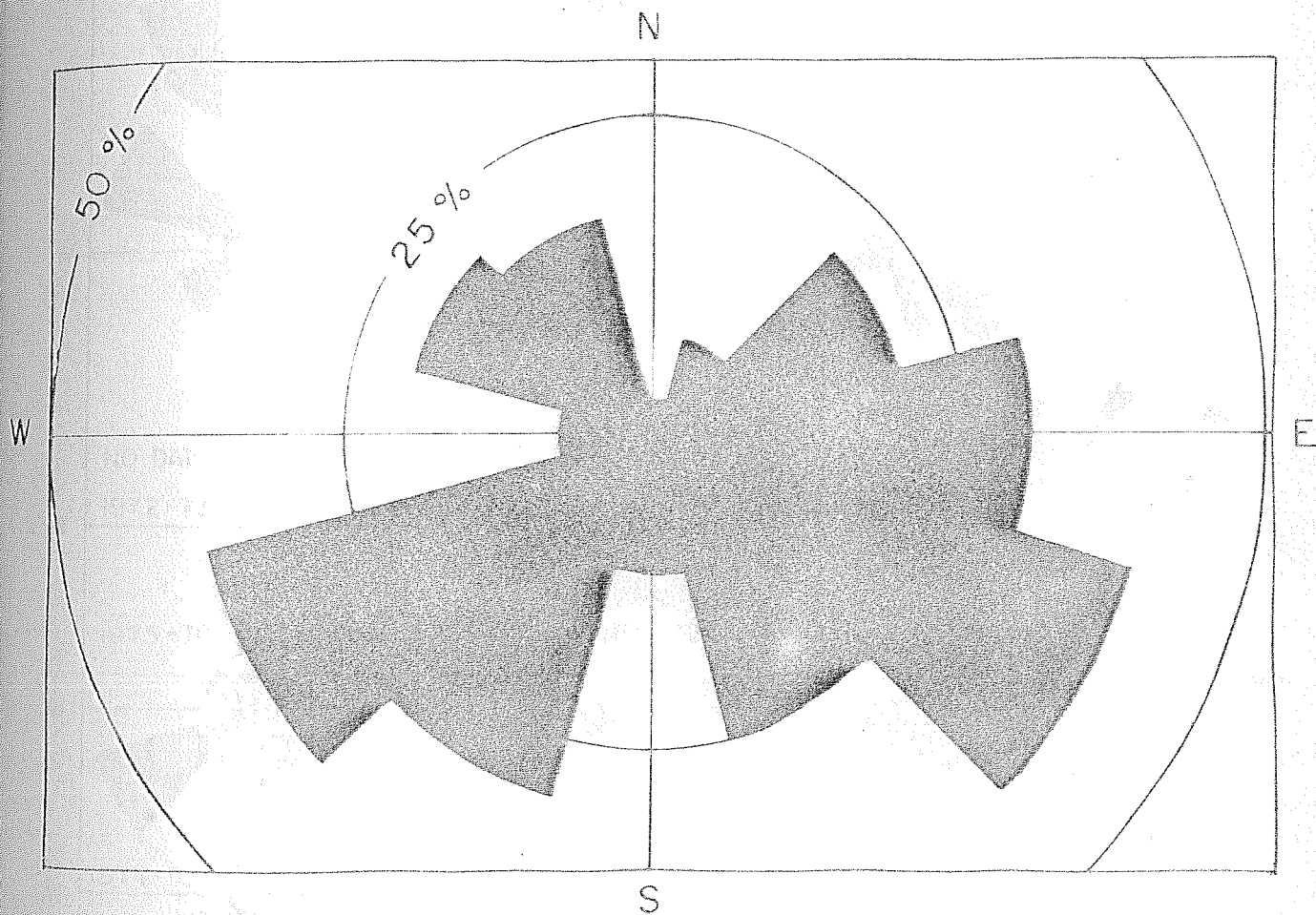


Fig.2.10 - Annual mean histogram of percentage occurrence of E-region drift direction at Ahmedabad during 1974.

AHMEDABAD

E - REGION

DAY TIME

WINTER

EQUINOXES

SUMMER

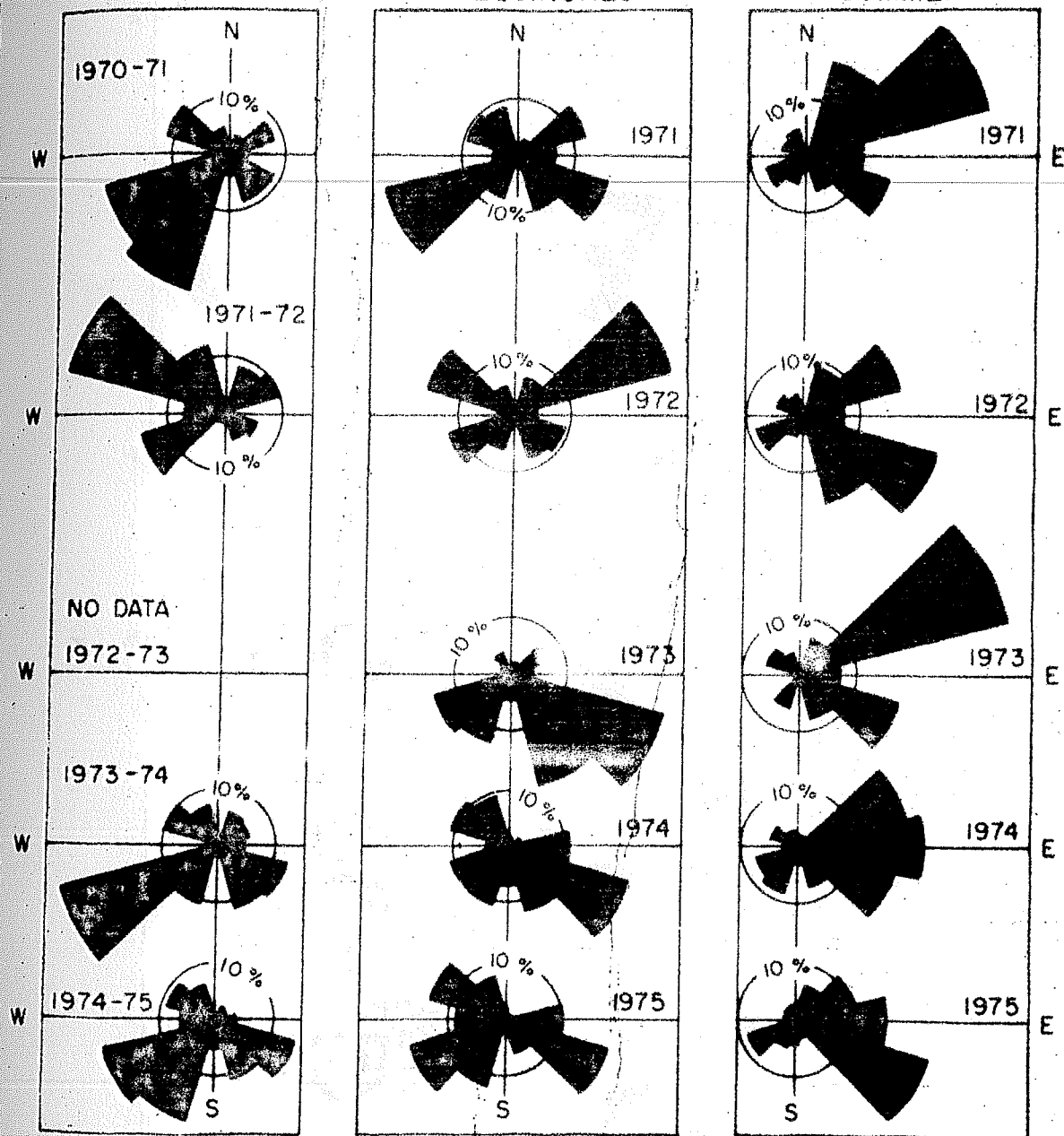


Fig.2.11 - Polar histograms of percentage occurrence of the drift direction (E-region day time) at Ahmedabad during each season in the period 1970-75.

AHMEDABAD E-REGION

1970-75

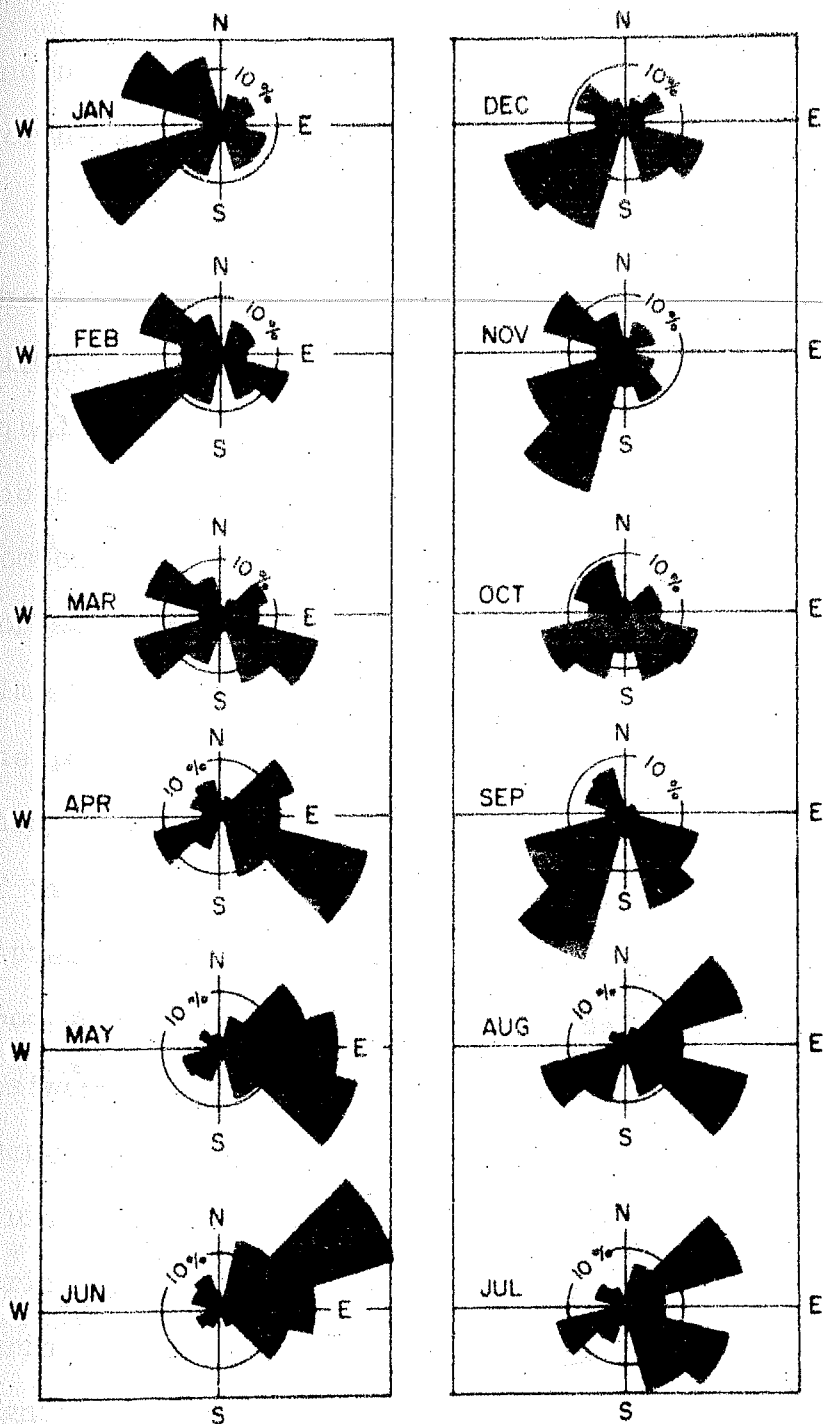


Fig.2.12 - Monthly mean histograms of percentage occurrence of the E-region drift direction at Ahmedabad for each of the months averaged over the period 1970-75.

and north-east. During summer the direction is mainly towards north-east, east or south-east.

Separate monthly histograms of drift direction averaged over the five year period (1970-75) are shown in Fig.2.12. The drift direction is mainly towards west during January with nearly equal peaks along N-W (north-west) and S-W (south-west) directions. The occurrence of eastward direction is very small. The eastward component increases progressively as seen from the histograms for subsequent months February, March etc., until June when almost all occurrences are towards east. From July onwards the percentage occurrence towards west increases till November when again westward direction is the dominant one. The transition of the zonal component is seen during March-April and then during September and October. Thus the consistent pattern which emerges from the histograms is that the drift direction has primarily westward component during winter, eastward component during summer. The transition in drift directions is observed during equinoxes. Another feature is that purely zonal or purely meridional drift is generally not observed at Ahmedabad except during summer when drifts towards the east are present significantly.

Fig.2.13 shows the year to year annual histogram of drift speed for the period 1970-75 alongwith mean, median and number of counts.

AHMEDABAD E-REGION

DAY TIME

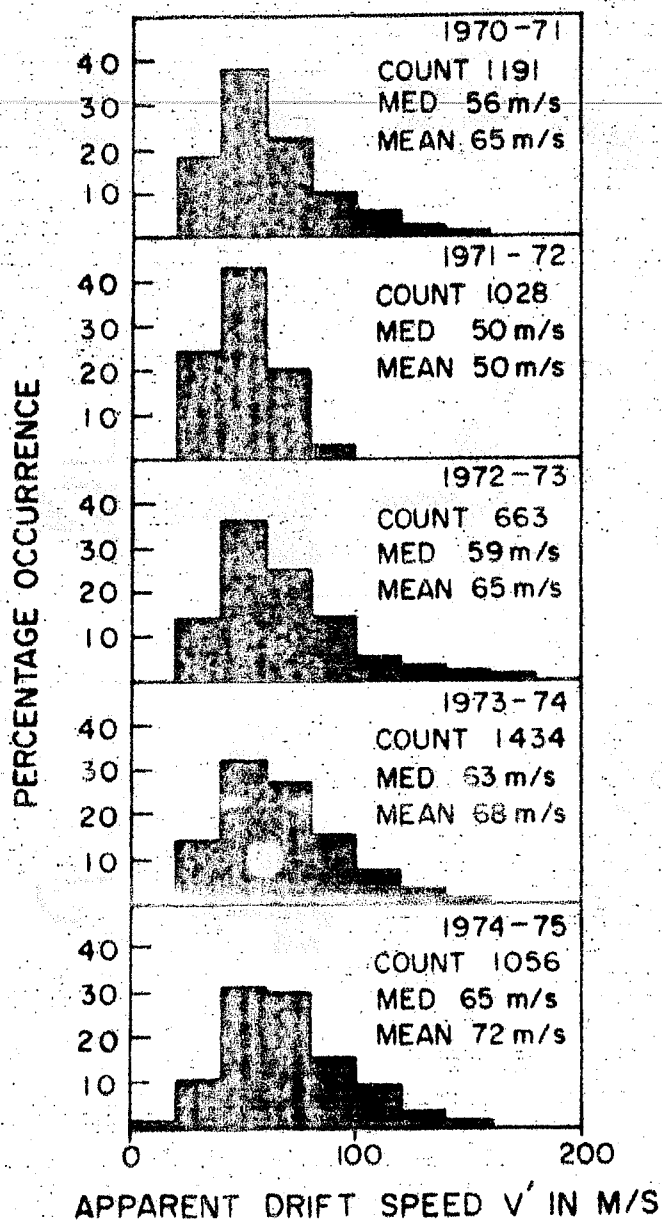


Fig.2.13 - Annual mean histograms of percentage occurrence of the E-region day time drift speed at Ahmedabad for the years 1970-75.

AHMEDABAD E-REGION DAY TIME

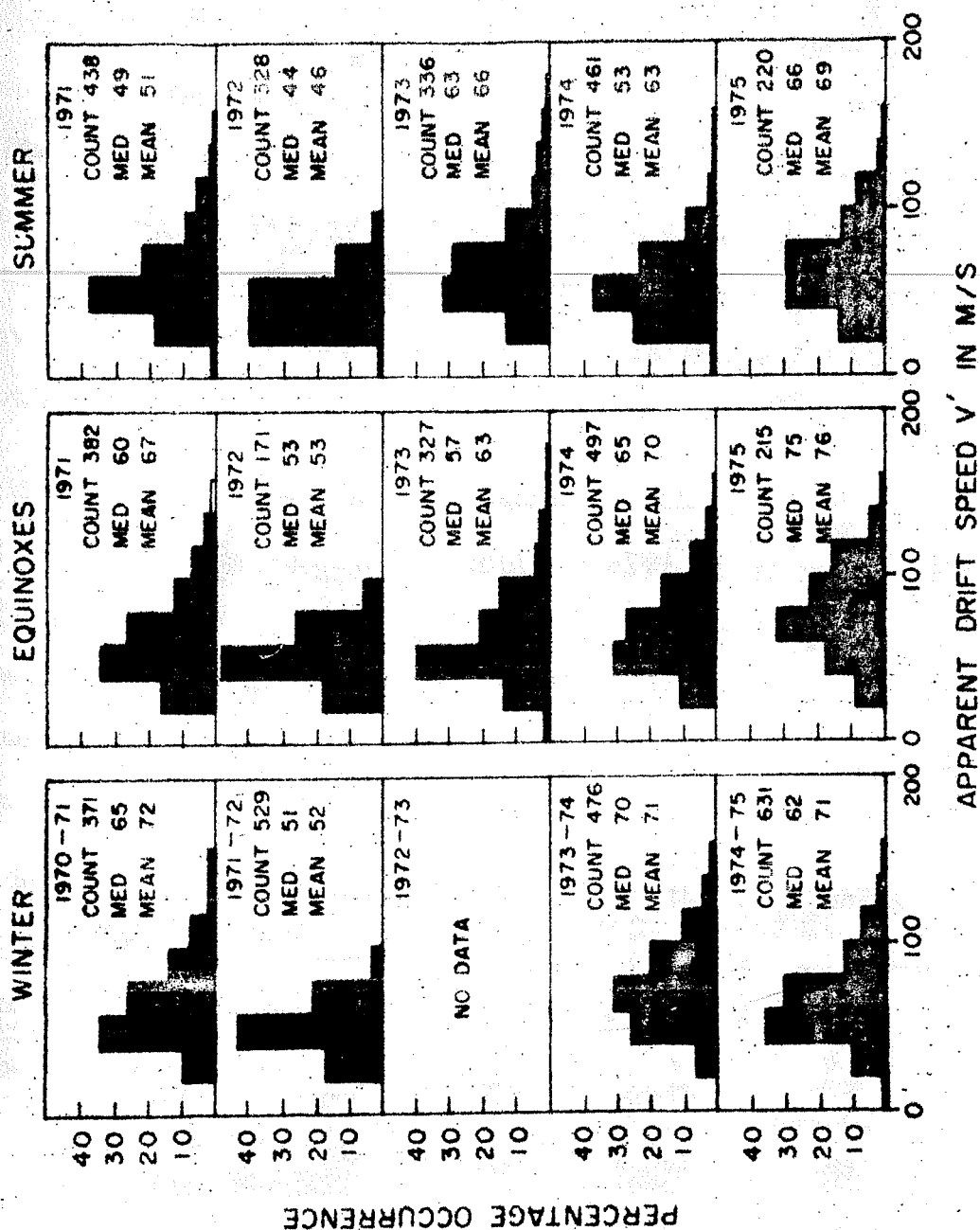


Fig.2.14 - Histograms of percentage occurrence of the E-region daytime drift speed at Ahmedabad during each season in the period 1970-75.

Distribution of drift speed during each season in this period is shown in Fig.2.14. Drift speeds are mostly ranging from 20 to 120 m/sec with most probable values lying in the range 40-80 m/sec. There is not much difference in the mean or median values from one year to another year or from one season to another season. However, the values during summer are in general little lower than in other two seasons.

2.4.2 Daily variation of drift speed

To study the variations of the drift speed with the time of day, seasonal mean values of the apparent drift speed and its eastward (V'_{E-W}) and northward (V'_{N-S}) components have been plotted in Fig.2.15 for different seasons averaged over the entire five year period (1970-75).

Referring to the daily variation of the apparent drift speed there is not much variation with the time of day. The drift speed varies between 60 and 70 m/sec during winter and equinoxes and is constant around 60 m/sec during summer.

Referring to the daily variation of the north-south component it is towards south throughout the daytime during winter and equinoxes. During summer, it is southward in the morning and evening hours and northward around noon hours.

A distinct change in the daily variation pattern with season is noticed in case of zonal component. It is westward during winter with mean values in the range 10-25 m/sec while during

AHMEDABAD E-REGION 1970-75

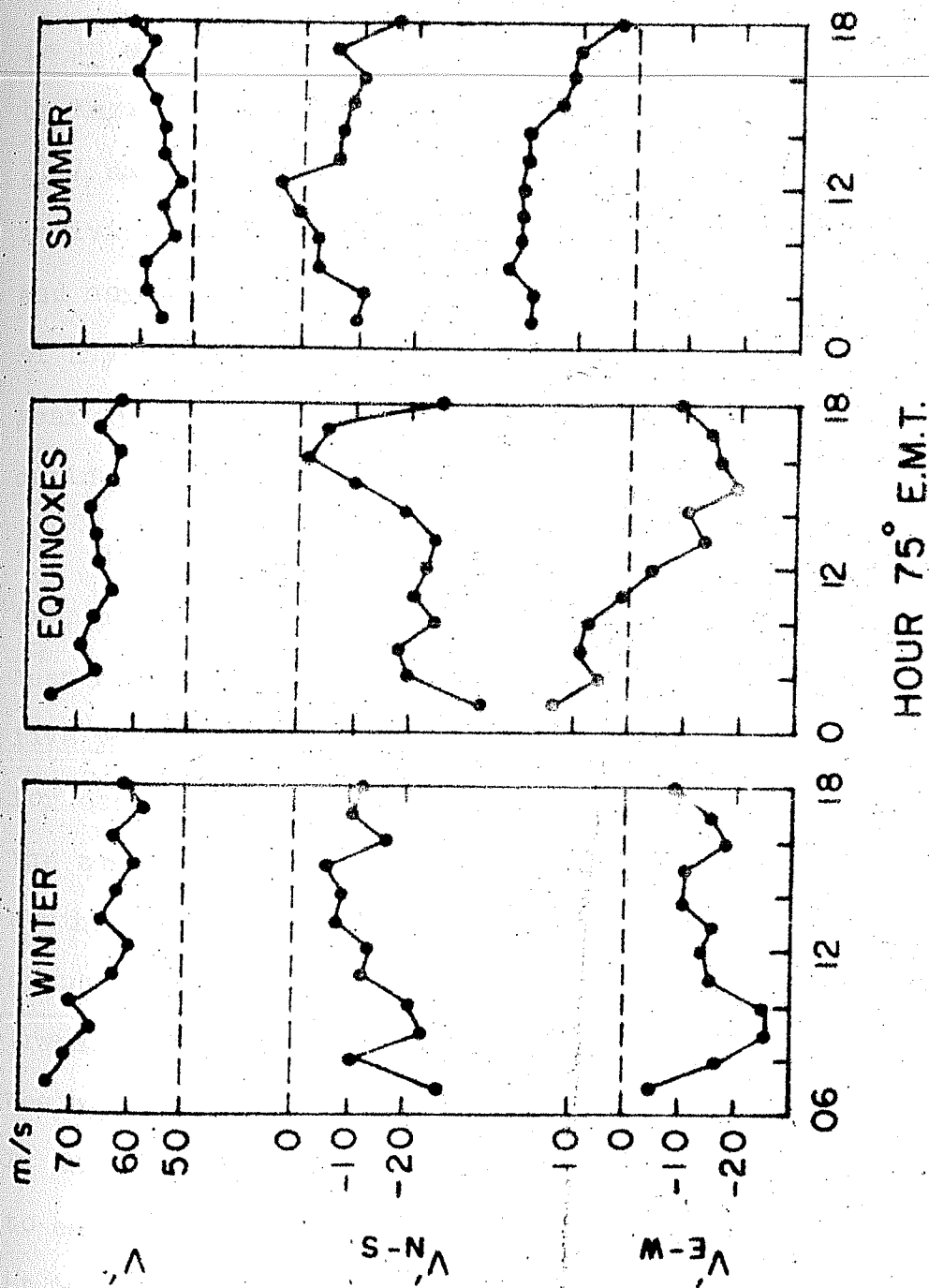


Fig.2.15 - Mean daily variation curves for the drift speed V , and its components V'_{E-W} and V'_{N-S} at Ahmedabad during different seasons averaged over the period 1970-75.

equinoxes it is eastward before noon and westward in the afternoon. During summer it is eastward with magnitude around 20 m/sec for most of the time. This pattern is seen repeating each year and is in accordance with the atmospheric circulation pattern shown by Kazimirovskiy (1962, 1963). This is shown in the Figs. 2.16, 2.17 and 2.18, where the daily variation curves for each individual season are shown for apparent drift speed, eastward and northward components. There is not much change in the nature of any of these parameters from one year to another except for the year 1971-72 when northward component is mainly towards north during winter.

To study the seasonal changes in the zonal and meridional components of the drift speed in more detail, we have computed mean daily variation curves for each of the months averaged over five year period. The daily variations of the zonal component for each months are shown in Fig. 2.19. As seen from Fig. 2.19 the zonal component is eastward throughout the daytime during the months of Jan. and Feb. During the month of March, zonal component is nearly absent in the afternoon period indicating a transition with equal number of chances of seeing eastward or westward component. In the afternoon hours the zonal component is still westward. During April zonal component has changed to eastward except in the late evening hours. During May and June it is eastward throughout the day. Thus the transition occurred during March-April period. The eastward component is little

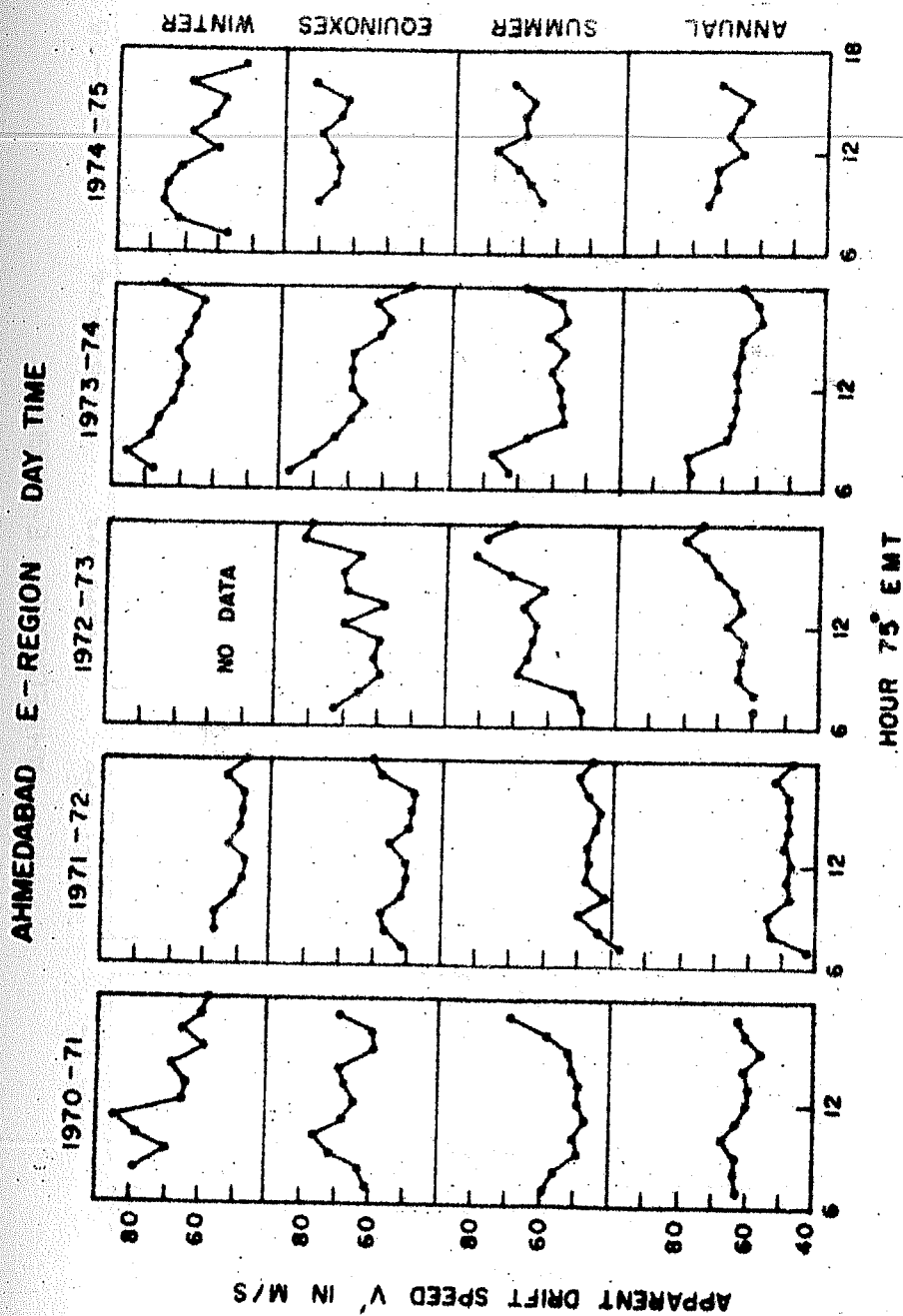


Fig.2.16 - Mean daily variation curves for the apparent drift speed for different seasons for each year during 1970-75.

AHMEDABAD E-REGION

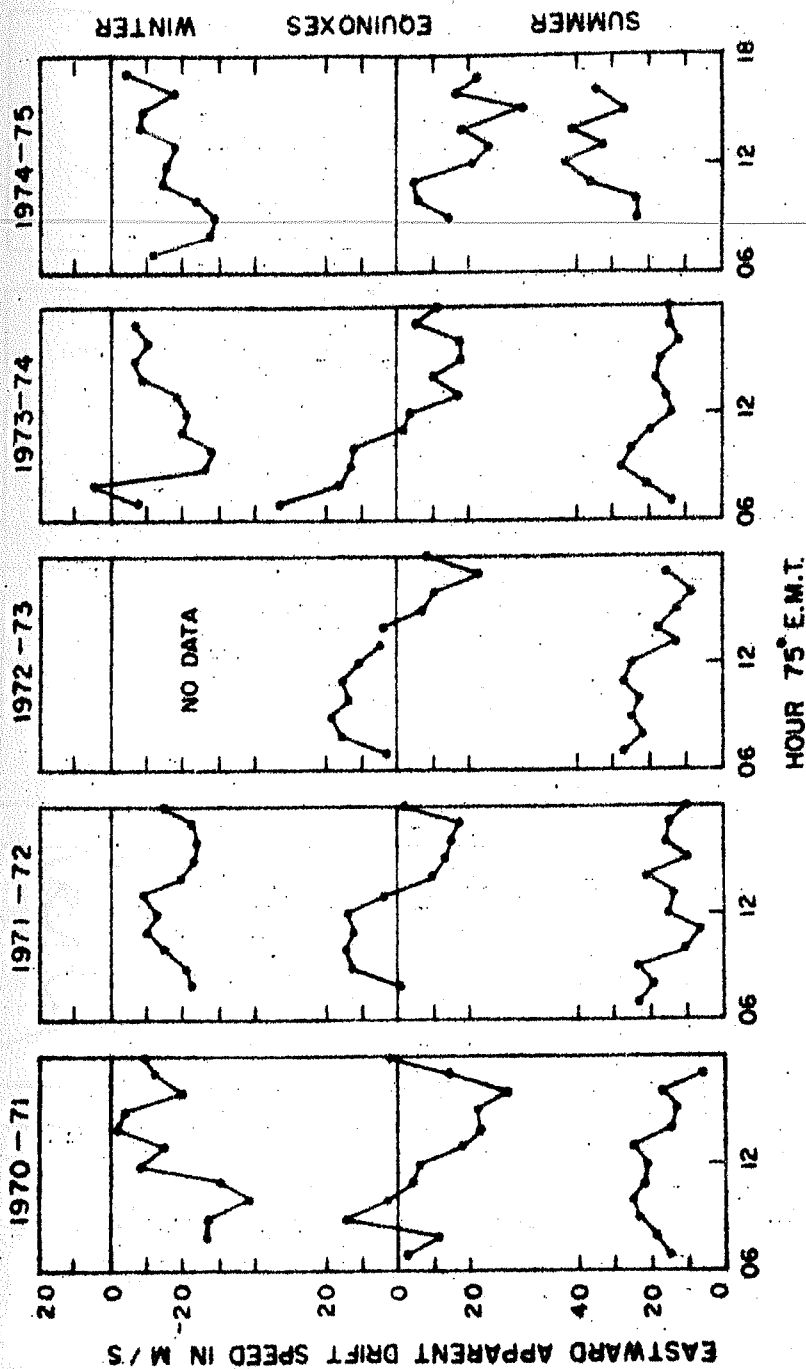


Fig.2.17 - Mean daily variation curves for eastward apparent drift speed for different seasons for each year during the period 1970-75.

AHMEDABAD E - REGION

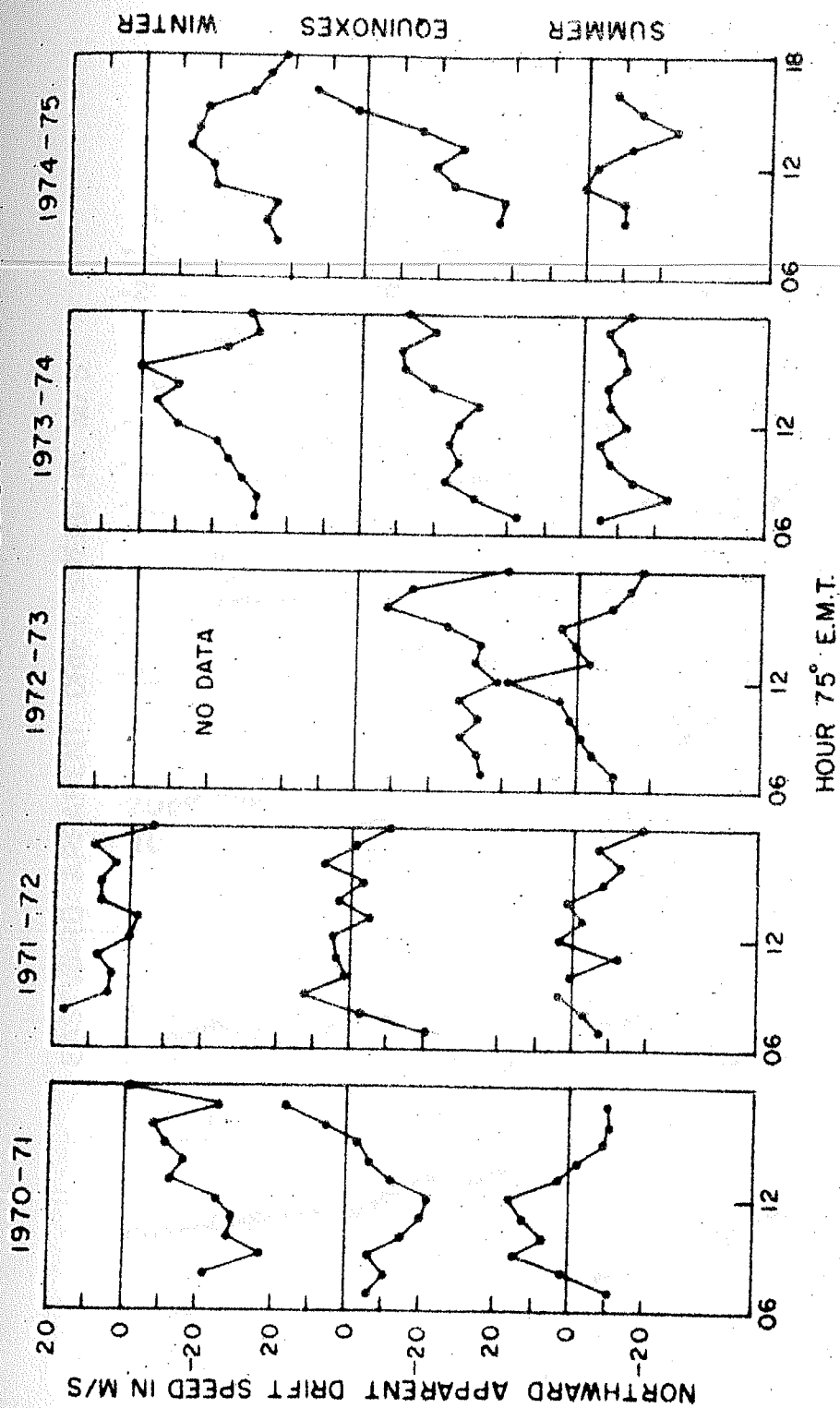


Fig.2.18 - Mean daily variation curves for northward apparent drift speed for different seasons for the period 1970-75.

AHMEDABAD E- REGION

1970-75

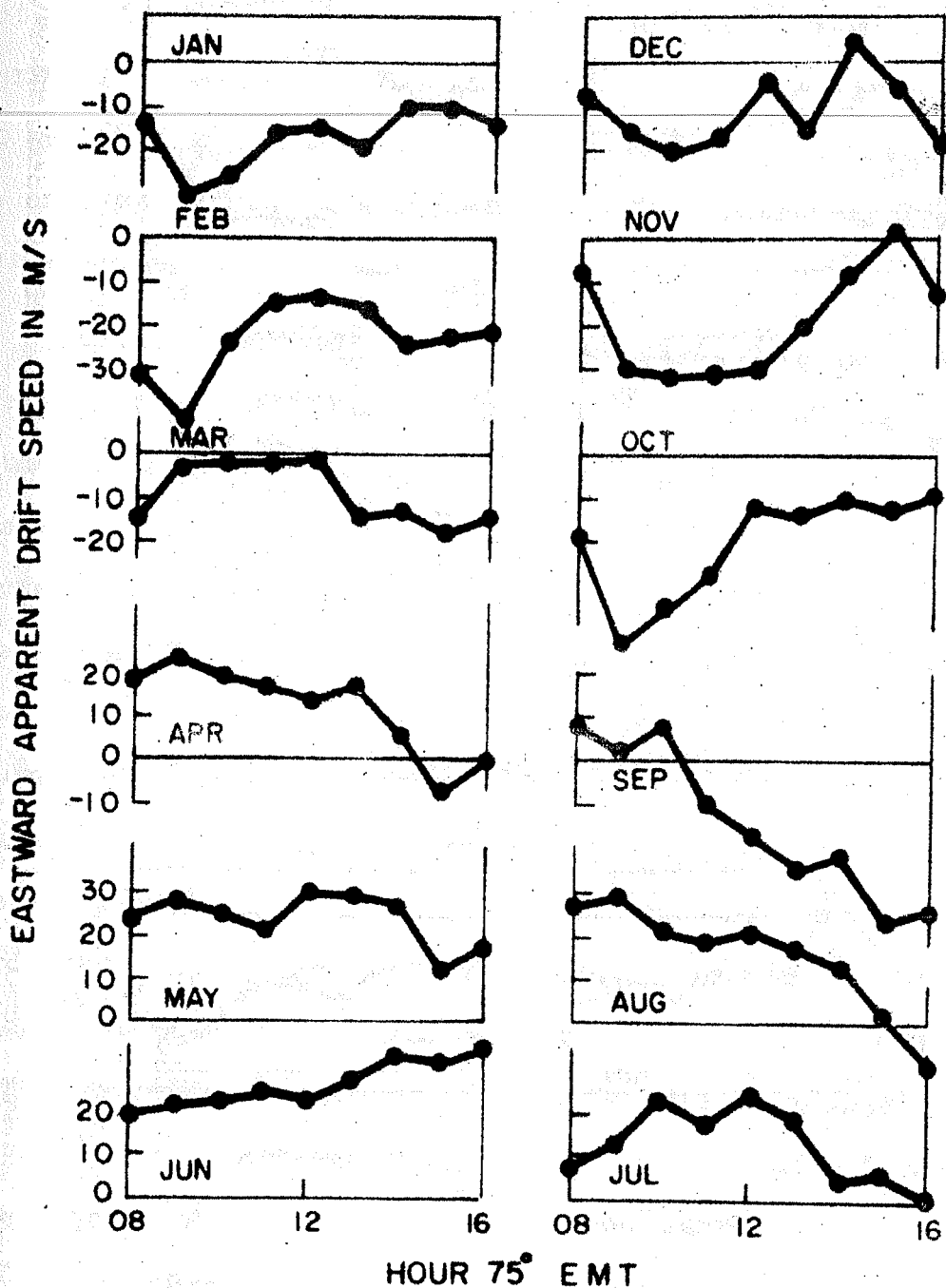


Fig.2.19 - Mean daily variation curves for the eastward component at Ahmedabad (E-region) for each of the months averaged over the period 1970-75.

weakened during July and in August it has changed to westward in the late evening, it being eastward at other times. During Sept. it is westward except in the morning hours while during Oct. it is westward throughout the day and it remains westward during Nov. and Dec. Thus transition from eastward in summer to westward in winter occurs during Sept. These results are again in conformity with the IGY studies of Kazimirovskiy (1962, 1963), who obtained instability in drift direction during equinoxes.

Month to month daily variations of meridional component averaged over the five year period are shown in Fig.2.20. It is southward during the forenoon hours for the month of Jan. and nearly absent in the afternoon hours. There is a progressive increase in the magnitude of this equatorward flow as shown in the curves for the months of Feb, Mar. and April - these curves show southward component throughout daytime. Decrease in the southward component is noticed for the month of May and complete change over to northward component is noticed in the month of June. July is again a transition period with low values, northward in the noon hours and southward at other hours. Complete change to southward flow is evident for the month of August and large magnitude throughout the day is noticed in Sept. The magnitude decreases gradually for the months of Oct. and Nov. Thus large equatorward flow is noticed during Mar-Apr. and then Sept. while poleward flow is noticed during June.

AHMEDABAD E-REGION

1970-75

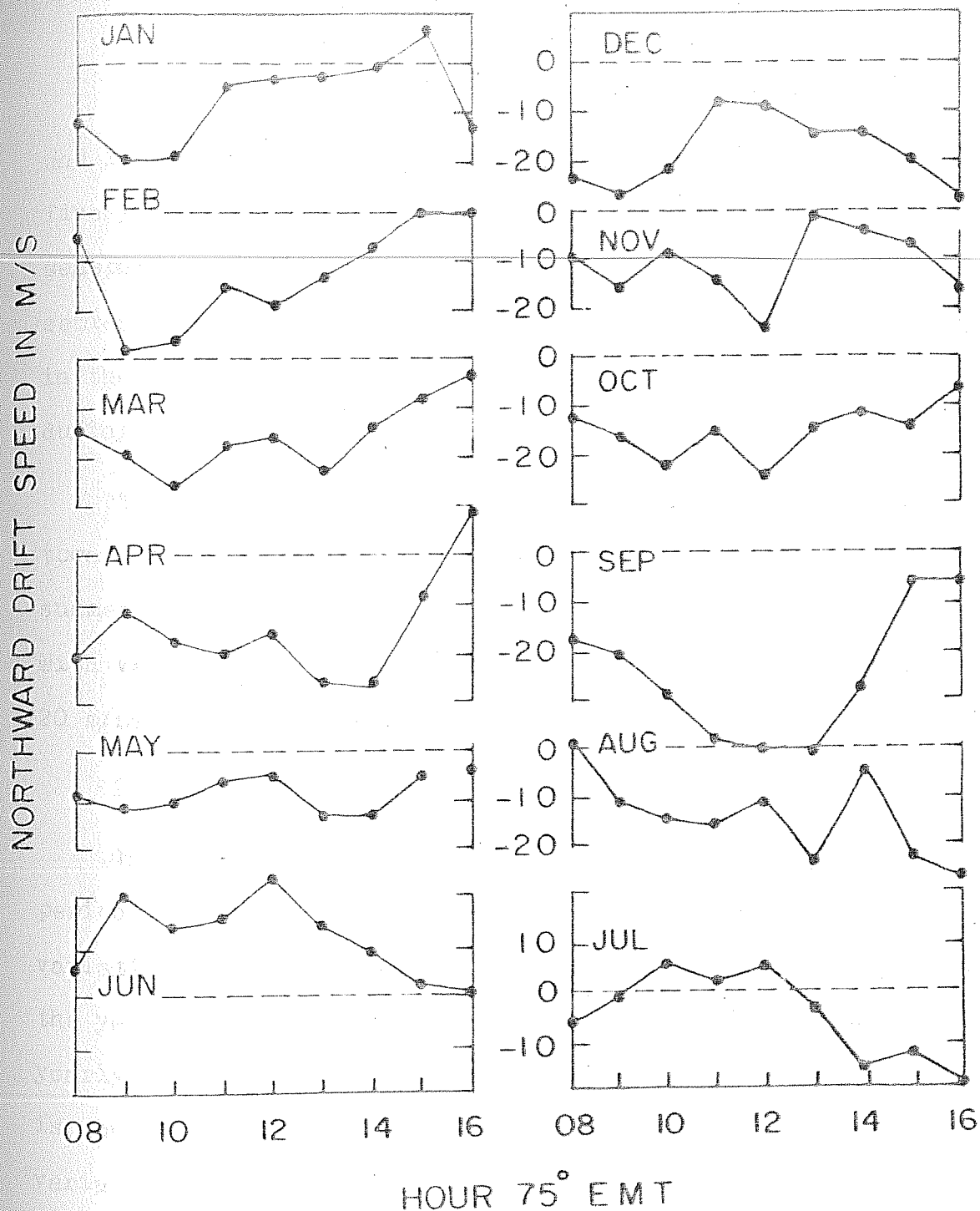


Fig.2.20 - Mean daily variation curves for the northward component at Ahmedabad (E-region) for each of the months averaged over the period 1970-75.

2.4.3 Seasonal variation of the midday drift velocity

To study the seasonal variation of the apparent drift speed and its components, monthly mean midday values averaged over the five years period have been computed and shown in Fig.2.21. The seasonal variation of apparent drift speed at noon shows a semi-annual variation with equinoctial maxima. The total range in the variation is from about 50 m/sec in June to about 70 m/sec during Feb. and March.

The seasonal variation of the zonal component is around 20 m/s toward west during winter and around 20 m/sec eastward during summer. The meridional component shows semi-annual variation with values of 20-30 m/sec southward during equinoxes and about 20 m/sec northward during summer.

2.4.4 Solar cycle variation

This long series of data (1970-75) as well as data for the periods 1956-59 and 1964-67 are used to study the solar cycle variation of E-region drifts. To study the solar cycle variation the yearly midday mean drifts values were plotted against the yearly mean sunspot number (R_z). This is shown in Fig.2.22. It is obvious that variation in the drift speed is remarkable. The variation of the drift speed is 73 m/sec corresponding to R_z 20 and 63 m/sec corresponds to R_z 80, sensitivity being 2.8×10^{-3} . The sensitivity is little higher than at equator. The comparison of the sensitivity at different latitudes is shown in the next chapter (Fig.3.1).

AHMEDABAD E-REGION
1970 - 75 (12 Hrs)

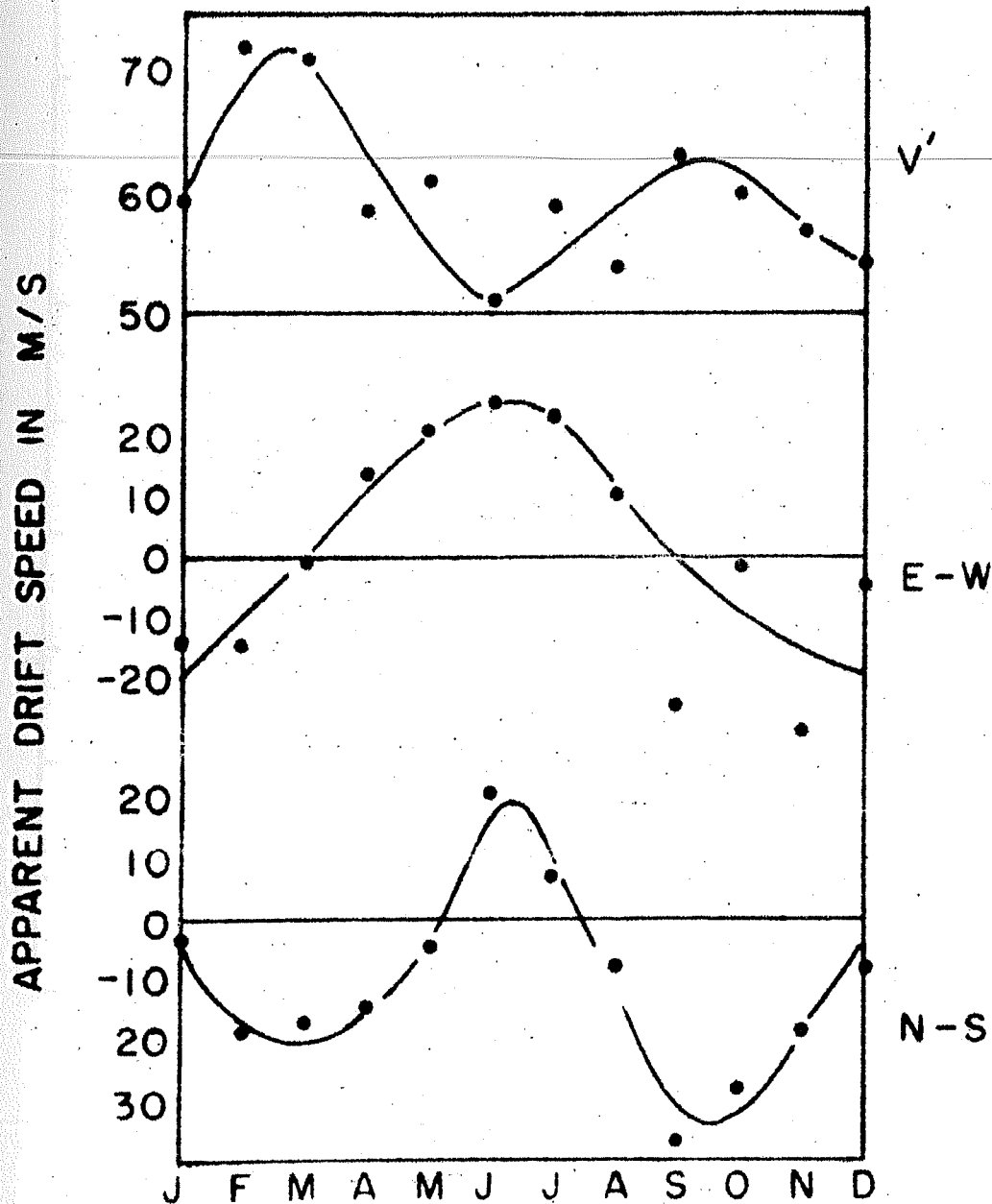


Fig.2.21 - Month to month variation of midday values of the apparent drift speed V' and its component V'_{E-W} and V'_{N-S} at Ahmedabad (E-region) averaged over the period 1970-75.

AHMEDABAD

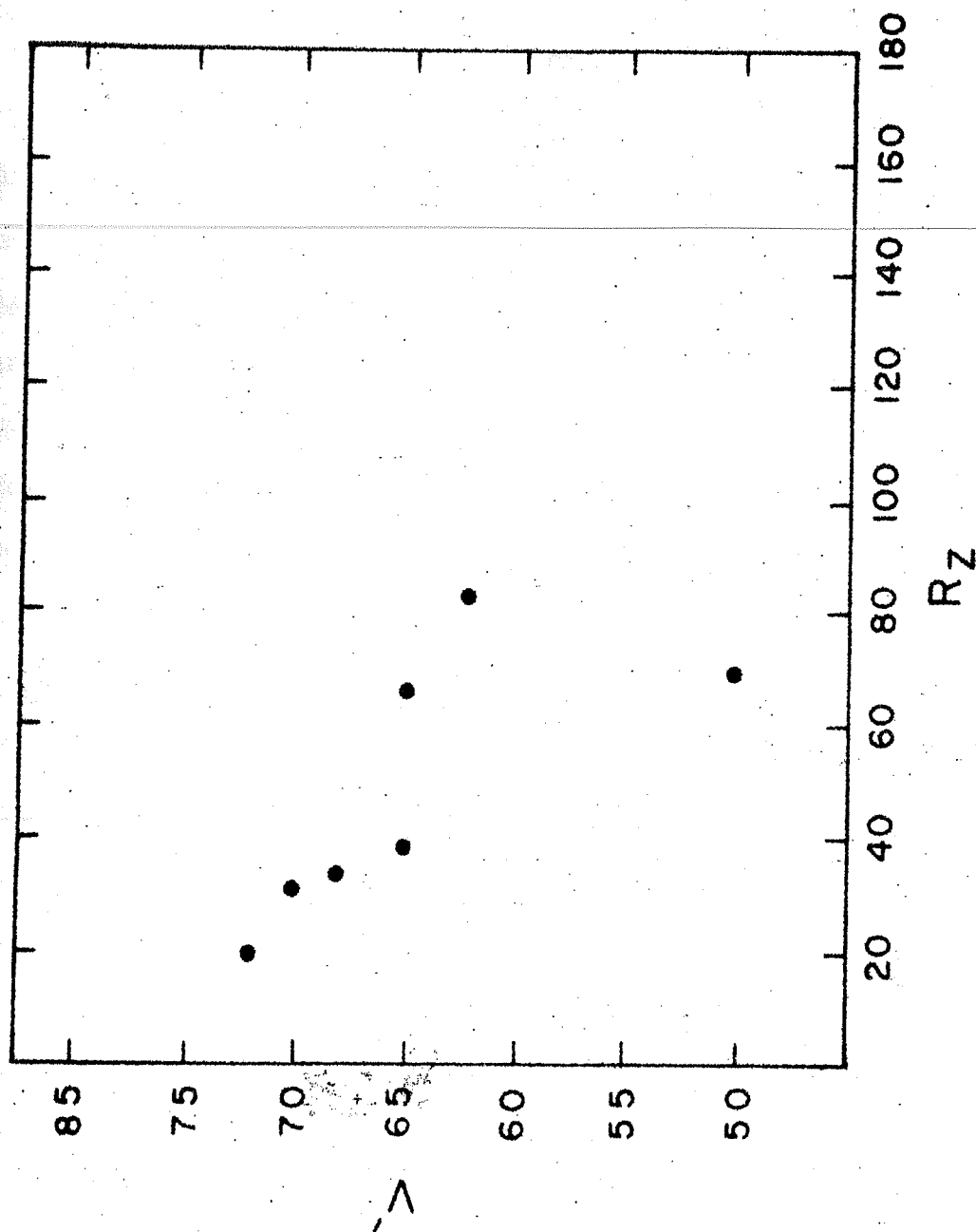


Fig.2.22 - Variations of apparent drift speed V' at Ahmedabad with respect to sunspot number R_z .

2.4.5 Magnetic activity effects in the E-region drifts

Here an attempt is made to find out magnetic activity effects in the drifts. Midday (1100-1300 hrs LT) values of apparent drift speed in the entire period of five years (1970-75) have been grouped and plotted against values of geomagnetic K_p index (Fig.2.23). The number of observations have been marked at every point. The bars indicate the standard error in the mean values. A slight decrease is noticed in the mean drift speed at high K_p index values. The total drop is from 59 m/sec for $K_p = 0$ to 51 m/sec for $K_p=6$.

These results confirm the earlier findings by Kaushika (1969) who also reported similar decrease from the daytime observations during the period 1965-66. Significant decrease of E- and F-region drift speeds have been reported at equatorial stations, viz. at Thumba (Rastogi et al. 1971), Tiruchirapalli (Vyas et al. 1978) and at Ibadan (Skinner et al. 1963). Slight increase in the E-region drift speed at Waltair during IGY (Rao 1969), however is in contradiction to all these observations and needs further examination from large set of data. Drift speeds are known to increase significantly at high latitudes with increase of magnetic activity (Briggs and Spencer, 1954).

2.4.6 Interplanetary magnetic field effects in the E-region

There is enough evidence now that the interplanetary magnetic field (IMF) does influence the electric fields at low latitudes

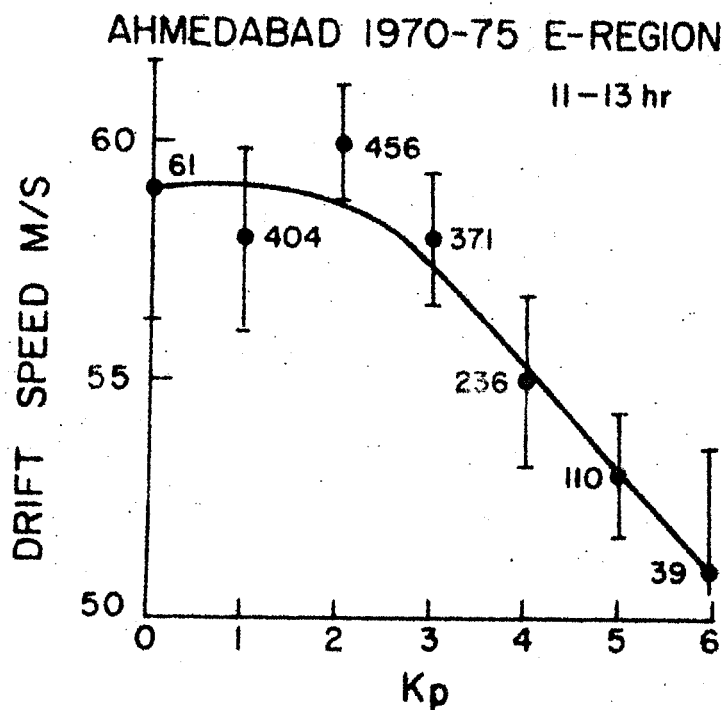


Fig.2.23 - Variation of the mean midday (1100-1300 hrs LT) drift speed with Kp for ionospheric E-region over Ahmedabad during the period 1970-75.

AHMEDABAD DRIFT E-REGION

1970 - 75

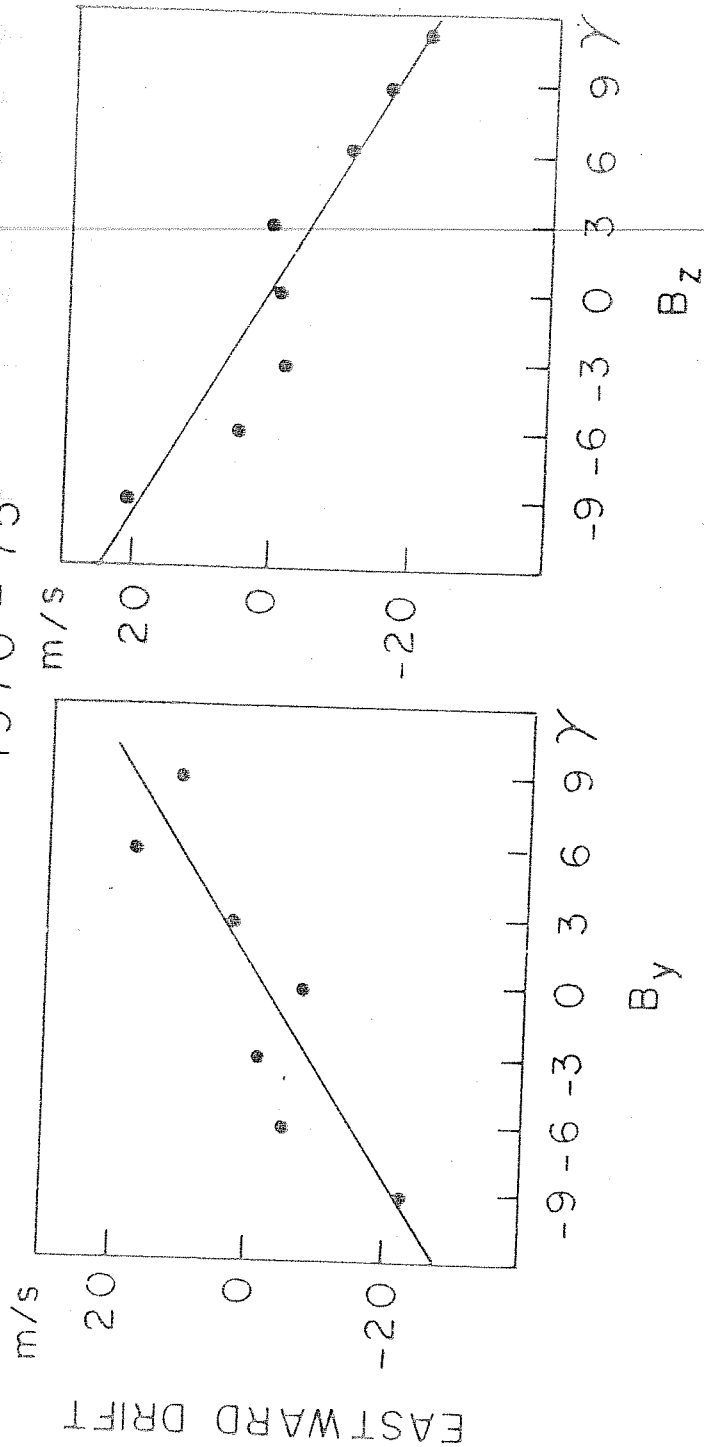


Fig.2.24 - Variations of the midday component of ionospheric E-region drift over Ahmedabad with B_z and B_y components of the interplanetary magnetic field.

(Matsushita and Balsley 1972, Rastogi and Chandra 1974, Vyas and Chandra 1979, Matsushita 1977, Galperin et al. 1978). There have been observed effects in the geomagnetic field variations at middle and low latitudes also (Matsushita 1977). Vyas et al. (1981) have examined in detail the relationship between the B_y and B_z components of IMF with the horizontal E and F region drifts at an equatorial station Tiruchirapalli. Recently Mithilesh et al. (1981) have studied IMF with horizontal E region drift at Udaipur (dip 36°N) and Ahmedabad. They have noticed decrease in the eastward drift with the increase in B_z component. To investigate the effects of the IMF parameters in the E-region drifts at low latitudes away from equator an attempt is made to examine the good series of ionospheric E-region drift data at Ahmedabad for the period 1970-75 and corresponding B_z and B_y values. Since electric fields will be primarily responsible for the E-W movement of the irregularities only this component is studied. Midday (11-13 hr LT) values of the eastward component of drift have been grouped according to the B_z or B_y value and the mean drift component has been plotted as a function of B_y or B_z . These are shown in Fig.2.24.

The mean eastward drift component of the velocity decreases linearly with the northward component of IMF, being 20 m/sec for B_z value of -9γ and about -20 m/sec for B_z value of 9γ . This result is consistent with the observed effect noted at the equatorial stations of Thumba (Rastogi and Chandra 1974) and

Tiruchirapalli (Vyas and Chandra 1979) and at low latitudes (Mithilesh et al. 1981). The rate of variation per \sqrt{V} however is smaller than those noted for equatorial stations. The variation of the mean eastward component of the velocity with B_y component is also linear. However, it shows an increase in the eastward velocity with increasing B_y component of IMF. The mean eastward component being about -20 m/s for B_y value of $-9\sqrt{V}$ and about 20 m/s for B_y value of $9\sqrt{V}$. This variation is opposite to the variation observed in the equatorial region (Vyas and Chandra 1979). These results give evidence to the IMF effects at low latitudes and further studies are needed to examine the correlation between the drifts and other ionospheric parameters with IMF fluctuations. Of more relevance would be to find the effects at different latitudes so that clear picture emerges about the possible physical mechanisms for the coupling between magnetosphere and ionosphere at low latitudes.

2.4.7 Lunar tides in the E-region drifts

Lunar tides in the ionospheric drifts have been studied at only a few stations, viz., Cambridge (Phillips 1952), Ottawa (Chapman 1953), Waltair (Ramanna and Rao 1962), Thumba (Misra 1973). One basic difficulty in obtaining lunar tidal oscillations is that the magnitude of lunar tidal oscillations is very small and therefore an extensive set of data is required for obtaining significant results. The long series of daytime drift speed

data (1970-75) has been used to study lunar tides.

Midday (1100-1300 hr LT) values of apparent drift speed over the entire period have been grouped into three seasons, winter (November to February), equinoxes (March, April, Sept. and Oct.) and summer (May to Aug.). Data on magnetically disturbed days have been excluded. The drift speeds in each season are grouped according to the lunar age \backslash at local noon and mean drift speeds at each lunar age computed. Plots of the mean drift speeds with lunar age \backslash at local noon for different seasons are shown in Fig.2.25 where the curves for the lunar age of 12 to 23 for depicting the lunar semimonthly tides. The lines drawn are the first harmonic values.

Amplitude of about 3 m/sec ~~is~~ noted during each of the season, the maximum occurring at about 05 lunar age for winter and equinoxes and at about 07 lunar age for summer. Misra (1973) had noted semimonthly oscillations in the E-region drifts at Thumba with amplitudes ranging from 6 m/sec to 9 m/sec with maximum around 04 lunar age. Lunar tidal studies in the geomagnetic H component at equatorial latitudes show similar maximum around 0300-0400 hr lunar age (Rastogi 1963,1965). The phases of the lunar semi-monthly oscillations at Thumba and Ahmedabad (except summer) occur at nearly same lunar age. Lunar barometric pressure oscillations at ground reported (Chapman and Westfold 1956) show nearly similar phase values for latitudes from Trivandrum to Tokyo.

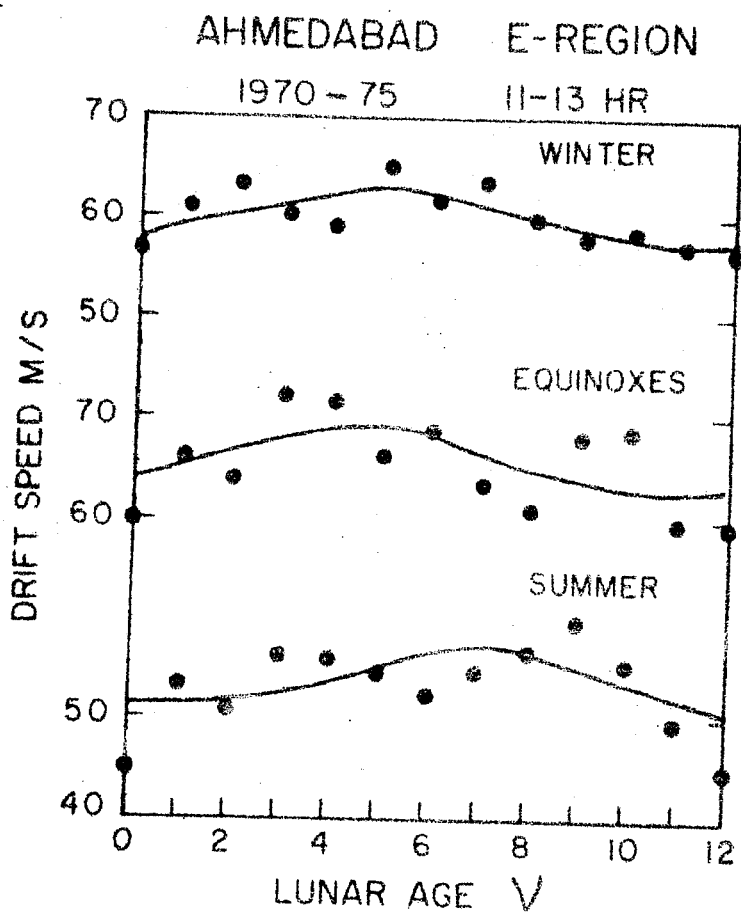


Fig.2.25 - Lunar tides in the midday E-region drift speed at Ahmedabad for different seasons of the period 1970-75.

2.4.8 Drifts at times of sporadic E

Based on the ionosonde observations at Ahmedabad we have separated drift speeds during E and Es layer reflections. A plot of eastward component of drift during winter and summer is shown in Fig.2.26. The average hourly values of the eastward drift vary between 20 m/sec and 40 m/sec directed towards west for E layer during the winter. However, the values for Es layer vary between 0 and 20 m/sec directed towards west. Thus on an average the drifts in the Es layer are about 25 m/sec less than those in the E layer. During summer the eastward component for E layer echoes varies between 0 and 20 m/sec, directed towards east. For Es echoes the values vary between 20 m/sec and 30 m/sec directed towards east. Thus there is again a change upto 20 m/sec in the average hourly values of eastward component. Thus it is concluded that the zonal component is clearly towards eastward wherever Es layer is present. This implies that an eastward drift is more favourable for the generation of Es.

AHMEDABAD 1970-75

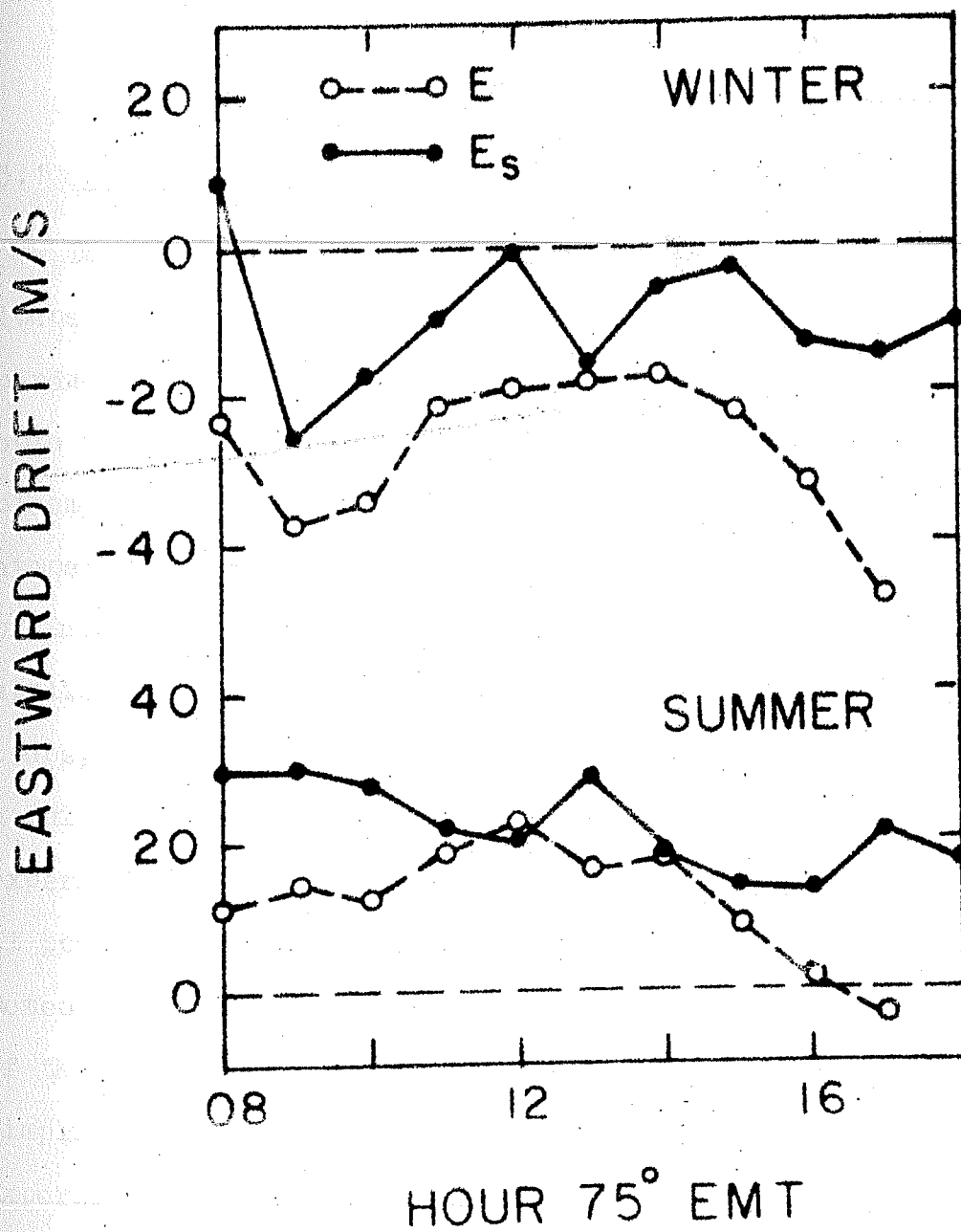


Fig.2.26 - Average daily variation of the eastward drift shown separately for E-layer echoes and Es echoes recorded at Ahmedabad for winter and summer seasons.

CHAPTER - III

E-REGION DRIFTS AT OTHER LATITUDES - CIRCULATION PATTERN

3.1 Introduction

The theoretical and experimental study of motions in the ionosphere has wide scope for further investigations. The parameters of the velocity field of neutral macroscopic motions both for the neutral and ionized component of the ionospheric plasma turned out to be necessary for constructing the upper atmosphere models for investigating the physical nature of interaction of different ionospheric layers and solving the applied problems. The view point adopted in the first decades of ionospheric studies, that upper atmosphere is meteorologically a quiet region, turned out to be erroneous. The development of experimental methods of measurements of ionospheric motions made it possible to lay down the foundations of the ionospheric meteorology. The theoretical pictures of the dynamical region of the upper atmosphere have until now suffered from over simplification and unrealistic assumptions. For this reason, experimental data is the basis for our considerations of the problem so far. The complexity of the ionospheric irregularities and the strong changeability of dynamical regime have all made doubtful the presence of regular atmospheric motions at ionospheric levels. It was necessary to organise the measurements of ionospheric motions by the world-wide network of stations using

common program and similar methods. Methodological experiments were needed to reveal whether the most utilised and comparatively simple methods of measurements of ionospheric motions - the so-called method of closely spaced receivers or D_1 method - were physically representative, a global data synthesis was needed to prove the presence of a certain motion system in the E and F regions of the ionosphere to reveal space-time variations of the prevailing winds and drifts as well as of the basic tidal components.

The horizontal drift measurements in the ionosphere have been reported earlier at high latitudes (Briggs and Spencer 1954) and at equatorial latitudes (Skinner et al. 1963, Deshpande and Rastogi 1966, Chandra 1977, Vyas and Chandra 1979). Systematic pattern of drift is emerged out at the equator, the drifts being westward during daytime and eastward during nighttime for all the seasons. E-region drifts at a low latitude station such as Ahmedabad are found to be highly seasonal dependent, being westward during winter and eastward during summer with a change over during equinoxes. Therefore it was felt necessary to investigate the global circulation pattern in the ionospheric E-region. Hence it was decided to examine drift data at a few more stations at different latitudes. For this drift data at Yamagawa (dip 43°N) for 1964 published by Science Council of Japan and at Sibizmir (dip 72°N) for the period 1970-75 published

by Academy of Sciences, USSR are analysed. The results separately obtained for both stations have been published. Reprint & preprint are attached at the end of this chapter for details. The inter-comparison of these results was done with the results at Ahmedabad (dip 34°N), Thumba (dip 0.6°S) and Tiruchirapalli (dip 4.8°N).

3.2 Circulation Pattern

A comparative study of the E-region drifts at Ahmedabad, Yamagawa and Sibizmir showed zonal flow westward during winter and eastward during summer. At the equatorial stations Thumba and Tiruchirapalli the drifts have been reported westward during day and eastward during night for all seasons (Deshpande and Rastogi 1966, Chandra 1977, Vyas and Chandra 1979). But there is decrease of about 50 m/s in the westward drift during day in the summer (Vyas et al. 1978). Thus circulation pattern is of a global scale (barring electrojet latitudes where electric fields determine the drift pattern).

3.3 Solar activity dependence of drifts at equatorial, low and high latitudes

Fig.3.1 shows dependence of drift speed on solar activity. The mean drift speeds at Thumba, Ahmedabad and Sibizmir are found to decrease with the increased solar activity. Possible reason for this may be higher ion neutral collisions during periods of high solar activity. Linear regression of R_z and drift showed increase in sensitivity with the increase of latitude.

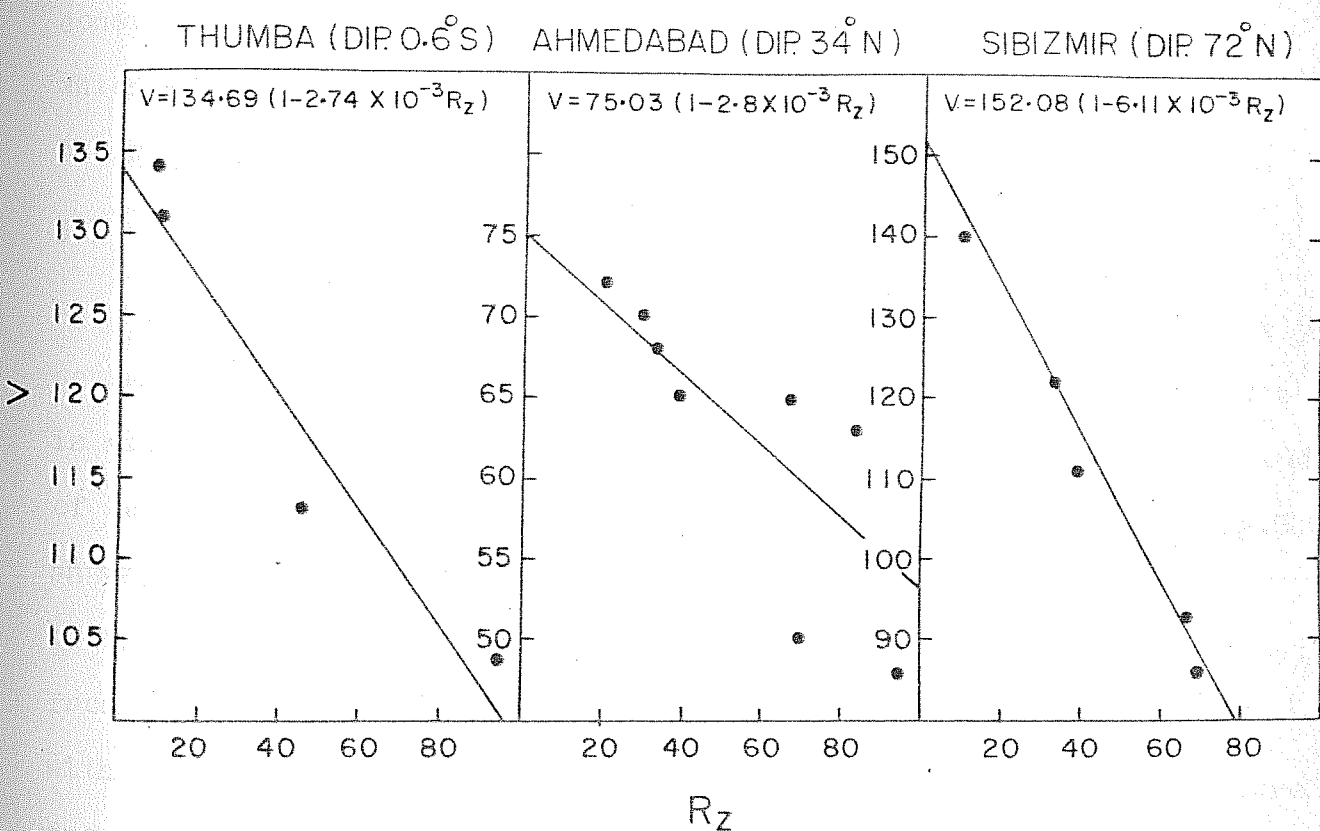


Fig.3.1 - Variation of drift speed with respect to sunspot number R_z at Thumba (dip 0.6°S), Ahmedabad (dip 34°N) and Sibizmir (dip 72°N).

3.4 Magnetic activity and drifts at different latitudes

A systematic change is observed in the magnetic activity effects in mean drift speeds. Drift speed increases with the increase of magnetic activity at high latitudes and decreases at the equator with a change over at about 40° dip. This is consistent with the electric field of magnetospheric origin which is opposite to the Sq field at equator but in phase at the high latitudes.

3.5 Lunar tidal effects in drifts at different latitudes

Lunar tidal effects in drift at all stations showed primarily semimonthly oscillations. The phase of semi-monthly oscillations is almost same at all stations. There is increase in the amplitude of lunar semimonthly oscillation in the equatorial region. Fig.3.2 shows amplitude of the semi-monthly oscillation as a function of dip (the amplitude of Yamagawa is excluded as it is derived from data of only one year). These results are consistent with the recent results of the lunar tides observed in temperature from satellite measurements which indicate increase in amplitude of semi-monthly oscillation in temperature at equator and constant phase at all latitudes for 80 km altitude (Schlapp 1981).

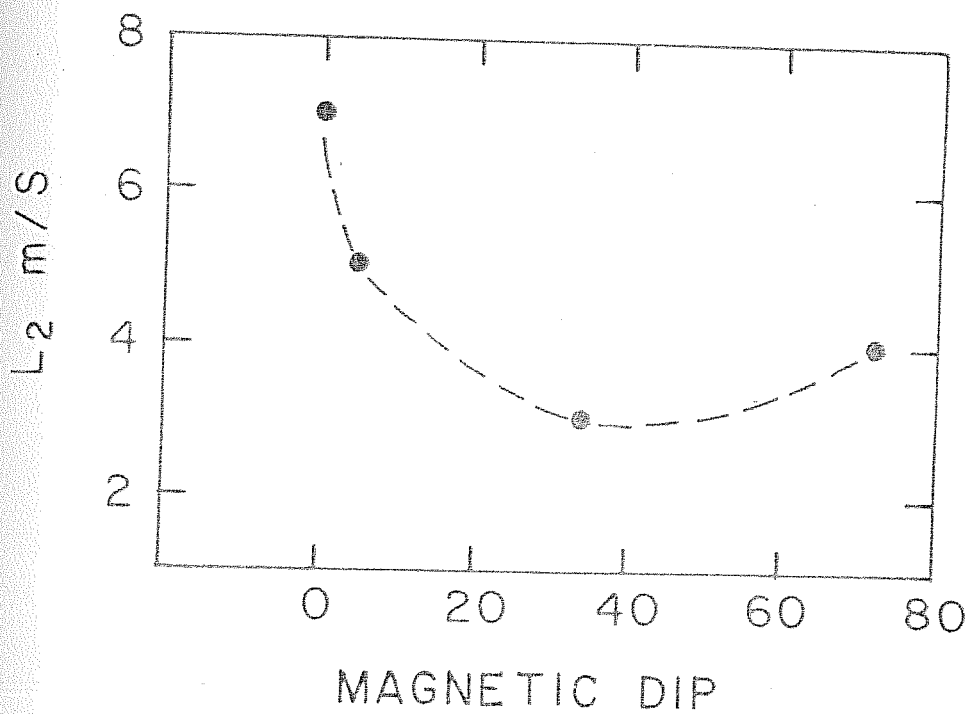


Fig.3.2 - Variation of lunar tidal amplitude L_2 with respect to magnetic dip.

Ionospheric *E*-Region Drifts at Yamagawa during IQSY

V. P. PATEL and H. CHANDRA

Physical Research Laboratory, Ahmedabad, India

(Received April 5, 1978; Revised January 9, 1979)

Ionospheric *E*-region drifts at Yamagawa are studied from the published

Ionospheric *E*-Region Drifts at Yamagawa during IQSY

V. P. PATEL and H. CHANDRA

Physical Research Laboratory, Ahmedabad, India

(Received April 5, 1978; Revised January 9, 1979)

Ionospheric *E*-region drifts at Yamagawa are studied from the published results for the year 1964. The drift pattern is highly seasonally dependent and similar to that reported for tropical latitude stations of Ahmedabad and Udaipur. Small changes due to lunar effects have been noted to occur.

1. Introduction

Horizontal drift measurements in ionosphere by MITRA's (1949) spaced receiver technique have been studied in detail at high latitudes (BRIGGS and SPENCER, 1954) as well as at equatorial latitudes (SKINNER *et al.*, 1963; RASTOGI *et al.*, 1972). Detailed investigations at tropical latitudes have been rather limited. From an extensive series of observations at Ahmedabad during the period 1970–1975 it was reported that there is a consistent pattern in the *E*-region drifts which is highly seasonally dependent with a drift towards west during winter and towards east during summer, the changeover occurring during the equinoxes (CHANDRA *et al.*, 1977; PATEL *et al.*, 1978). A comparative study of the ionospheric *E*-region drifts from simultaneous measurements at two close stations at tropical latitudes viz. Ahmedabad (dip 34°N) and Udaipur (dip 36°N) separated by about 200 km has shown a remarkable agreement which suggests a large scale circulation pattern at *E*-region heights (RASTOGI *et al.*, 1978). To investigate further the ionospheric *E*-region drift system it was decided to examine data at a few more stations at different latitudes. The published drift results at Yamagawa (dip 43°N) for the year 1964 (SCIENCE COUNCIL OF JAPAN, 1966) were looked into with this view and the broad features are reported in this paper. Measurements for the daytime hours 0600 to 1800 hr LT) only are considered and three seasons namely winter (Nov. to Feb.), equinoxes (Mar., Apr., Sept., and Oct.) and summer (May to Aug.) have been separated out.

2. Results

Entire data have been grouped into different seasons and histograms of

the percentage occurrence of drift direction for each season as well as for the complete year are shown in Fig. 1. The predominant direction is towards south-west during winter and towards east during equinoxes and summer. Thus the zonal component is mainly towards west during winter and mainly

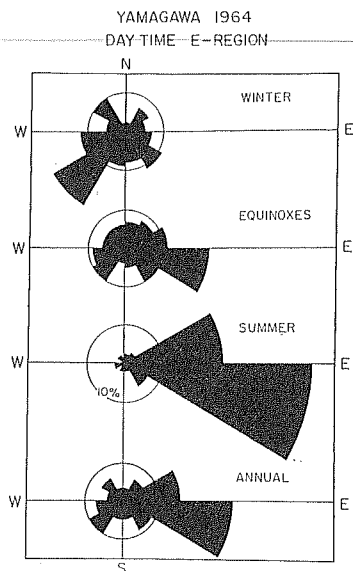


Fig. 1. Histograms of percentage occurrence of the drift direction at Yamagawa for each season as well as for the complete year 1964.

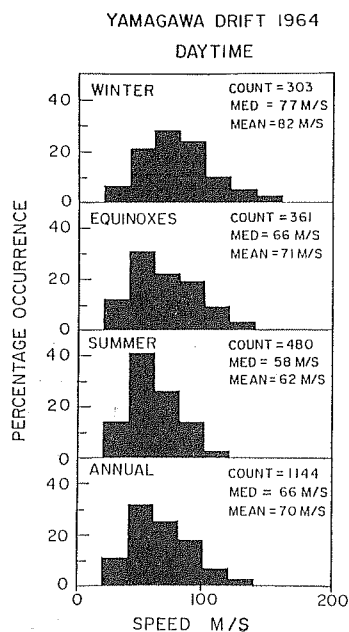


Fig. 2. Histograms of percentage occurrence of the drift speed at Yamagawa for each season as well as for the complete year 1964.

towards east during equinoxes and summer. Meridional component is mainly towards south during each of the seasons. GROVES (1969) has constructed a model to represent the wind profiles at different latitudes and at different altitudes derived from the rocket measurements and a few meteor wind measurements. The features noted here agree closely with those contained in GROVES's model.

Similar histograms for the drift speed are shown in Fig. 2. The number of observations, mean and median values are also shown in the figure. Drift speeds range from 20 m/s to 160 m/s during winter, 20 m/s to 140 m/s during equinoxes, and 20 m/s to 120 m/s during summer. The median values are 77 m/s, 66 m/s, and 58 m/s for the seasons winter, equinoxes and summer, respectively. These results are very similar to the *E*-region results at Ahmedabad during periods of similar sunspot activity viz. 1965–1966 (RASTOGI, 1969) and during 1973–1974 (PATEL *et al.*, 1978).

3. Daily Variations of the Drift Speed

To study daily variations of drift parameters hourly mean values of the apparent drift speed V' as well as eastward (V'_{E-W}) and northward (V'_{N-S}) components for each season and for whole of the year have been computed and are plotted in Fig. 3. The daily variations of the eastward component

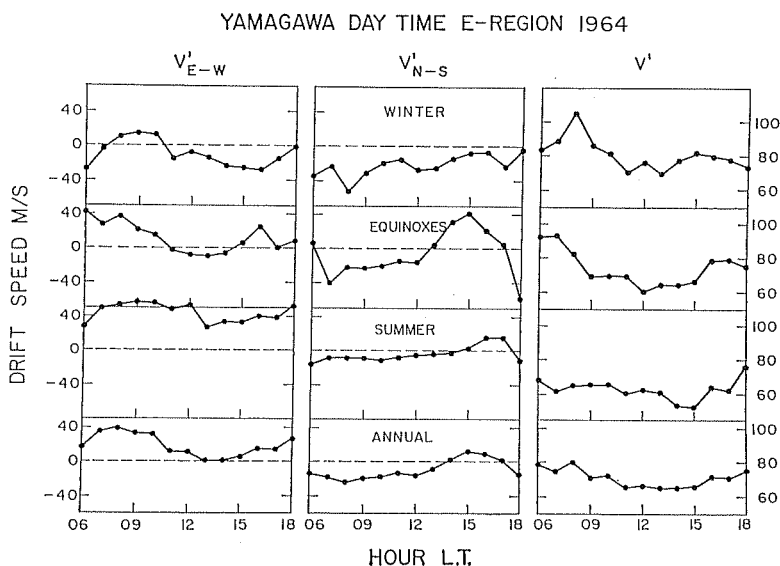


Fig. 3. Mean daily variation of the eastward drift speed (V'_{E-W}), northward drift speed (V'_{N-S}) and the apparent drift speed (V') at Yamagawa for each season as well as for the complete year 1964.

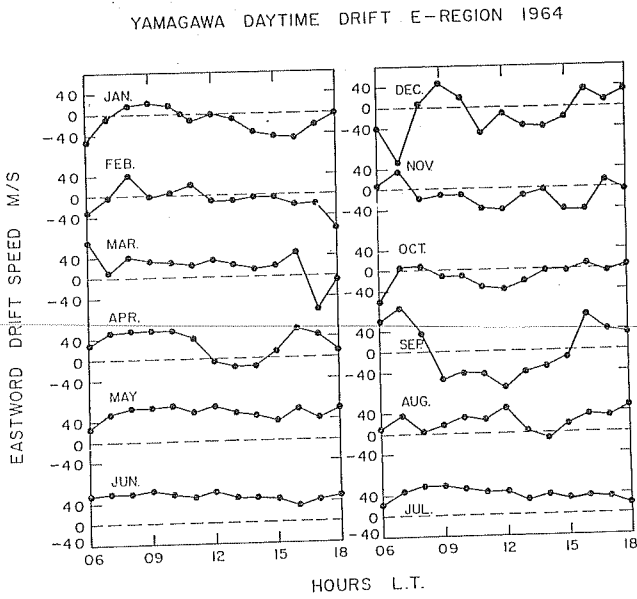


Fig. 4. Mean daily variation of eastward component of drift speed at Yamagawa for each month of the year 1964.

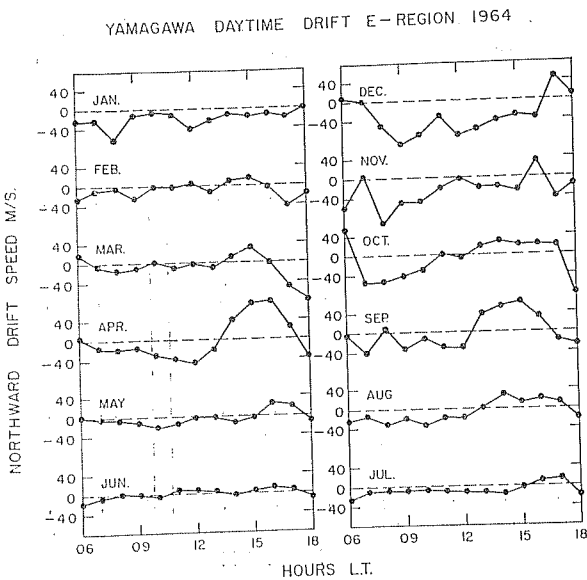


Fig. 5. Mean daily variation of northward component of drift speed at Yamagawa for each month of the year 1964.

are towards west during the winter (except in the morning hours) and towards east during the summer (except around noon) and the equinoxes. The northward component is towards south throughout the day during winter but during equinoxes and summer it is southward before noon and changes to northward in the afternoon hours. The minimum of the apparent drift speed is around noon during winter and equinoxes and fairly constant values are observed during summer season. The trend of these variations during winter and summer agrees very well with earlier IGY results at Yamagawa (SHIMAZAKI, 1959). Month to month changes in the daily variation pattern of the eastward and northward component can be clearly seen in Figs. 4 and 5 which show the mean daily variations for each month.

4. Seasonal Variation of the Noon Drift Speed

To study the seasonal variation of the midday drift pattern the monthly mean values of the eastward and northward components for noon (1100–1300 hr LT) have been plotted for each month (Fig. 6). There is an annual variation of the eastward component with the drift being westward during winter months and eastward during summer. The change over occurs during Feb.–March and September. Comparing these with the similar results obtained for Ahmedabad (PATEL *et al.*, 1978) there is very good similarity in the seasonal variation of E–W component at the two latitudes. The seasonal variation of the midday northward component is not very consistent but shows southward drift throughout the year.

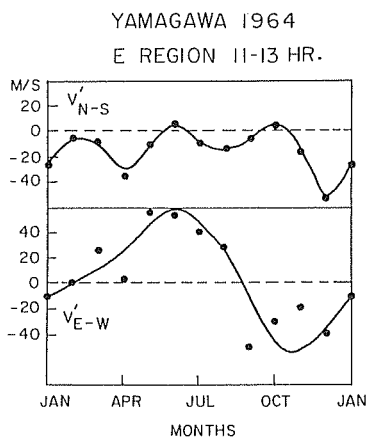


Fig. 6. Month to month variation of midday (1100–1300 hr LT) values of the eastward (V'_{E-W}) and northward (V'_{N-S}) components of the drift speed at Yamagawa for the year 1964.

5. Variation with Magnetic Activity

To investigate the effect of magnetic activity on *E*-region drift speeds at Yamagawa midday (1100–1300 hr LT) values have been grouped into three different K_p ranges i.e. low (less than 2), medium (between 2 and 4) and high (greater than 4) and the plot of mean drift speed with K_p is shown in Fig. 7. No significant change in the mean drift speed is noted with increasing K_p index. The small variation seen is within the error limit and hence not significant statistically. From a much larger number of observations at Yamagawa during the period 1966–1971, OHYAMA *et al.* (1974) reported no change in the daytime drift speed with K_p . However, the drift speed at Ahmedabad decreases slightly with increasing K_p (KAUSHIKA, 1969; PATEL and CHANDRA, 1978).

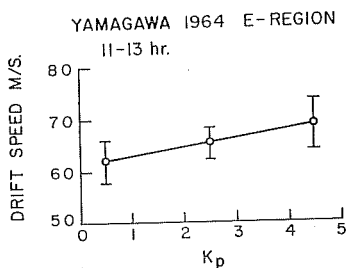


Fig. 7. Variation of mean midday drift speed with magnetic activity index K_p .

6. Lunar Tides in Drift

Lunar tides in the drifts have been studied only at a few locations. These are the high latitude stations, Cambridge (PHILLIPS, 1952) and Ottawa (CHAPMAN, 1953), the low latitude station, Waltair (RAMANA and RAO, 1962) and the equatorial station, Thumba (MISRA, 1973). To examine lunar influence in the *E*-region drifts at Yamagawa midday (1100–1300 hr LT) values of the drift speeds were grouped into different lunar ages. Since the variation of the mean drift speed with the lunar age showed a purely semimonthly oscillation we have averaged the curve for 0–11 lunar age with that for 12–23 lunar age. The resulting mean curve is shown in Fig. 8 which shows a semimonthly oscillation with an amplitude of about 9 m/s and a maximum occurring at 3.6 lunar age. This agrees very well with the results of MISRA (1973) for Thumba who reported a semimonthly oscillation of about 7 m/s with maximum at about 5 lunar age obtained from a large series of data covering the period 1964–1969. It seems, therefore, that the lunar oscillations in the *E*-region drifts at Thumba and Yamagawa have same phase.

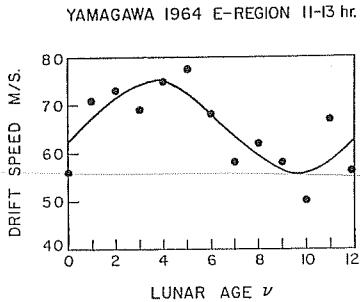


Fig. 8. Variation of mean midday (1100-1300 hr LT) drift speed with lunar age.

The lunar barometric pressure oscillations on ground at Trivandrum and Tokyo (CHAPMAN and WESTEOLD, 1956) also show nearly similar phase.

7. Conclusions

The results presented lead to following conclusions:

- 1) The drift pattern at Yamagawa is highly seasonal dependent, with zonal winds towards west during winter and towards east during summer, similar to that obtained at other tropical stations like Ahmedabad and Udaipur. The meridional component is mainly towards south. These features match with GROVES (1969) model.
- 2) There is no significant change in the midday drift speed with increasing magnetic activity.
- 3) Lunar semimonthly oscillations of about 9 m/s are noted in the midday drift speed.

REFERENCES

- BRIGGS, B. H. and M. SPENCER, Horizontal movement in the ionosphere, *Rep. Prog. Phys.*, **17**, 245-280, 1954.
- CHANDRA, H., V. P. PATEL, and R. G. RASTOGI, Ionospheric E-region drift pattern at low-latitudes, *Curr. Sci.*, **46**(20), 835-836, 1977.
- CHAPMAN, J. H., Study of the winds in the ionosphere by radio methods, *Canadian J. Phys.*, **31**, 120-131, 1953.
- CHAPMAN, S. and K. C. WESTFOLD, A comparison of the annual mean solar and lunar atmospheric tides in barometric pressure, as regards their world-wide distribution of amplitude and phase, *J. Atmos. Terr. Phys.*, **8**, 1-23, 1956.
- GROVES, G. V., Wind models from 60 to 130 km altitude for different months and latitudes, *J. Br. Interplanet. Soc.*, **22**, 285-307, 1969.
- KAUSHIKA, N. D., Effect of magnetic activity on drifts and anisotropy of E-region ionisation irregularities over Ahmedabad, *J. Atmos. Terr. Phys.*, **39**, 1127-1129, 1969.
- MISRA, R. K., Lunar tidal oscillations in the horizontal ionospheric drift at the equator, *Planet. Space Sci.*, **21**, 1109-1114, 1973.

- MITRA, S. N., A radio method of measuring winds in the ionosphere, *Proc. Inst. Elect. Engrs.*, **96**(III), 441-446, 1949.
- OHYAMA, H., S. NAKASHIMA, M. NAKAJIMA, and S. KAMIZHIKIRYO, Observation of ionospheric drifts at Yamagawa, *Rev. Rad. Res. Lab.*, **20**, 419-438, 1974 (in Japanese).
- PATEL, V. P., H. CHANDRA, and R. G. RASTOGI, Ionospheric drift measurement over Ahmedabad during 1970-75, *Ind. J. Rad. Space Phys.*, **7**, 22-25, 1978.
- PATEL, V. P. and H. CHANDRA, Magnetic activity effects in the *E*-region drifts at Ahmedabad, *Ind. J. Rad. Space Phys.*, **7**, 263, 1978.
- PHILLIPS, G. J., Measurements of winds in ionosphere, *J. Atmos. Terr. Phys.*, **2**, 141-154, 1952.
- RAMANA, K. V. V. and B. R. RAO, Lunar daily variation of horizontal drifts in the ionosphere at Waltair, *J. Atmos. Terr. Phys.*, **24**, 220-221, 1962.
- RASTOGI, R. G., Studies of horizontal drift in the *E*-region of the ionosphere at Ahmedabad, *J. Inst. Telecom. Engrs.*, **15**, 216-226, 1969.
- RASTOGI, R. G., H. CHANDRA, and R. K. MISRA, Features of the ionospheric drift over the magnetic equator, *Space Research*, **12**, 983-992, 1972.
- RASTOGI, R. G., H. CHANDRA, K. P. SINGHAL, R. K. RAI, A. V. JANVE, and V. KUMAR, Simultaneous investigation of ionospheric *E*-region irregularities at low-latitude stations by spaced receiver technique, *Ind. J. Rad. Space Phys.*, **7**, 6-8, 1978.
- SCIENCE COUNCIL OF JAPAN, IQSY data of ionospheric drift at Yamagawa in Japan, 1966.
- SHIMAZAKI, T., World-wide measurements of horizontal ionospheric drifts, *Rep. Ionos. Space Res.*, Japan, **13**, 21-47, 1959.
- SKINNER, N. J., A. J. LYON, and R. W. WRIGHT, Ionospheric drift measurements in the equatorial region, *Proc. Int. Conf. on Ionos.*, edited by A. C. Stickland, pp. 301-309, Phy. Soc. London, 1963.

PREPRINT

Ionospheric E-region Drifts at Sibizmir during 1970-75

V.P. Patel* and H. Chandra
Physical Research Laboratory
Ahmedabad-380009
India

Abstract

Features of the ionospheric E-region drifts during daytime hours at Sibizmir (dip 72°N) are described, based on the spaced receiver data for the years 1970-75 published by the Academy of Sciences, USSR. The drift pattern is highly seasonal dependent with westward drift during winter and eastward drift during summer. The magnitude of the drift velocity decreases with increasing sunspot number but increases with increasing magnetic activity (K_p). Small changes due to lunar tidal effects have also been isolated.

V.P. Patel and H. Chandra
Physical Research Laboratory
Ahmedabad-380009
India

*Department of Physics, M.G. Science Institute, Ahmedabad 380009.

1. Introduction

Ionospheric drifts obtained by the most widely used radio methods viz. the closely spaced receiver method of Mitra (1949) at a worldwide network of stations provides a unique method of understanding the general atmospheric circulation at ionospheric heights. The observations in the equatorial stations at Thumba (Rastogi et al., 1972) and Tiruchirapalli (Vyas and Chandra, 1979) show westward drift during daytime hours which is well correlated with the equatorial electrojet. At a low latitude station Ahmedabad (dip 34°N), drift is highly seasonal dependent which is westward during winter and eastward during summer (Chandra et al. 1977, Patel et al.. 1978). Similar trend was also noticed at Yamagawa (dip 43°N) reported by Patel and Chandra (1980). To investigate the drift pattern at a higher latitude station, we have examined the apparent velocities at Sibilizmir (dip 72°N) in USSR for the years 1970-75 obtained from the similar radar method of analysis, which was published by the Academy of Sciences, USSR, and the main results are reported here. Measurements during the daytime hours (0600- to 1800 hr) only are considered and divided into three seasons namely winter (Nov. to Feb.), equinoxes (March, April, Sept. and Oct) and summer (May to Aug.).

2. Results

The entire data for the period 1970-75 has been grouped into three seasons and the histograms of the percentage occurrence of the drift direction for each season and for the annual are shown in Fig.1. The drift direction is predominantly in the S-W quadrant during winter and in N-E quadrant during summer. During equinoxes directions are little more towards east than towards west. Thus the zonal component is mainly towards west during winter and mainly towards east during summer and equinoxes. This is not in agreement with Grove's model (1969), Meridional component is mainly towards south during winter and towards north during summer.

Similar histograms for the drift speed are shown in Fig.2. The number of observations alongwith mean and median values are also shown in the figure. The drift speeds range between 20 m/s to about 240 m/s with median values of 109 m/s, 86 m/s and 84 m/s respectively for winter, equinoxes and summer. The trend of the seasonal variation is similar to the one observed for Yamagawa (Patel and Chandra, 1980) and for Ahmedabad (Patel et al. 1978) with winter values higher than other seasons. Higher neutral-ion collisions in summer could be possible reason for this behaviour.

SIBIZMIR
1970 - 1975

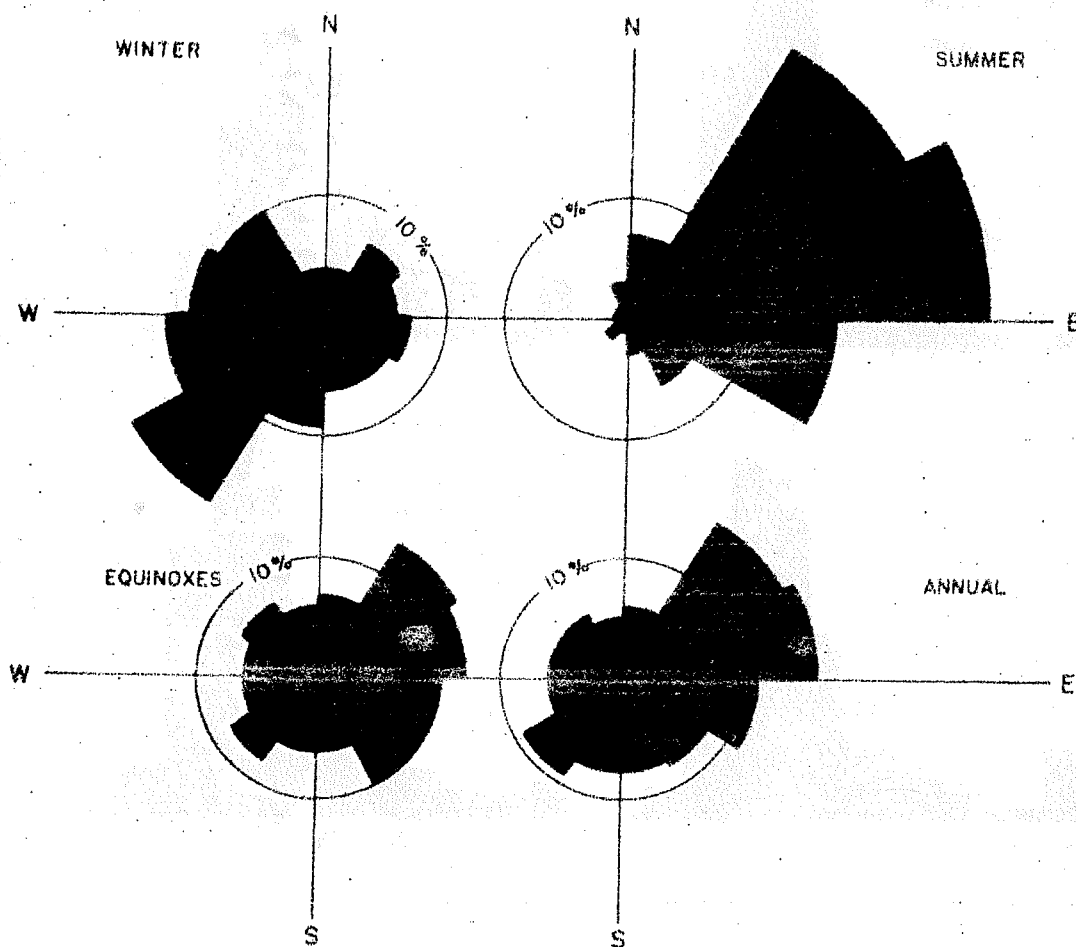


Fig.1 Seasonal mean and annual mean histograms of percentage occurrence of E-region drift direction at Sibizmir averaged for the years 1970-75.

SIBIZMIR
1970 - 1975

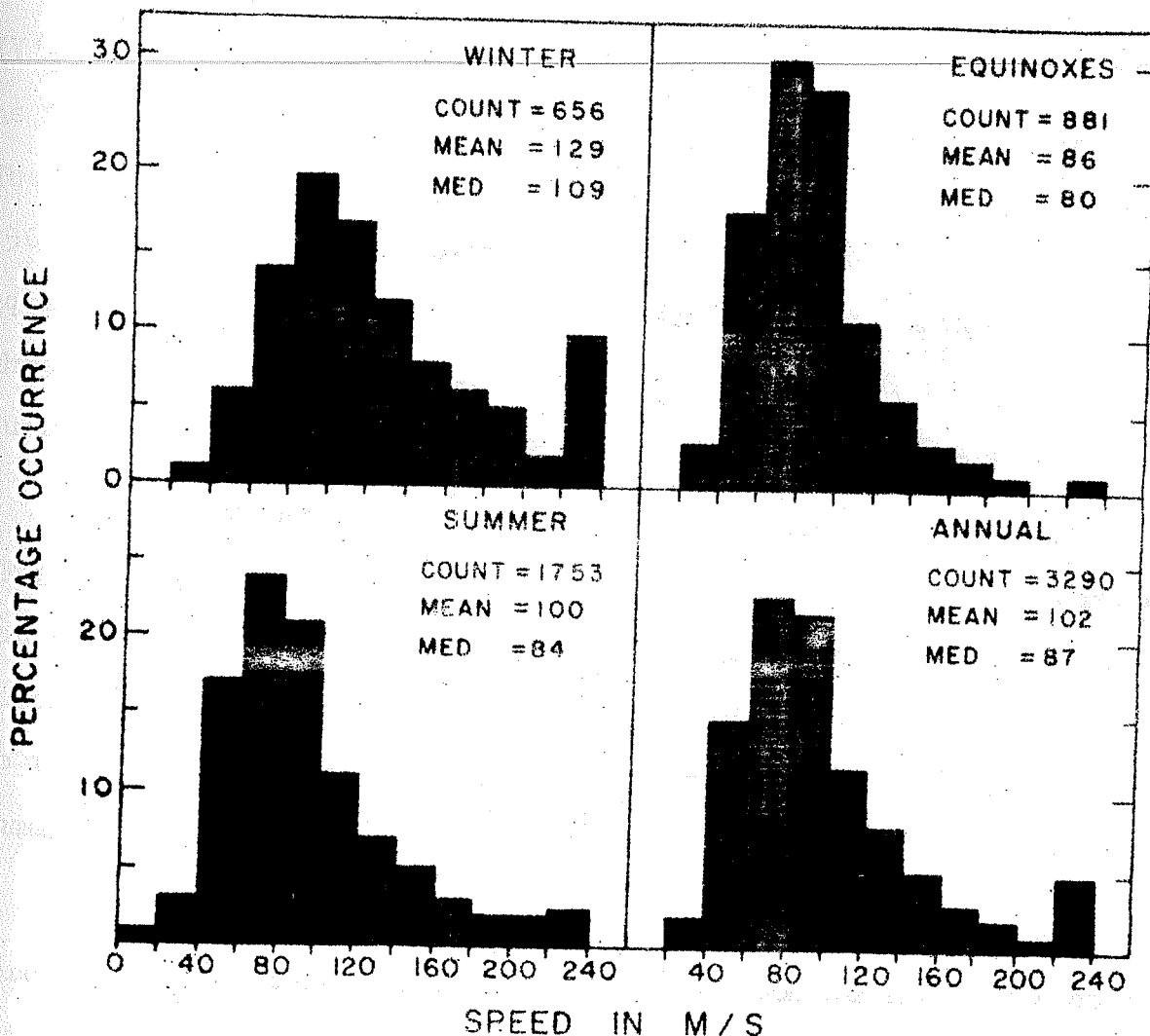


Fig.2 Seasonal mean and annual mean histograms of percentage occurrence of the E-region drift speed at Sibizmir averaged for the years 1970-75.

3. Daily and Seasonal Variations of the Drift Speed

To study the daily variations of drift parameters, hourly mean values of the apparent drift speed V' as well as the eastward (V'_{E-W}) and northward (V'_{N-S}) components for each season as well as for the annual have been computed and shown in Figs.3 to 5. The apparent drift speed (Fig.3) for winter vary between 110 m/s to 150 m/s with a suggestion of a peak around 09 hr. During equinoxes and summer the drift speeds are fairly uniform throughout the day with speeds ranging between 90 m/s to 110 m/s during equinoxes and between 80 m/s to 100 m/s during summer.

The daily variations of the eastwest component of drift (Fig.4) shows westward drift during winter except in the morning and evening hours. During equinoxes it is eastward in the morning and evening hours but westward during the hours from 11 to 15. The drift is however eastward throughout the day in summer.

The N-S component (Fig.5) shows southward drift in the forenoon and northward drift in the afternoon during the winter and equinoxes. During summer, however, it is northward both in the morning and evening hours with midday values either very small or southward.

The seasonal behaviour of zonal component reveals that zonal component is mainly westward during winter and eastward

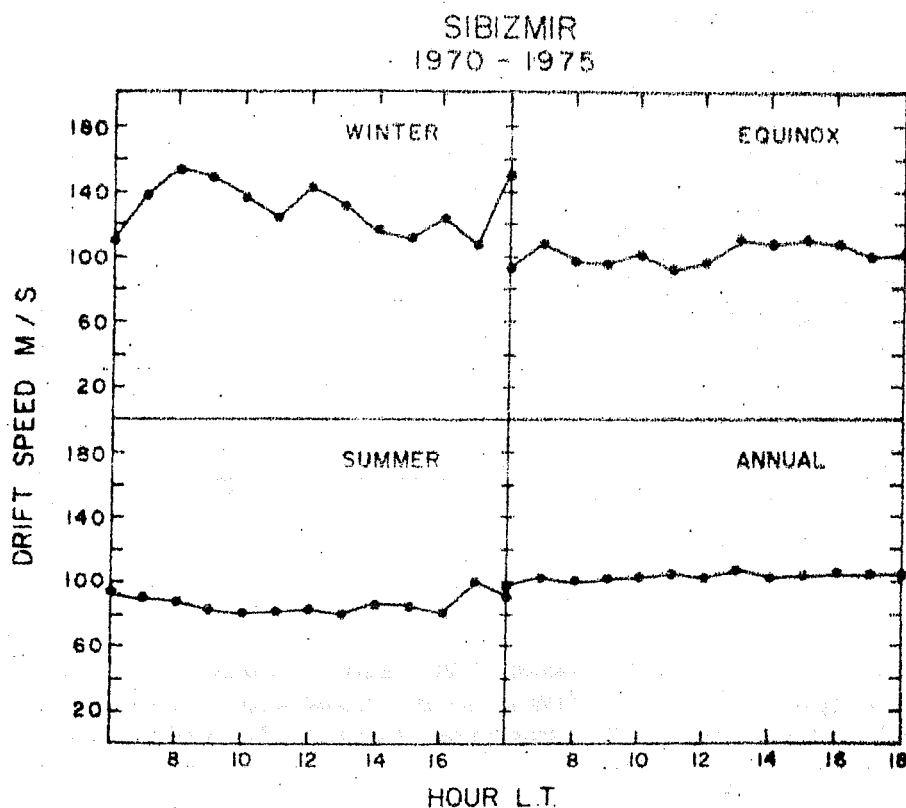


Fig.3 Seasonal mean and annual mean daily variations of the E-region drift speed over Sibizmir averaged for the years 1970-75.

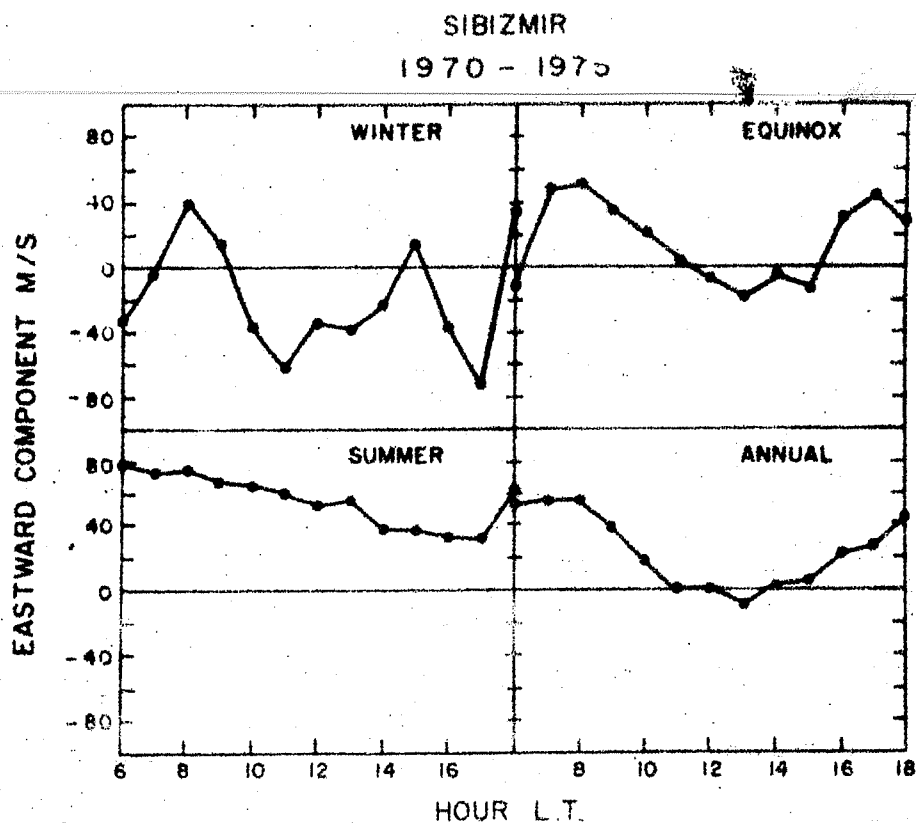


Fig.4 Seasonal mean and annual mean daily variations of the eastward component of the E region drift speed over Sibizmir averaged for the years 1970-75.

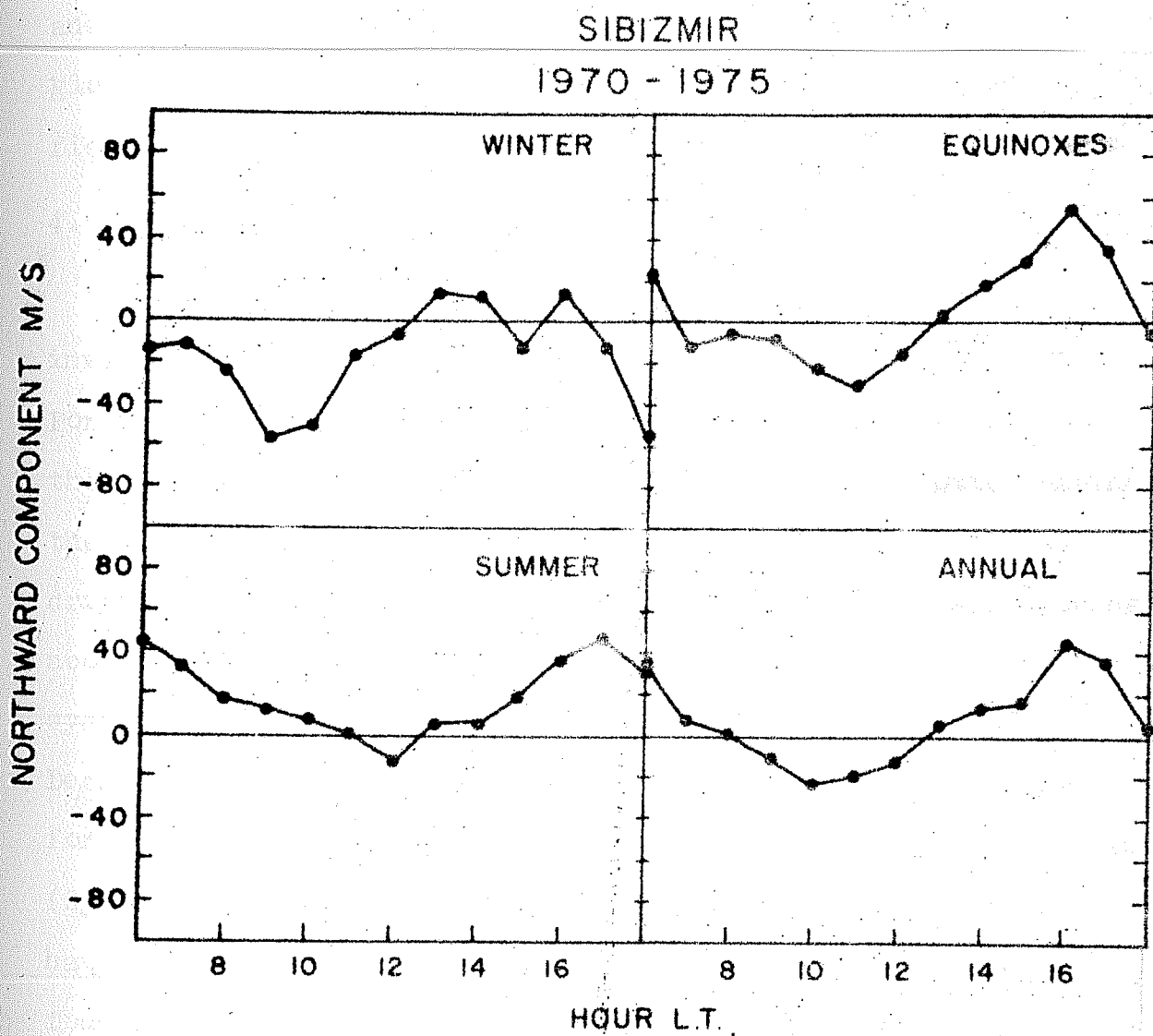


Fig.5 Seasonal mean and annual mean daily variations of the northward component of the E region drift speed over Sibizmir averaged for the years 1970-75.

during summer with a change over during equinoxes. Thus the behaviour of the zonal and meridional component is similar to those reported earlier for Yamagawa (Patel and Chandra, 1980) and Ahmedabad (Chandra et al. 1977). This appears to be a global phenomenon barring electrojet region where electric fields (polarisation fields) govern the drifts.

4. Solar Cycle Variation

The long series of data at Sibizmir has permitted to investigate the solar cycle variation of the drift speed. For this the annual mean values for each year averaged over the entire daytime hours have been computed and plotted against the yearly mean sunspot number in Fig.6. A decrease of the drift speed with R_z is clearly noticed. The drift speed being about 140 m/s for R_z values of about 15 and then dropping systematically to about 90 m/s at R_z values of about 80. Decrease in the drift velocities have been reported earlier for equatorial stations, Thumba (Misra et al. 1971) and Ibadan (Oyinloye and Onalaja 1977). All available data at Ahmedabad have been examined and similar decrease with R_z has been found (unpublished). The decrease of the drift speed with sunspot could again be possibly explained by higher values of ion neutral collisions during high sunspot numbers.

5. Variation with Magnetic Activity

To investigate the effect of magnetic activity on E-region drift speed at Sibizmir, midday (1100-1300 hr LT) values of drift

SIBIZMIR

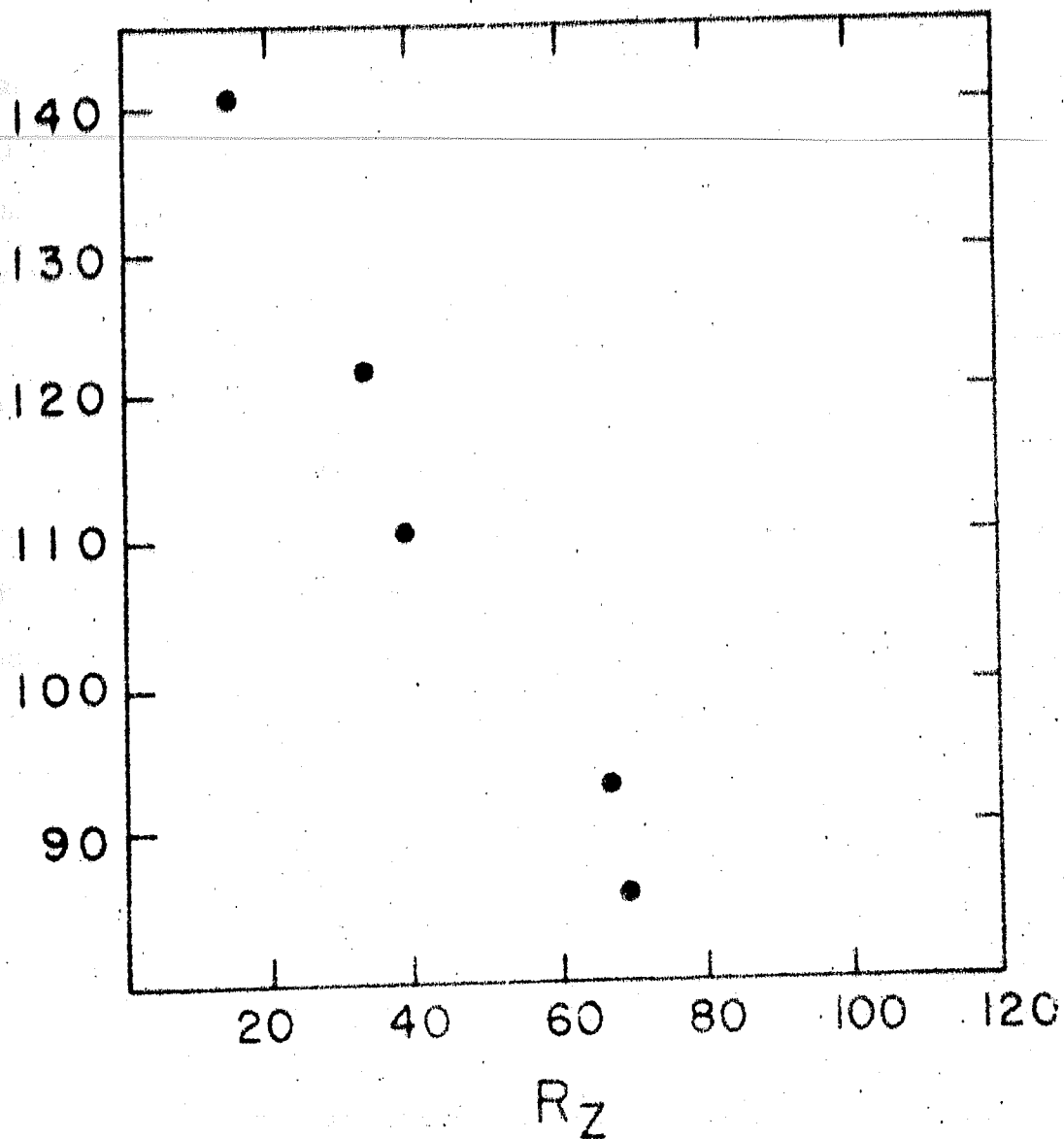


Fig.6 Variations of mean E region drift speed over Sibizmir with the sunspot number R_z .

speed have been grouped according to different K_p values and the plot of mean drift speed with K_p is shown in Fig.7. The vertical bars represent the standard errors in the mean. An increase in the drift speed with K_p is clear with speeds being about 95 m/s for $K_p = 0$ and increasing to about 125 m/s for $M_p = 6$. To examine the latitude dependence, the earlier results have been taken for Yamagawa (Patel and Chandra 1980), Ahmedabad (Patel and Chandra 1978) Thumba (Rastogi et al. 1971) and Tiruchirapalli (Vyas et al. 1978) and reported in Fig.8. Large increase at Sibizmir, a small increase at Yamagawa, slight decrease at Ahmedabad and large decreases at Tiruchirapalli and Thumba are noted. Thus there is a systematic change in the magnetic activity effects on E-region drifts from equator to high latitudes. These are consistent with the direction of the electric field of magnetospheric origin which are opposite to the Sq field near equator but in phase at auroral region.

6. Lunar Tides Effects

The lunar tidal effects have been studied by grouping the midday (1100-1300 hr LT) values of drift speeds into different lunar ages and then finding the variation of the mean drift speed with lunar age. The resulting lunar monthly oscillation obtained is shown in Fig.9. Semimonthly wave with an amplitude of about 6 m/s and maximum occurring at about lunar age of 5 hr is seen. This agrees well with the results obtained earlier at Thumba where semimonthly oscillations of about 7 m/s and maximum of about 5 lunar age was obtained

SIBIZMIR

1970 - 1975

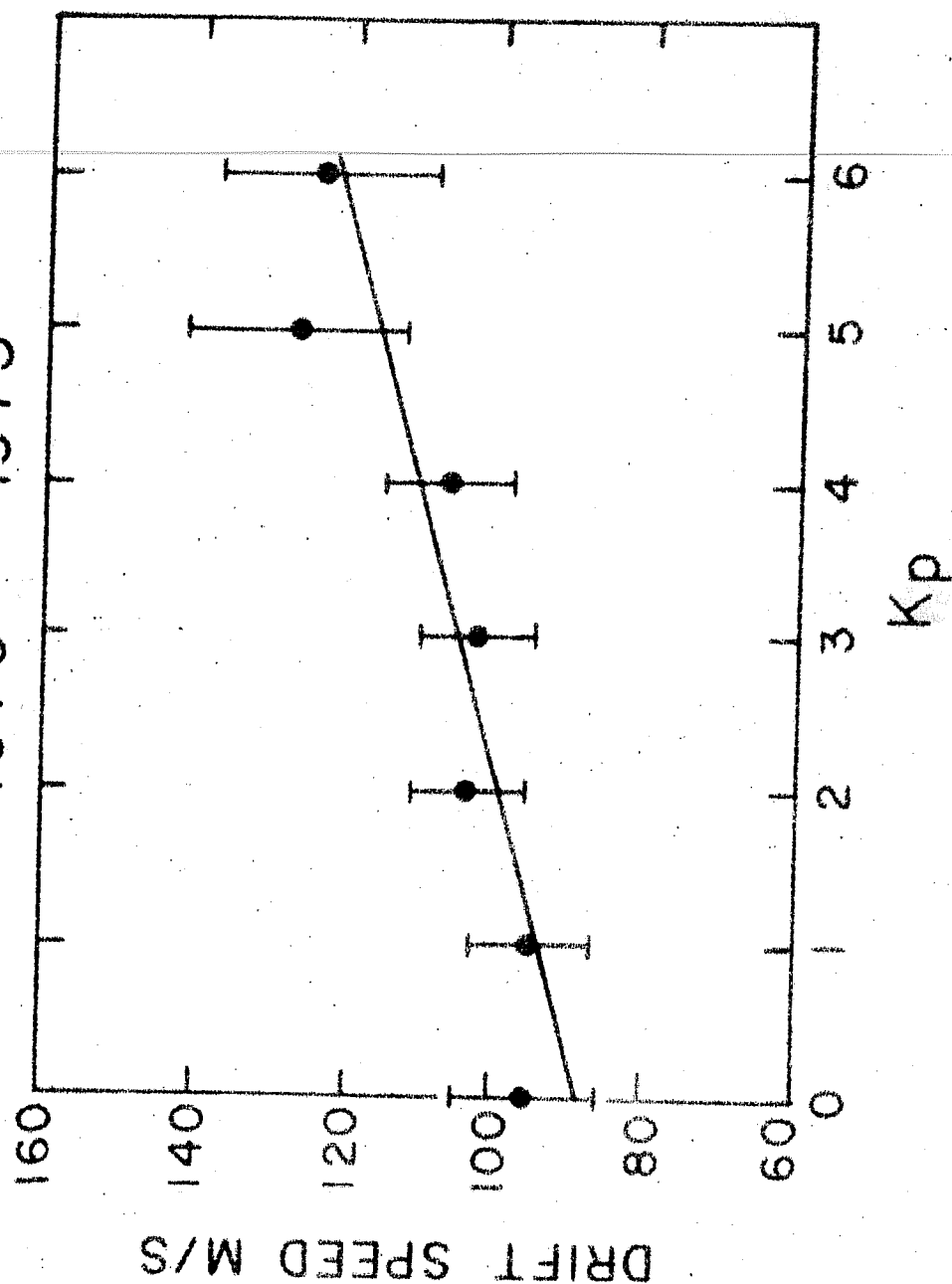


Fig.7 Variation of mean midday E-region drift speed over Sibizmir with magnetic activity index K_p .

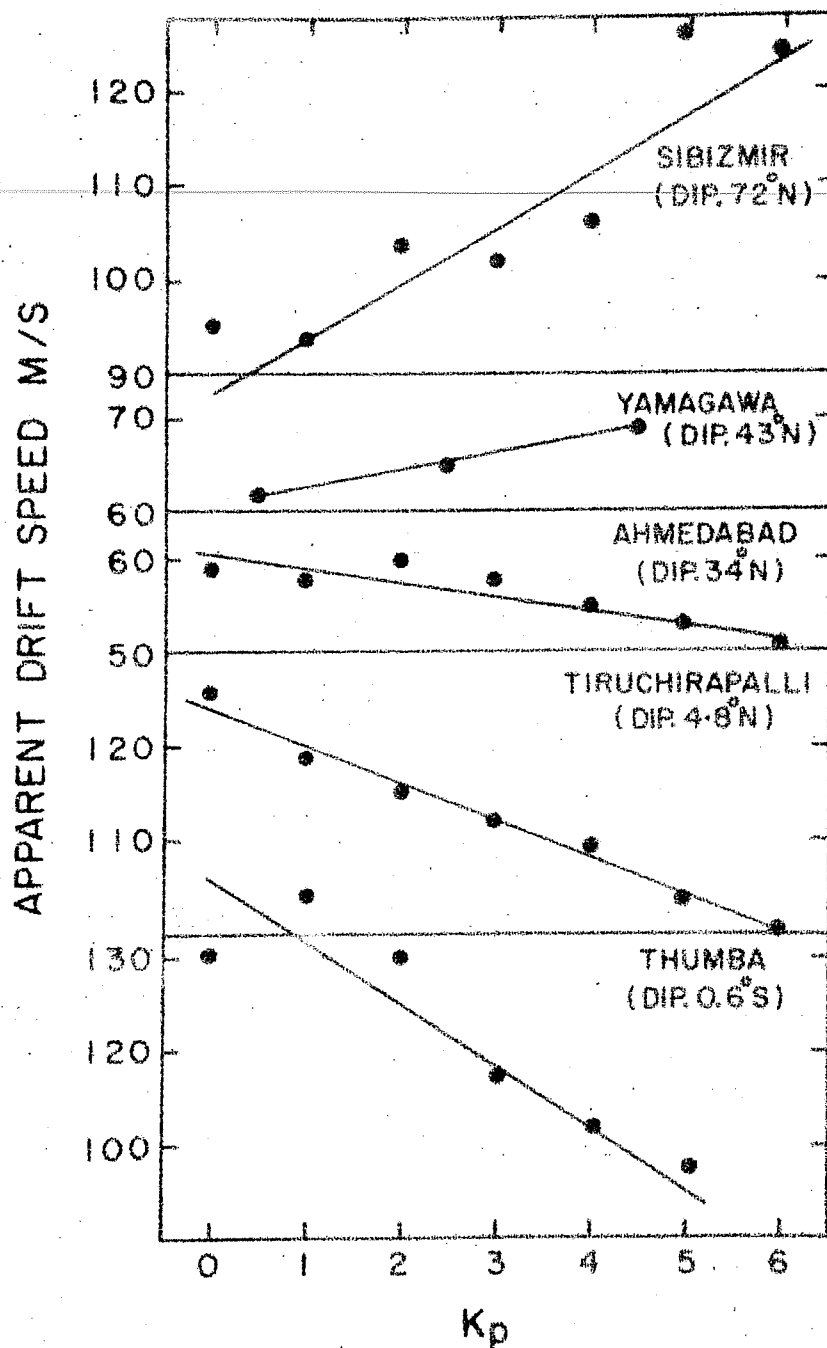


Fig.8 Variation of mean midday E region drift speed over different stations with magnetic activity index K_p .

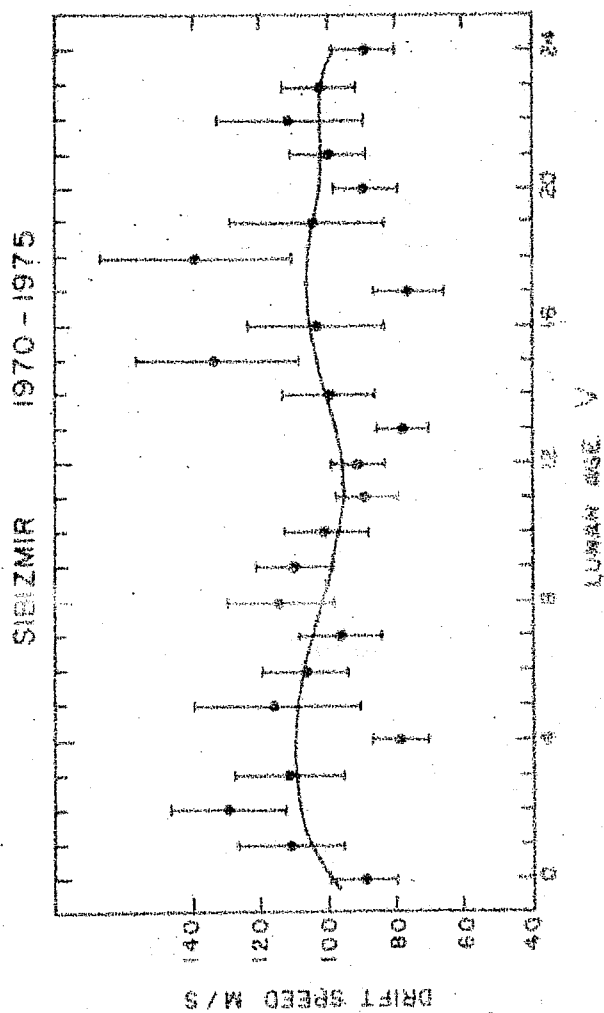


Fig.9 Variation of mean midday E-region drift speed over Sibizmir with lunar age.

(Misra, 1973). At Yamagawa the maximum was found around 4 lunar age even though the data was only for one year period (Patel and Chandra, 1980). It appears that the phase of the lunar oscillations is same at all the latitudes.

7. Conclusions

- 1) The drift pattern at Sibizmir showing westward zonal flow during winter and eastward zonal flow during summer is similar to those obtained at Yamagawa and Ahmedabad. Thus the circulation pattern is of a global scale (barring electrojet latitudes where electric fields determine the drift pattern).
- 2) The mean drift speeds are found to decrease with increasing sunspot number.
- 3) The mean drift speeds increase with increasing K_p value.
- 4) Lunar semi-monthly oscillations with an amplitude of about 6 m/s and maximum occurring at about 5 lunar age is clearly noticed.

Acknowledgements

Thanks are due to Suchita Desai and Chhaya Shah for computational assistance.

References

- Chandra H, V.P. Patel and R.G. Rastogi, Curr. Sci., 46(20) (1977), 835.
- Groves G.V., J. Br. Interplanet. Soc., 22 (1969), 285.
- Misra R.K., Planet. Space Sci., 21 (1973), 1109.
- Misra R.K., H. Chandra and R.G. Rastogi, J. Geomag. Geoelectr., 23 (1971), 181.
- Mitra S.N., Proc. Inst. Elect. Engrs., 96(III) (1949), 441.
- Patel V.P. and H. Chandra, Ind. J. Rad. Space Phys., 7 (1978), 263.
- Patel V.P. and H. Chandra, J. Geomag. Geoelectr., 32 (1980), 129.
- Patel V.P., H. Chandra and R.G. Rastogi, Ind. J. Rad. Space Phys., 7 (1978), 22.
- Rastogi R.G., H. Chandra and R.K. Misra, Nature, 233 (36) (1971), 13.
- Vyas G.D. and H. Chandra, "Ionospheric drift studies near equatorial electrojet region", Low Latitude Aeronomical Processes (Advances in Space Exploration), COSPAR Symp. Series, ed. By A.P. Mitra, 8 (in press), 1979.
- Vyas G.D., H. Chandra and R.G. Rastogi, Proc. Ind. Acad. Sci., 87A (1978), 215.

CHAPTER-IV

SOME ASPECTS OF THE GEOMAGNETIC VARIATIONS AT LOW LATITUDES

4.1 Quiet day variation of geomagnetic H-field at low latitudes- Solar and seasonal effects

4.1.1 Introduction

The study of solar daily variation of the geomagnetic components has attracted many workers since the beginning of this branch of science. The daily variation of the geomagnetic field has been attributed to the ionospheric dynamo currents (Schuster 1908, Chapman 1919). Significant seasonal variations are seen in the H field components and different sources have been suggested for these variations (Vestine 1954, McIntosh 1959, Price 1963, Currie 1966).

The geomagnetic data at low latitudes are of special importance because within a narrow belt of 4° - 5° centred over the magnetic dip equator, the daily variation of geomagnetic H-field on quiet days i.e. $rSq(H)$ is abnormally large compared with other places in the low latitude region. This large $Sq(H)$ variation is due to large ionospheric currents in the dynamo region over the dip equator and has been named as "Equatorial electrojet" by Chapman (1951). This enhanced current arises due to the special geometry of the geomagnetic field at the dip equator which causes a vertical Hall polarisation field resulting in the P field components and different sources have been suggested for these variations (Vestine 1954, McIntosh 1959,

in enhanced conductivity in the eastward direction. During night-time the currents are very weak due to the depletion of E-layer ionisation (Chapman and Raja Rao 1965). Another way of representing the low latitude ionospheric currents is to consider the currents to be due to the normal Sq current extrapolated from the tropical latitudes over which is added another current system which is entirely due to electrojet (Forbush and Casaverde 1961, Onwumechilli 1967).

At low latitudes the horizontal component is the major part of the total field and the vertical component is significantly affected by the geological and geographic surroundings of the station. Therefore, we have studied only the horizontal component of the geomagnetic field. Recently, Rastogi and Iyer (1976) have studied quiet day variation of geomagnetic field at low latitudes including IGY-IGC period.

One of the oldest and foremost geomagnetic observatories at low latitudes is at Huancayo, Peru operating since 1922. In this study we have examined quiet day solar variation of geomagnetic H field at equatorial station Huancayo for the period 1922-73 and comparison of these results is made with those at Trivandrum, an equatorial station in the Indian region where the mean magnetic field is high as compared to that in American region.

4.1.2 Data analysis and results

The mean daily variation of the H field at Huancayo averaged for the five international quiet days of each month from 1922 to

1973 was computed applying non-cyclic correction. The corrected annual mean daily curves for each of the years were subjected to harmonic analysis to obtain the amplitudes and times of maximum of the diurnal and semidiurnal components. Fig.4.1 shows the year to year variation of zurich sunspot number (R_z), amplitudes (a_1, a_2) as well as times of maximum (T_1, T_2) of the diurnal and semidiurnal components of daily variation. It is clearly seen that both the amplitudes a_1 and a_2 very faithfully follow the variation of R_z . The time of maximum of diurnal component also varies between 1100 and 1200 LT with the variation of R_z . The daily maximum occurs close to noon during high sunspot years but it is at an hour earlier during low sunspot years.

The time of maximum of semi-diurnal component shows variation with R_z for certain epochs while for others it is not very evident. Further the range of the variation is relatively smaller for T_2 than for T_1 .

The dependence on R_z of amplitudes and phases of the harmonic components were computed using the following equations:

$$a = A_0 + A_1 R_z + A_2 R_z^2 \quad (4.1)$$

$$\text{and } T = A'_0 + A'_1 R_z + A'_2 R_z^2 \quad (4.2)$$

Fig.4.2 shows graphically the variation of these factors with sunspot number together with the best-fitting quadratic line. It is seen that the harmonic amplitude increases linearly

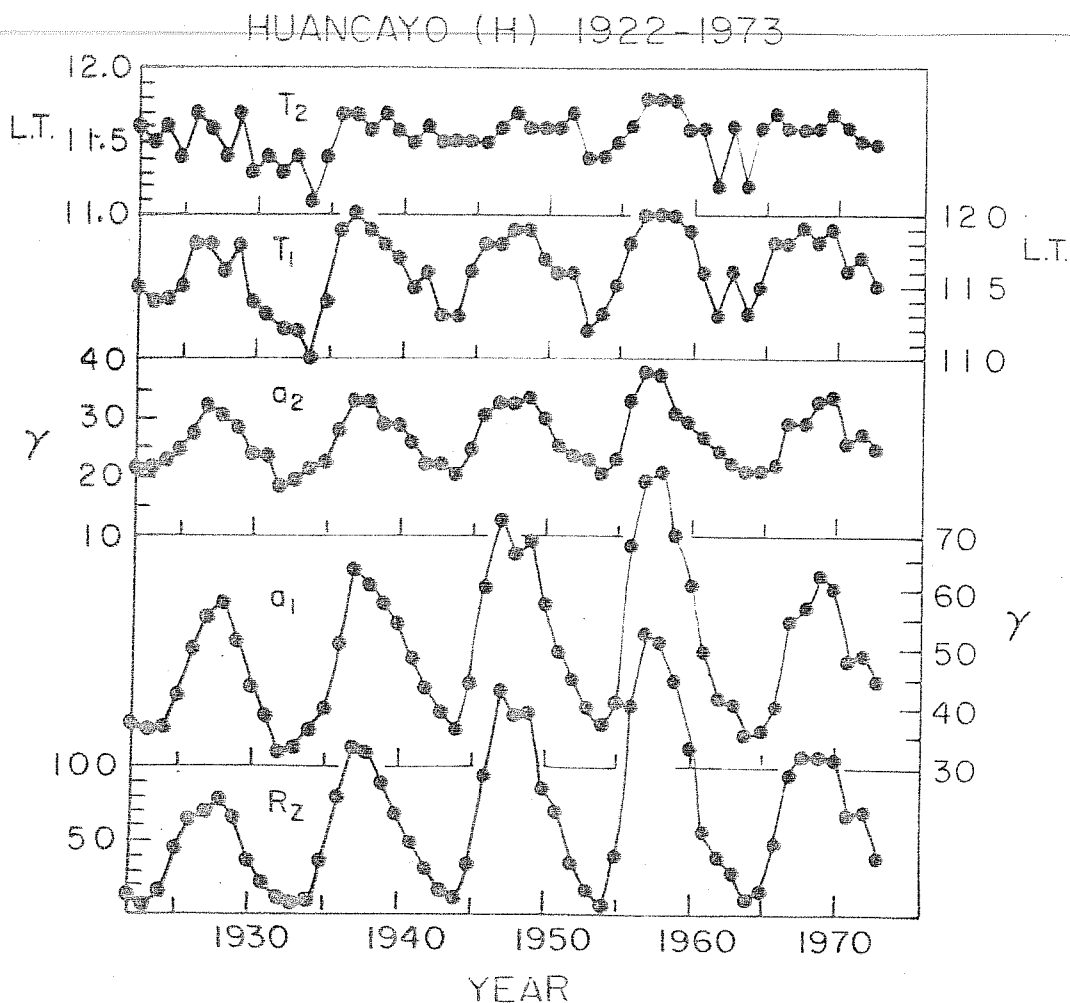


Fig.4.1 - Solar cycle variation of amplitude of first harmonic (a_1) and second harmonic (a_2) and the time of maximum of first and second harmonics (T_1) and (T_2) of yearly mean $Sq(H)$ at Huancayo. R_z is the annual average zurich sunspot number.

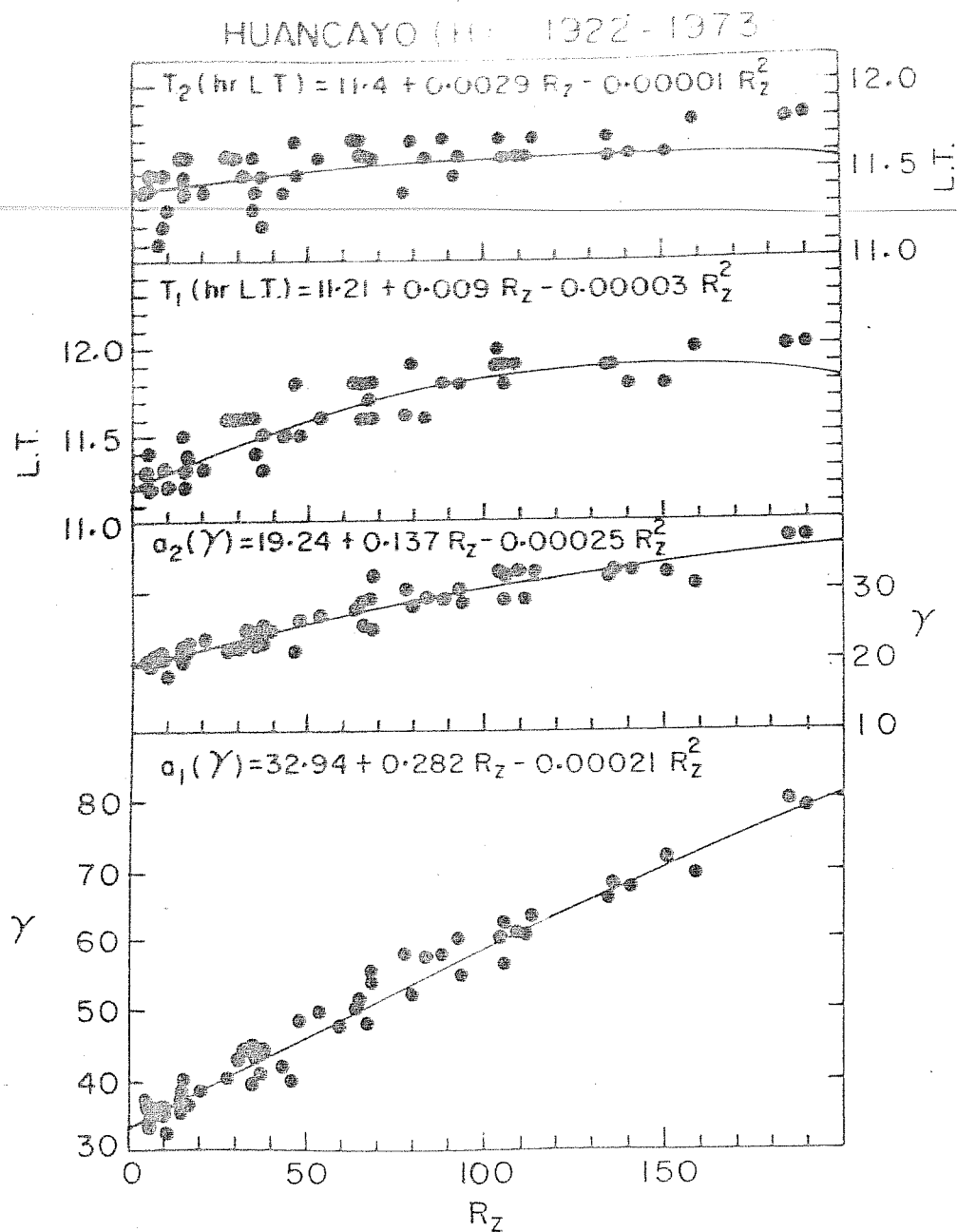


Fig.4.2 - Variation of amplitudes a_1 and a_2 and time of maximum T_1 and T_2 of first and second harmonics of the yearly mean daily variation with annual average zurich sunspot numbers.

with sunspot number but beyond sunspot number 100 a kind of saturation effect sets in. The coefficient for T_2 is much smaller than for T_1 .

Similar analysis was done separately for each month for each harmonic component. Further for each particular month the value of the coefficient (denoted by A) extrapolated for zero sunspot number as well as the sensitivity of these factors to sunspot number (denoted by B) were calculated using linear relationship between the components and the sunspot number.

Similar analysis was done for the geomagnetic H field at Trivandrum for the period 1958 to 1973. The results are shown in Fig.4.3.

Comparing the amplitude extrapolated for zero sunspot number shown on the left hand of Fig.4.3 it is seen that the diurnal wave at Huancayo is larger than that at Trivandrum for any of the months of the year. Further at both the stations the amplitude a_1 is maximum during equinoctial months. The amplitude a_2 is also maximum at either of the stations during equinoctial months but the value of a_2 is greater at Huancayo than that at Trivandrum only during the months September to March. For the months April to August the amplitude of a_2 is greater at Trivandrum than that at Huancayo. Thus the amplitude a_1 has the semi-annual effect at different parts of the world

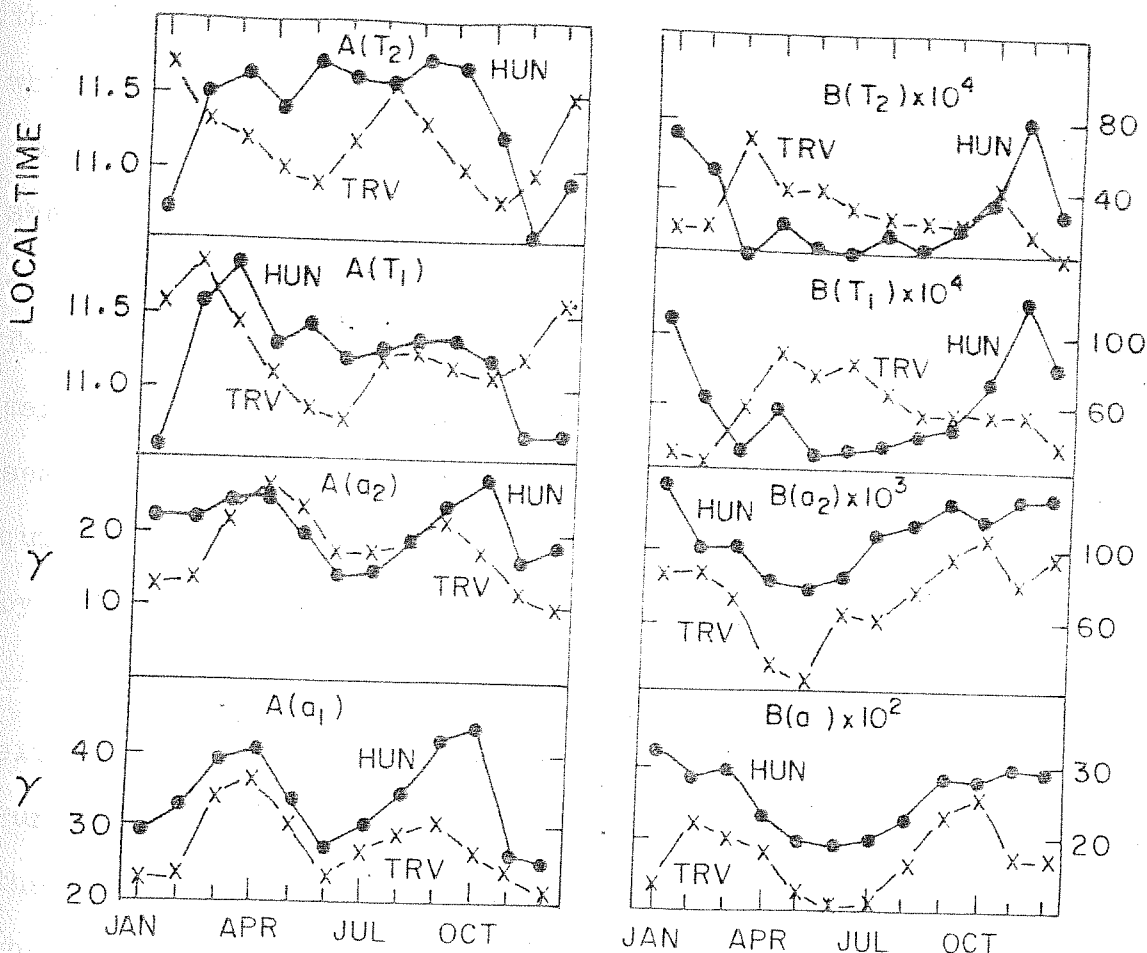


Fig.4.3 - Annual variation of coefficients A and B in the linear regression equation between a or T and monthly mean zurich sunspot numbers. a and T are the amplitudes and times of maximum of first and second harmonics of monthly mean daily variation of quiet day H field. Dashed line for Trivandrum and solid line for Huancayo.

whereas semidiurnal component a_2 is further affected by local seasons, with increased value during local summer months. This means that at both the places electrojet is maximum during equinoxes. Further the electrojet is much stronger at Huancayo than that at Trivandrum during D (Nov, Dec, Jan, Feb.) months while the difference is least during J (May, June, July, Aug.) months. Referring to time of maximum of diurnal component it is seen that it is earliest at Huancayo around Nov., Dec., Jan. and at Trivandrum during May and June months. To some extent similar features are noticed in the seasonal variation of the time of maximum of the semidiurnal component. Thus it seems that the seasonal variation of the time of daily maximum of $Sq(H)$ (solar quiet day variation of H field) at equatorial station is governed by certain parameters which depend upon local seasons.

The sensitivity of the values of a_1 or a_2 to sunspots for either Huancayo or Trivandrum seems to be least for J months. Further for any months of the year a sensitivity of either of these values is greater for Huancayo than for Trivandrum. Thus the difference in the electrojet currents over Huancayo and Trivandrum would increase with the increasing sunspot number. The seasonal variation of the sensitivity of the times of maximum T_1 and T_2 seems to be opposite in nature at Huancayo and at Trivandrum. Thus the time of maximum of the daily variation again seems to be controlled by the local seasons of the station.

4.2 Counter-electrojet - Geomagnetic effects at different latitudes

4.2.1 Introduction

The large depressions of the H field which are noticed in the afternoon hours at Huancayo were first reported by Bartels and Johnston (1940). Gouin (1962) reported an event in which daily variation of H at Addis Ababa (within the electrojet) was depressed during noon hours below the night-time level. This phenomenon of decrease of H field during the daytime at an equatorial station was named 'counter-electrojet' by Gouin and Mayaud (1967). On counter-electrojet events the electrojet seems to reverse its flow pattern during early morning and/or afternoon hours.

Rastogi et al. (1971) showed that the depression in H at Kodaikanal (counter-electrojets) were associated with simultaneous reversal of the drift velocities of ionospheric irregularities over the equator (measured at Thumba) and sudden disappearance of q type equatorial Es. Later it was confirmed that the counter-electrojet events at Huancayo were associated with simultaneous reversal of the electron drift velocities measured by VHF backscatter radar at Jicamarca (Rastogi 1973a). Such an association has been shown to be true on a very small time scale of minute or so and even during geomagnetically disturbed periods (Rastogi et al. 1977).

Using a large network of closely spaced ground-based magnetometers in the equatorial region ($\pm 5^\circ$ dip latitude long. 14° - 19° E) in Chad in the Central African Republic during Nov. 1968 to March 1970, Fambitakoye and Mayaud (1976, a, b) reported the results on counter-electrojet events. Separating the regular solar (S_R) variation into two components viz. S_R^P representing the effect due to mid-latitude "planetary" S_q current system and S_R^E representing the "supplementary" equatorial electrojet current confined to a narrow latitude band along the dip equator, they showed (i) the permanence of counter-electrojet in the morning hours and frequent occurrence in the afternoon hours, (ii) frequent occurrence in the afternoon of a secondary reversal current ribbon, roughly twice as double as the main ribbon, (iii) large variability in the ratio of S_R^E to S_R^P , (iv) significant north-south asymmetries in the total field and S_R^P , (v) shifting of the electrojet centre by about 40 km to the north during the counter-electrojets and (vi) inhibition of the normal development of S_R^E (reduction in the electrojet strength) when irregular short-term fluctuations occur on some days. Fambitakoye et al. (1976) have offered explanations for some of these in terms of possible ionospheric east-west winds at high altitudes (125-200 km) and plasma instabilities as envisaged in the physical mode of the electrojet suggested earlier by Richmond (1973, a).

A much more extensive network was operated in Ethiopia (long 36° - 44° E) from Dec. 1970 to May 1971 in a much restricted latitude ($\pm 5^{\circ}$ dip lat.) but consisting of 35 stations.

Preliminary results were presented by Porath et al. (1973) who showed that (i) there was a north-south asymmetry in the daily range. The similar dip latitudes in the southern region showing larger ranges, (ii) the Z variation showed north-south asymmetries not only in amplitude and sign but in spectral composition also, the 24 hr, 8 hr and 6 hr components showing dissimilar behaviours, (iii) the planetary S_q and equatorial supplementary electrojet seem to be mostly unrelated, (iv) assuming the electrojet effect as equivalent to that due to three model line currents at dip latitudes 0° , $\pm 1.5^{\circ}$ and $\pm 3.0^{\circ}$, it was observed that the inner line currents were stronger, indicating essentially a centering on the dip equator but during afternoon counter-electrojet, the current intensities seemed to decrease more gradually with distance (or latitude) than the normal electrojet currents did indicating possibly different mechanisms and/or altitudes for the reverse current flows in the ionosphere, (v) on some days, electrojet showed depression near local noon and its magnitude decreased more gradually with latitude than the normal electrojet strength and the depression occurred slightly earlier away from the equator, (vi) morning counter-electrojet magnitudes decreased more rapidly with latitude than normal electrojet, (vii) on storm

day, the electrojet part could have counter-electrojet too, and (viii) SSC had larger magnitude nearer equator for some events.

Rastogi (1975) had suggested that the observed variation of H-field at the ground in the electrojet region is due to the superimposition of two current systems one of which associated with world-wide S_q and flowing always eastward during daytime at a height of about 107 km; another a simultaneous current at about 100 km which may flow eastward or westward.

Hutton and Oyinloye (1970) reported that there was no connection between the occurrence of counter-electrojet and the moon as the phenomenon had been observed at all times of the lunar day, even though they found that the counter electrojets were most frequent around 0300 and 1500 lunar hours. Sastri and Jayakar (1972) showed that major afternoon counter-electrojet events at Trivandrum occurred most frequently around lunar age 0000 and 1200 hrs (new and full moon days) and were practically absent around lunar age 0600 and 1800 hrs (first and third quarter moon days).

Marriot et al. (1979) noted that the afternoon counter-electrojets occur most often at all stations when lunar phase is 1 hr and the morning counter-electrojet occurs most frequently for lunar phase 5, 6 and 7 hrs. It is quite reasonable to conclude the additional field on the days with afternoon counter-electrojet events detected by Bhargava and Sastri (1977) is of

lunar tidal origin. Sastri and Bhargava (1980) had examined the variation of the additional magnetic field present on afternoon counter-electrojet days over the latitudes from the dip equator to Sabhawala (dip = 45°N) separately for January and the summer months. They had given a picture of variation of the additional magnetic field on the days of counter-electrojet events and also had represented approximately the overhead current vectors during daytime on those days, which demonstrates the two vertexes of the additional current system and position of which is seasonal dependent.

Schieldge et al. (1973) simulated worldwide magnetic variations observed at four universal times of quiet day on the basis of coupled numerical models of the global ionospheric dynamo

consisting of a tilted dipole field within realistic conductivity lunar tidal origin. Sastri and Bhargava (1980) had examined the contribution and height varying tidal winds and allowed for variation of the additional magnetic field present on afternoon field line currents. They found that in addition to the diurnal component, days over the latitudes from the dip equator to Sabhawala (dip = 45°N) separately for January and the summer months. They had given a picture of variation of the additional magnetic field on the days of counter-electrojet events and also had represented approximately the overhead current vectors during daytime on those days, which demonstrates the two vertexes of the additional current system and position of which is seasonal dependent.

Raghavarao and Anandarao (1980) showed that only vertical wind can reverse the electrojet most effectively and to identify a latitudinal model of vertical winds that can produce the observed features of counter-electrojet in the presence of additional current system and position of which is seasonal dependent. They had given a picture of variation of the additional magnetic field on the days of counter-electrojet events and also had represented approximately the overhead current vectors during daytime on those days, which demonstrates the two vertexes of the additional current system and position of which is seasonal dependent.

vertically upward winds the ions are lifted up cancelling or even reversing the vertical polarisation field depending on the wind speed only. An upward velocity of about 13 m/sec can

simulate the features of counter-electrojet in the presence of additional current system and position of which is seasonal dependent. They had given a picture of variation of the additional magnetic field on the days of counter-electrojet events and also had represented approximately the overhead current vectors during daytime on those days, which demonstrates the two vertexes of the additional current system and position of which is seasonal dependent.

annual the vertical polarisation field engendered by a primary eastward field of 0.5 mv/m at the dip equator in the Indian zone ($B = 0.38$ gauss at 105 km altitude).

Rastogi and Patel (1975) had demonstrated that a number of events of counter electrojet were associated with IMF (Interplanetary magnetic field). They had concluded that large and quick changes in the latitude of IMF from its southward to northward direction would impose an electric field in the ionosphere from the evening to the morning sector of the earth, which would be superimposed on S_q electric field. Depending upon the magnitude of the magnetospheric electric field and S_q electric field at the concerned field on the equator may be decreased still maintaining the normal direction or even reversed from its normal direction, causing a partial or complete counter-electrojet events. Recently Rastogi (1981) has discussed the characteristics of equatorial counter-electrojet events associated with reversal of interplanetary magnetic field (IMF) and compared with those events associated with semi-diurnal luni-solar tides.

4.2.2 Counter-electrojet effects in geomagnetic field components at different latitudes

The study refers to the quiet sun year of 1964 and geomagnetic data for the equatorial locations Trivandrum (dip angle $-1.6^\circ S$), Kodaikanal ($+2.5^\circ N$) and Annamalainagar ($+5.2^\circ N$) and

the non-equatorial locations Alibag (+23.0°N), Sabhawala (+45.2°N), Tashkent (+60.6°N), Sverdlovsk (+73.6°N) and Dixon (+83.6°N) all about 70°E longitude were used.

A major difficulty in studying counter-electrojet is the distortion of H plots during disturbed conditions. In particular, the local time dependent storm effects DS are known to have a profile of a dawn maximum and dusk minimum (Sugiura and Chapman 1960). The latter can be easily mistaken for afternoon counter-electrojets. A possible way out would be to confine the study only to quiet days ($A_p = 0$ to 7). However, A_p is an average daily index and there is no guarantee that all individual hours on that day will be free from disturbances. A method to eliminate these was suggested by Kane (1973_a) in which a parameter Sd_I is calculated as follows:

$$Sd_I = H(\text{equator}) - H(\text{low lat.}) + \overline{S_q}(\text{low lat.}) \quad (4.3)$$

Here the H values at low latitude location (outside the electrojet region) are subtracted from the H values at an equatorial location, thus eliminating all magnetospheric effects which are expected to be common to both these locations. Since the low latitude S_q is also eliminated unjustifiably, a compensatory factor $\overline{S_q}(\text{low lat.})$ obtained as the mean of either 5 internationally quiet days or all quiet days ($A_p = 0$ to 7) in any particular month is added. The plots of Sd_I show the counter-electrojets very satisfactorily even on disturbed days.

Fig.4.4 shows the frequency of occurrence of negative values of Sd_I (deviation of Sd_I from the average of pre-dawn hours 00-03 LT) at different LT in different seasons in 1964 where Sd_I is obtained as Trivandrum minus Alibag. The outer histograms are for all negative magnitude while hatched parts represents negative magnitude exceeding 10 gamma. The negative magnitude is confined mostly to the morning and afternoon hours specially for larger values, thus indicating that these are the most suitable hours for occurrence of counter-electrojets. Negative magnitudes between 0 and 5 gamma occur at other hours too; but since these seem to occur even during night, we believe that this indicates the level of inaccuracy of the parameter Sd_I .

Days were sorted out according to whether the minimum value of Trivandrum Sd_I during the interval 12-16 LT was in the following ranges (a) positive (b) negative between 0 and 10 gamma, (c) negative exceeding 10 gamma. Thus group (a) would represent days having no counter-electrojets while group (c) would represent days of strong counter-electrojets. The average daily variation of the horizontal component H and its northward component X and eastward component Y at all locations were obtained for these three groups separately for the three seasons (Summer = May, June, July, August; Winter = Jan., Feb., Nov., Dec.; Equinoxes = March, April, Sept., Oct.) separately. Since events in winter were few winter and equinoxes were combined.

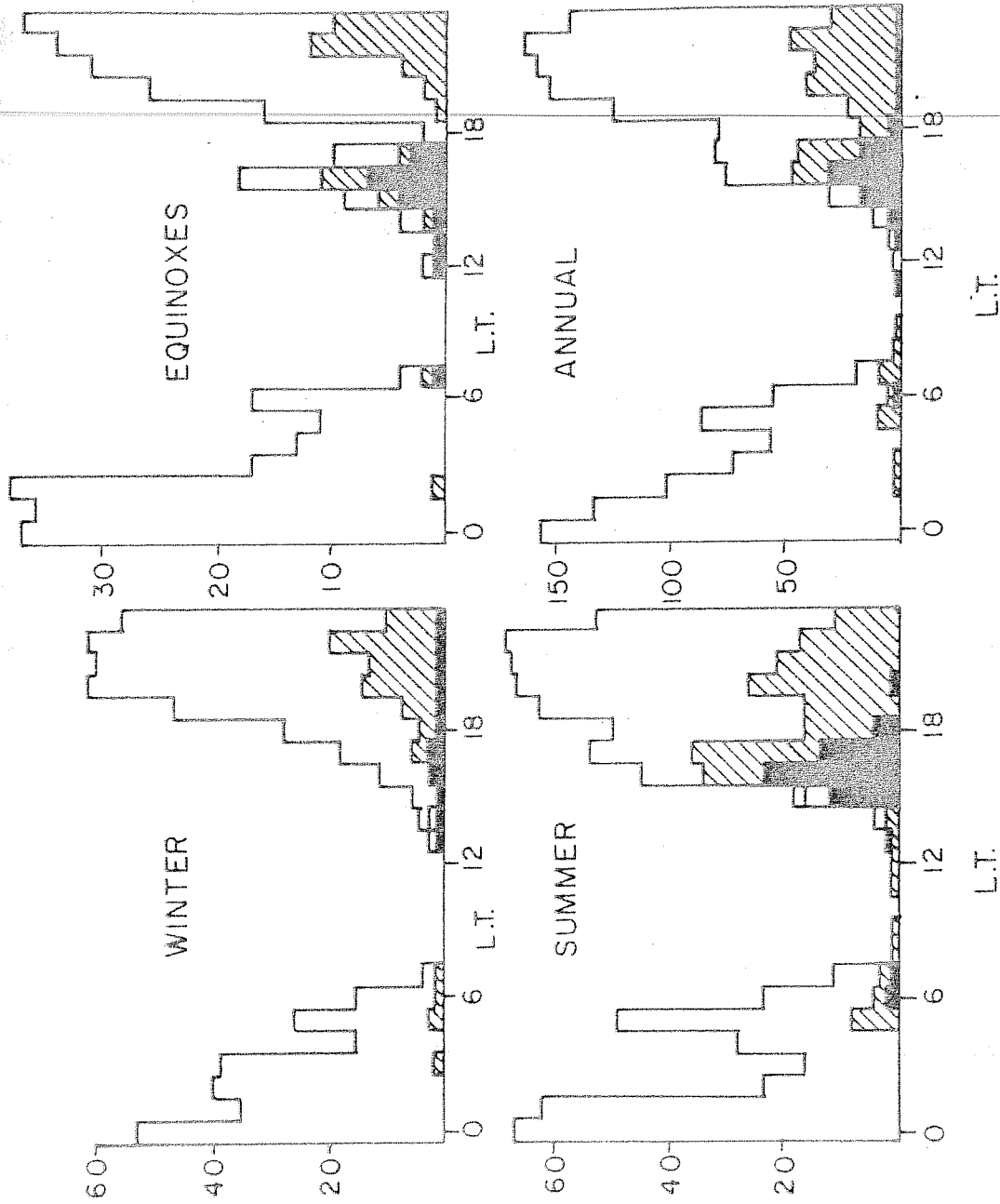


Fig. 4.4 - Occurrence frequency of negative values of SdI (counter-electrojet) at various local time in various seasons. Outer histogram refers to all negative values - Washed for negative values exceeding 5 gamma and black for negative values exceeding 10 gamma.

In Fig.4.5 the left half shows average diurnal H plots for the equatorial stations Trivandrum, Kodaikanal and Annamalainagar for summer months. The top triplet is for days of group (a) i.e. days not having any counter-electrojet. The middle triplet is for group (b) (small afternoon counter-electrojet) and the bottom triplet is for group (c) (strong afternoon counter-electrojet). In each case the superposed dashed curve represents the average of groups (a), (b), (c) and is plotted to show the distinguishing features of these groups. Thus in group (a) the full curves show larger H values than the dashed curves for the afternoon hours indicating a complete lack of counter-electrojet. In contrast the full curves in group (c) are far below the dashed curves during afternoon hours indicating a strong counter-electrojet (shown hatched).

The question we are posing is, are the low and middle latitude daily variation profiles of H, X or Y different for these three groups? The right half of Fig.4.5 shows the average diurnal plots of H, X and Y for Alibag, Sabhawala, Tashkent, Sverdlovsk and Dixon for group (a), (b) and (c) separately. On each full curve the superposed dashed curve is the average of groups (a), (b) and (c) together.

From these plots for summer it seems that the profiles at low, middle and high latitudes are not different for days of counter-electrojets as compared to those for days having no counter-electrojets.

1964
SUMMER

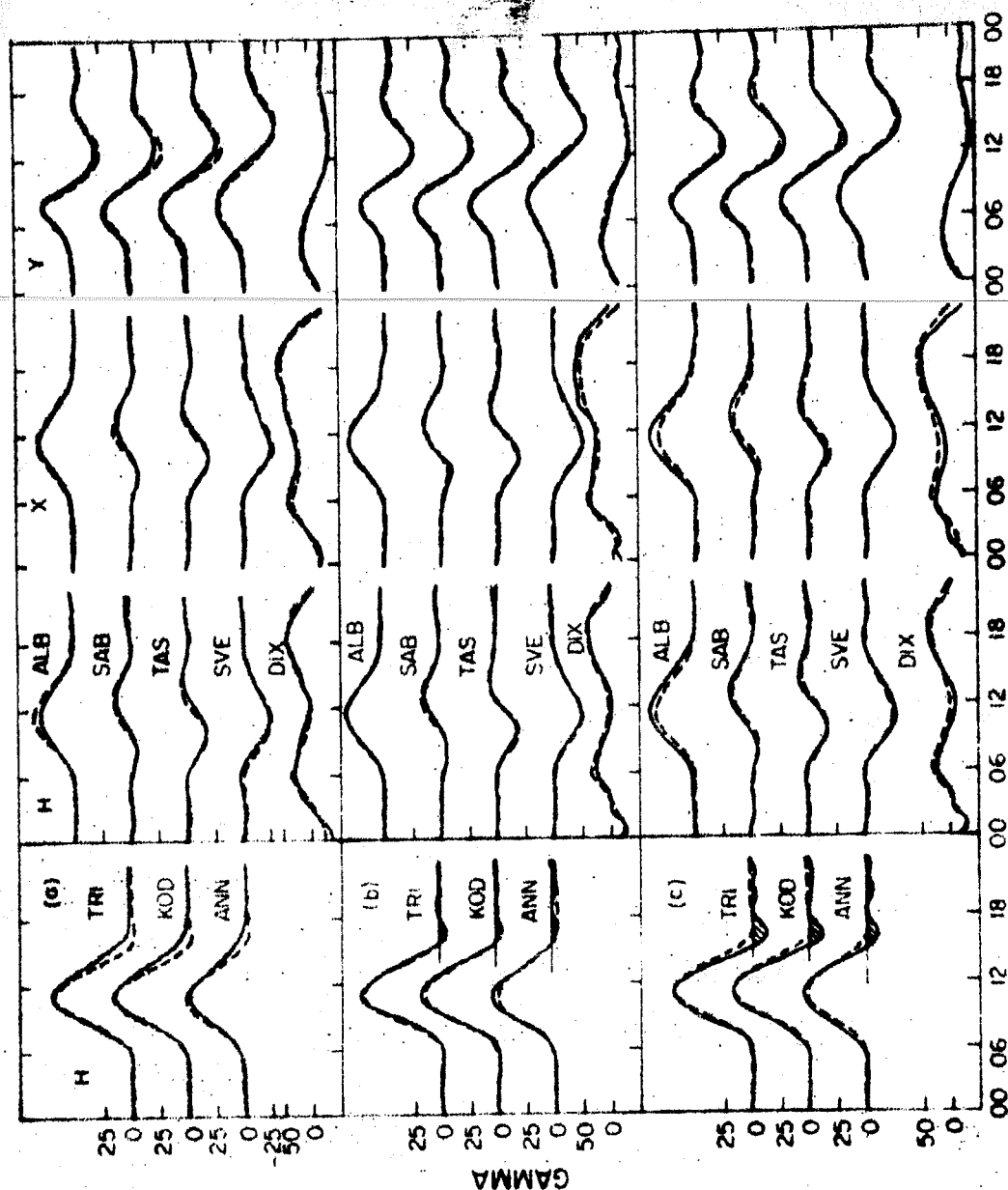


Fig.4.5- Average daily variation curves for summer H at Trivandrum, Kodaikanal, Annamalaiagar (left portion) and H, X and Y at Alibag, Sabhawala, Tashkent, Sverdlovesk, Dixon (right portion) for group (a) days not having any afternoon counter-electrojet and group (b) and group (c) days having respectively small and large afternoon counter-electrojets (shown hatched) as judged from negative Sd_1 at Trivandrum. Dashed curves are averages of group (a), (b) and (c) i.e. average of all quiet summer days for each station separately.

Fig.4.6 shows similar plots for the other seasons viz. winter and equinoxes which have combined together as days for group (c) (large counter-electrojets) were fewer in these seasons. Here the group (c) of large counter-electrojet shows considerable variations in H, X and Y. Incidentally, Bhargava and A Sastri (1977) have reported that on days of afternoon counter-electrojets there is an additional northward component near noon hours i.e. a large amplitude of the normal electrojet at Trivandrum. From Figs.4.5 and 4.6, this is true for winter whereas this effect is not much clear for summer. Recently Sastri and Bhargava (1980) have suggested an additional field on the days of strong counter-electrojet events and have shown changes of the additional field by an approximate representation of the horizontal current vectors. According to them the magnitude of H is high in forenoon hours and in afternoon hours it is low compared to a day which is quiet day and selected nearby counter-electrojet event day. This thing is clearly seen during winter and equinoxes as shown in Fig.4.6 whereas it is not clearly seen during summer referring to Fig.4.5.

In calculating Sd_I , we subtract Alibag H from Trivandrum H. However, since on quiet days, H patterns are not distorted, a similar analysis could be done for Trivandrum H alone rather than for Sd_I . Fig.4.7 shows the average results for three groups of counter-electrojets for Trivandrum H on the left side

1964

WINTER AND EQUINOXES

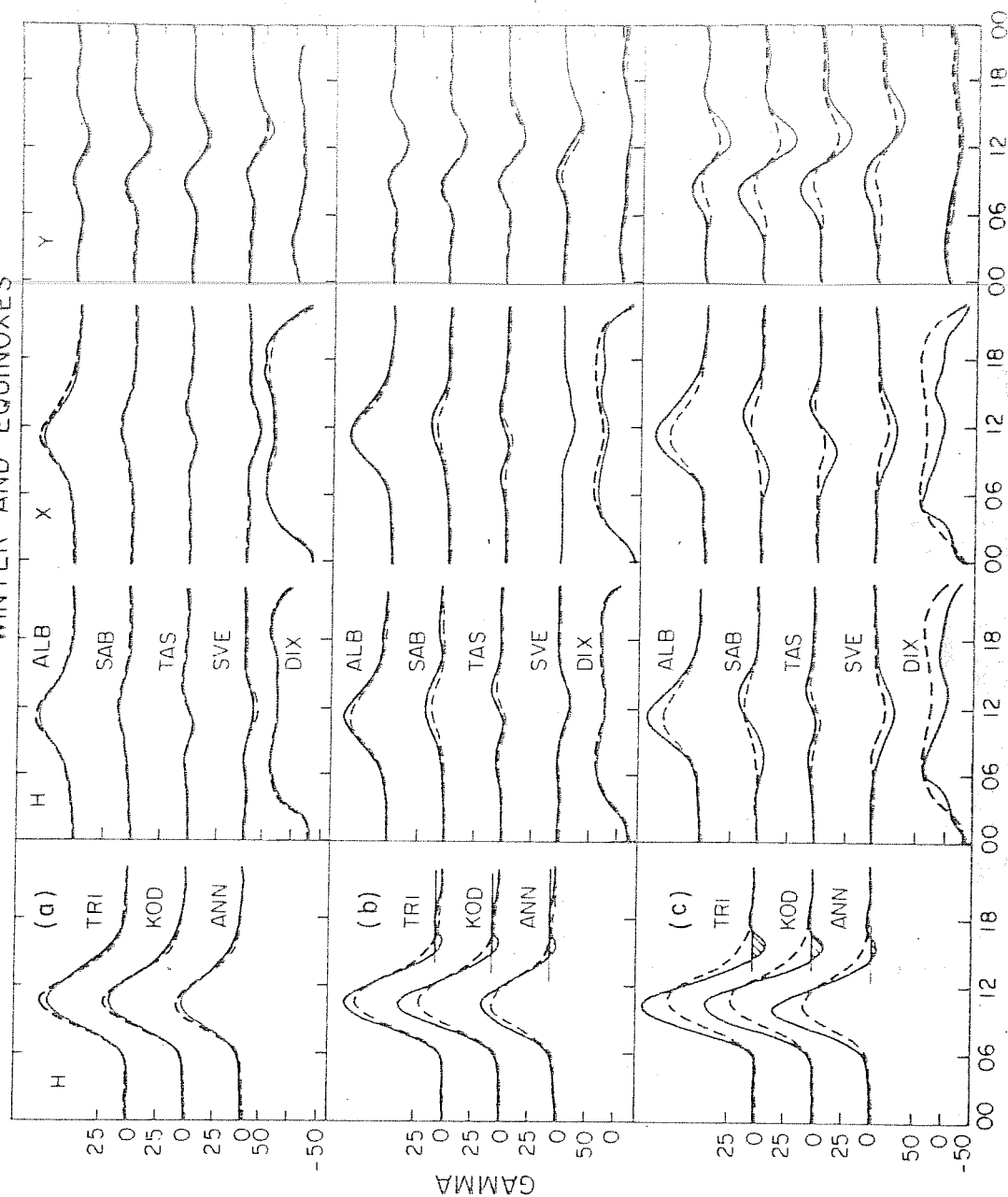


Fig.4.6 - Same as Fig.4.5 for winter and equinoxes combined. Dashed lines are averages for all quiet days in winter and equinoxes.

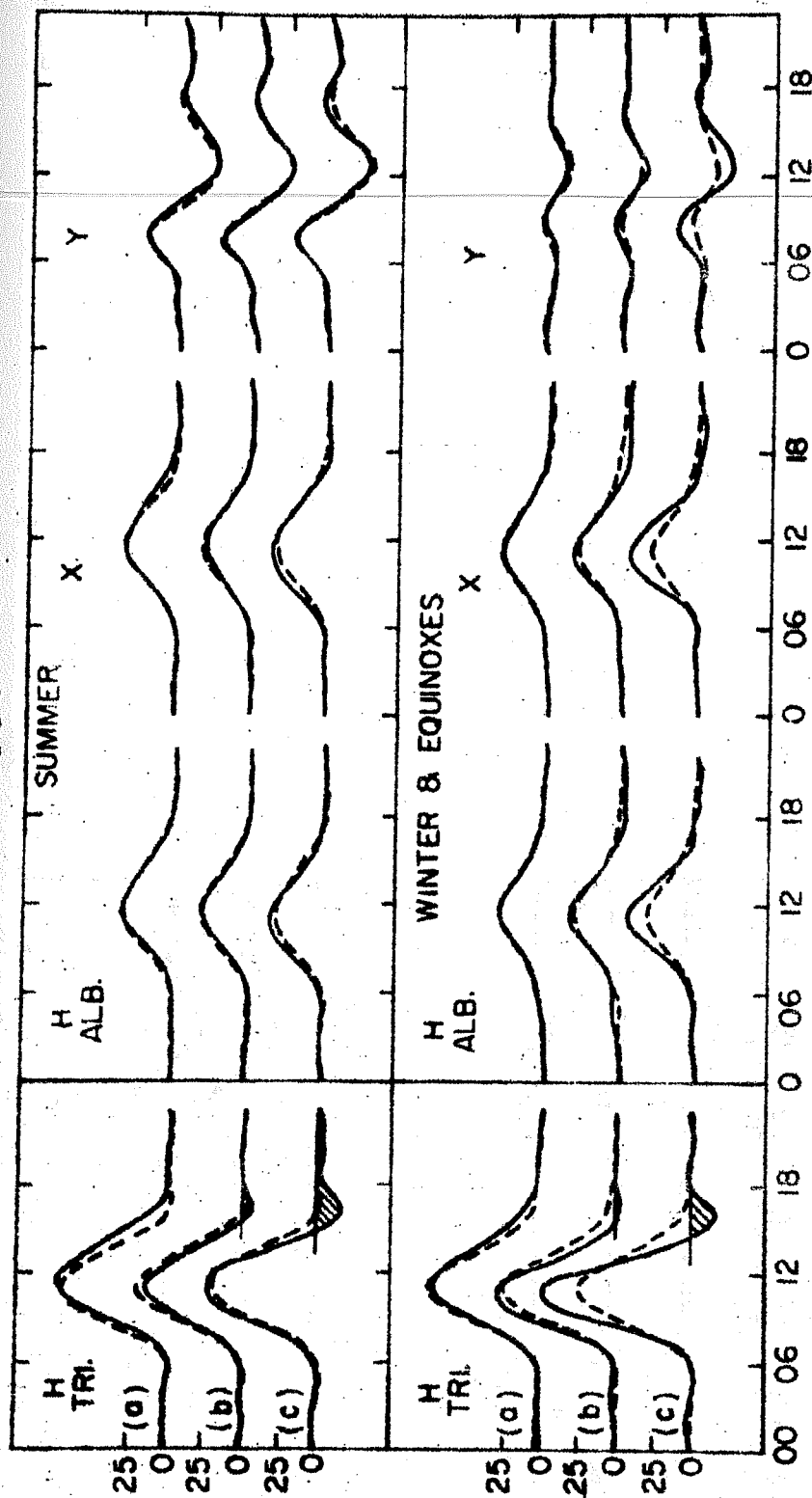


Fig.4.7 - Average daily variation plot for H at Trivandrum (left portion) and H, X and Y (right portion) for summer (upper half) and winter and equinox combined (lower half) for groups (a) of no counter-electrojet days and groups (b) and (c) of small and large counter-electrojet days respectively (shown hatched) as judged from actual H values (and not from S_d as in earlier figures). Dashed curves are averages of groups (a), (b) and (c).

and Alibag H, X and Y on the right-side. Alibag H, X and Y curves are similar for the three groups in summer; but in winter, average amplitude at Alibag is higher during strong counter-electrojets.

To study the H patterns on individual days, Fig.4.8(a) shows diurnal curves for H at Trivandrum for selected days when large afternoon counter-electrojets occurred (shown hatched in summer). Fig.4.8(b) shows the curves for H, X and Y at Alibag. Alibag patterns vary widely from event to event with no consistent feature in the afternoon hours (15, 16 LT) when counter-electrojets occurred at Trivandrum. The dashed curves are the averages for all quiet days in summer. The X and Y patterns are larger than average on some days and smaller than average on others but not necessarily simultaneously in X and Y. On some days, Y patterns are distorted (hour of maximum and/or minimum shifted). Thus on 16 June, 1964, both Trivandrum and Alibag show afternoon decrease below the night level. One would normally conclude that the counter-electrojet at Trivandrum coincided with a reverse S_q at Alibag in the afternoon. However, even though A_p was low ($=7$) on this day, the afternoon drop is most probably not an ionospheric effect at all but magnetospheric effect as it was seen at other locations too. On Aug.6, 1964, the H pattern at Trivandrum is strikingly odd. In Fig.4.9 we show a plot for continuous 5 days including Aug.6, 1964. The top curve is geomagnetic D_{st} (Sugiura and Poros 1971) and shows a mild storm on Aug.4, 1964.

1964

SUMMER

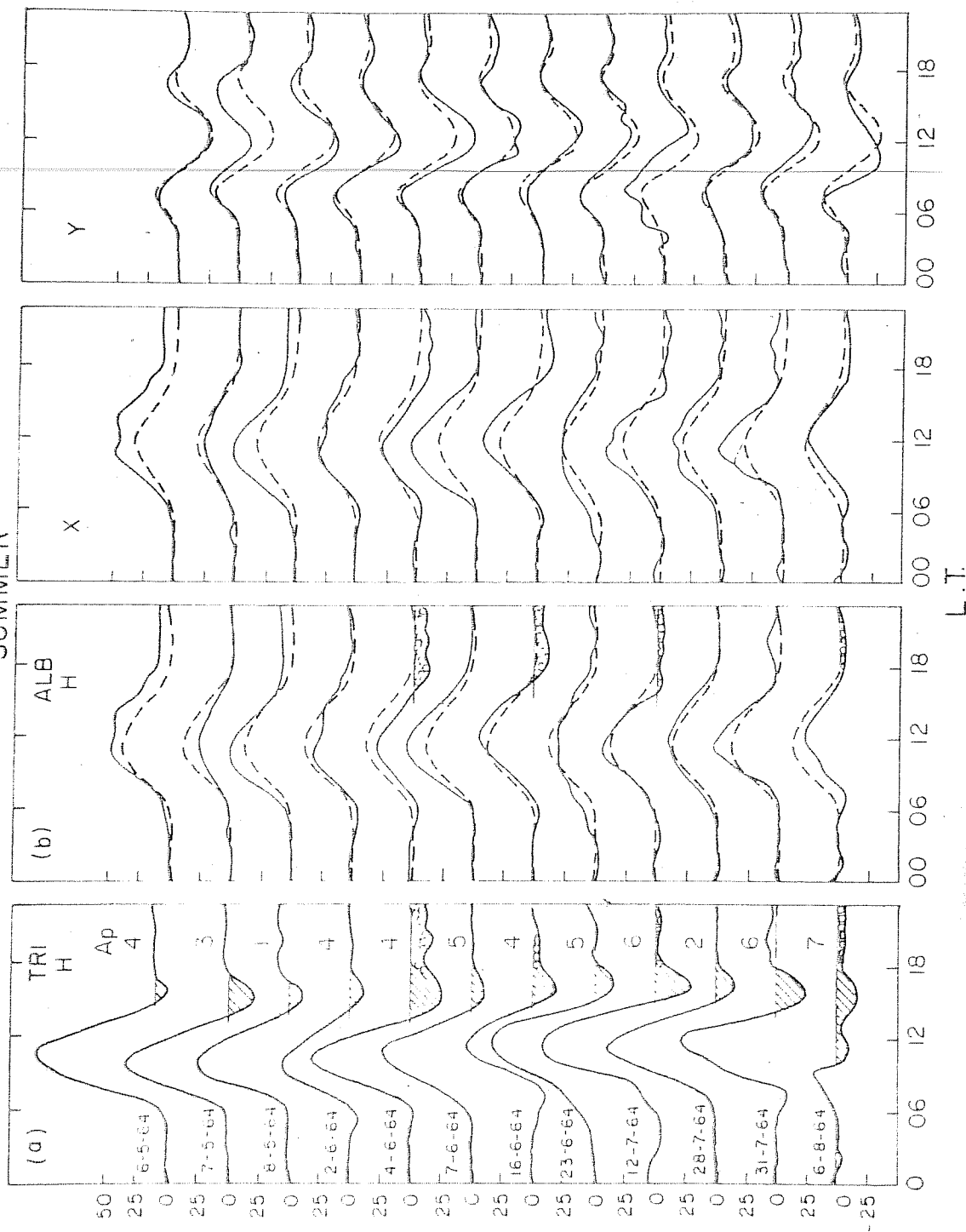


Fig. 4.8 - Actual H plots for (a) Trivandrum H and (b) Alibag H, X and Y for some selected days when strong counter-electrojets occurred at Trivandrum (shown hatched) in northern summer. Superposed dashed lines at Alibag are averages of all quiet days in summer.

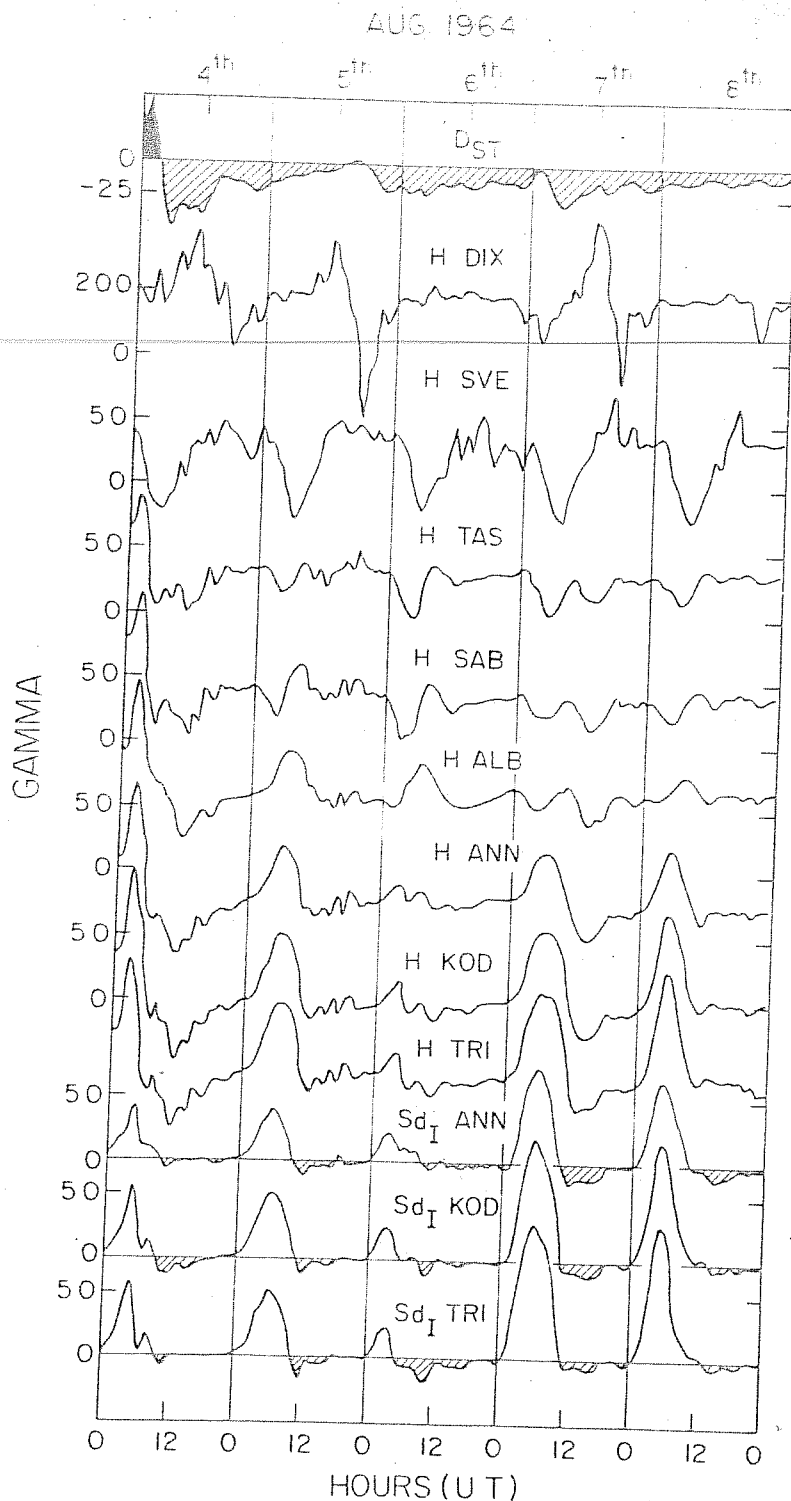


Fig.4.9 - Plots of D_{st} , H values at Dixon, Sverdlovsk, Tashkent, Sabhawala, Alibag, Annamalainagar, Kodaikanal and Trivandrum and Sd_I at the latter three stations for the 5 day interval Aug.4-8, 1964. Counter-electrojets are shown hatched.

On succeeding days the storm recovers. On Aug.6 the A_p was only 7. However, the electrojet at all equatorial locations (Trivandrum, Kodaikanal and Annamalainagar) is highly distorted. Upto about 09 LT, the electrojet seems to have developed normally. But from 10 LT onwards, something very drastic happened and the electrojet reversed for the whole day. At Alibag, the H values are slightly depressed at 06-08 LT but from 08 LT onwards the H values are normal. At Sabhawala, Tashkent and Sverdlovsk nothing very extra-ordinary happened. But at Dixon, the daily variation is different in that the usual maximum at 17-18 LT is missing. However, this maximum is missing at Dixon on Aug.8 also but the electrojet is normal at equator on Aug.8. This Aug.6 event is very peculiar indeed when equatorial electrojet disappeared and even reversed (counter-electrojet) near noon hours even under apparently quiet conditions (low A_p). Unfortunately, no data of interplanetary plasma were available for this day for a comparative study. From the odd behaviour of H at Dixon on Aug.6 a possibility arises that the equatorial counter-electrojet may have some connection in the polar region. Now it is known that magnetic changes in polar regions are intimately connected with changes in interplanetary magnetic fields. Hence an attempt was made recently by Kane (1978) to see whether equatorial counter-electrojets were related to changes in interplanetary magnetic fields. The results were inconclusive.

In Fig.4.10(a) we show the hourly plots of X at Trivandrum on some selected individual days when counter-electrojets occurred in winter and equinoxes and the corresponding H, X and Y plots at Alibag are shown in Fig.4.10(b). The dashed curves are average for all quiet days in winter and equinoxes. On almost all days, the H and X amplitudes are higher. The Y amplitudes are also higher with some distortion of phase too.

This study revealed that in the northern summer, the low and middle latitude H and/or X and Y pattern do not seem to have any behaviour consistently different from the normal. But in the northern winter and equinoxes the H, X and Y variations at low latitudes have abnormally high amplitudes on counter-electrojet days. Thus counter-electrojets at equator could be related to intensifications on certain days of the normally weak winter hemisphere S_q current system in the Indian region. Whether the counter-electrojets at Trivandrum in the northern summer were related to S_q current system intensification in the southern hemisphere could not be checked as there are no magnetic observatories directly south of Trivandrum in the Indian ocean.

The above evidence indicates a possibility that the neutral winds might have an intimate connection with the change in the neutral wind patterns of winter hemisphere. To check this we have studied changes in the low latitude E-region drifts on counter-electrojet days in winter.

1964

WINTER & EQUINOXES

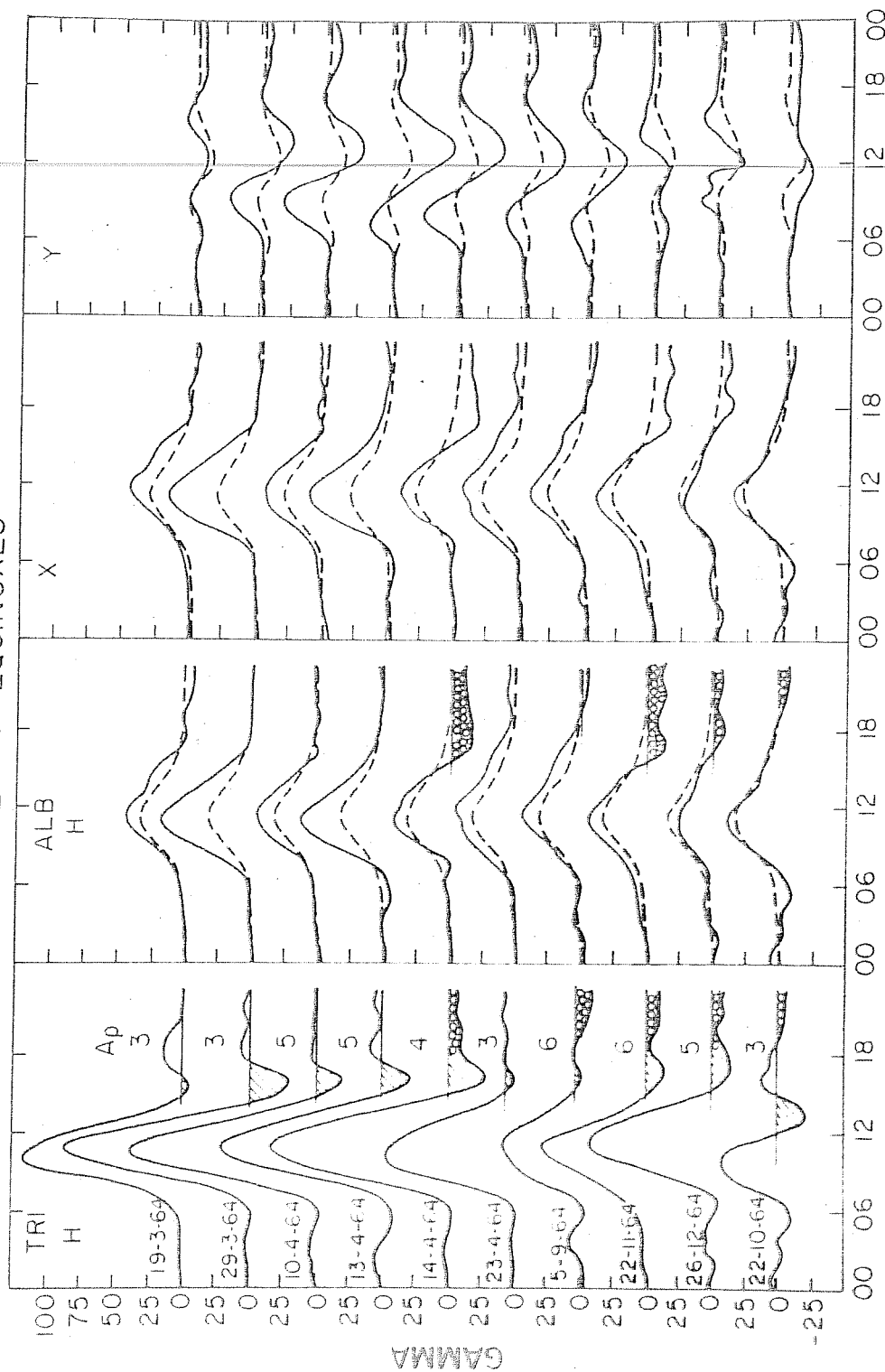


Fig.4.10 - Actual H plots for (a) Trivandrum H and (b) Alibag H, X and Y for some selected days when strong afternoon counter-electrojets occurred (shown hatched) in northern winter and equinoxes. Superposed dashed lines are averages of all quiet days in winter and equinoxes.

4.2.3 Changes in the low latitude E-region drifts on counter-electrojet days

In an attempt to examine the relationship between the drifts at low latitudes and the counter-electrojet we have studied the counter-electrojet events during the year 1974 and the corresponding E-region drift velocities at Ahmedabad. The drifts at Ahmedabad show a marked seasonal change in the zonal wind with a flow towards west during winter and towards east during summer (Chandra et al. 1977, Patel et al. 1978). This is in contrast to the westward day-time drift throughout the year in the electrojet region (except during counter-electrojet events). Counter-electrojet days were identified from ground magnetic data recorded at Trivandrum and Alibag and later confirmed from the E-region drift measurements made at an equatorial station Tiruchirapalli (dip 4.8°N). In Fig.4.11 the eastward component of E-region drift is plotted for Ahmedabad as well as for Tiruchirapalli for a counter-electrojet day (22 November 1974) alongwith the magnetic field variations (Sd_I) which shows a depression around midday. To show the change in drifts from the normal pattern the mean values of the drifts for the month are also plotted by broken lines. The drift at Tiruchirapalli shows a change to eastward around the time of counter-electrojet event. The drift at Ahmedabad on this day is eastward throughout and shows large eastward velocity around midday. Another example

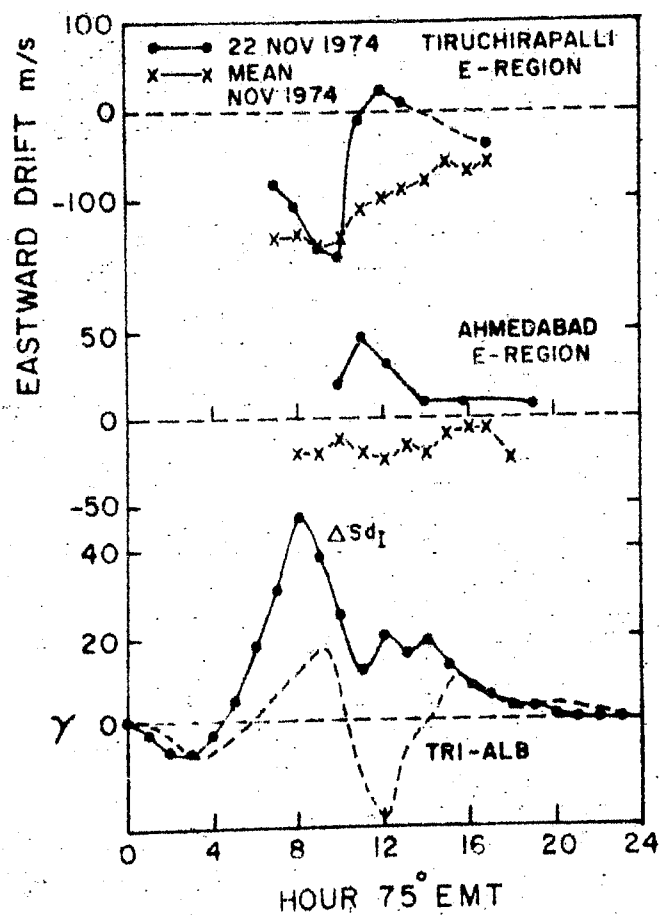


Fig.4.11 - Daily variation of E-region drifts at Tiruchirapalli and Ahmedabad, of geomagnetic H variations Sd_I and (Trivandrum-Alibag) on 22nd Nov. 1974.

on 20 December 1974 is shown in Fig.4.12. There is counter-electrojet between 12 and 15 hr LT centred around 14 hr LT on this day. The drifts at Tiruchirapalli show reversal at 14 hr while the drifts at Ahmedabad are eastward throughout daytime. We have examined some other events during winter and all of them show eastward drifts at Ahmedabad.

Thus the counter-electrojet events are probably associated with the eastward shift of the global scale wind pattern. We conclude, therefore, that counter-electrojet events are probably caused by changes in the atmospheric circulation pattern rather than the localised change near magnetic equator.

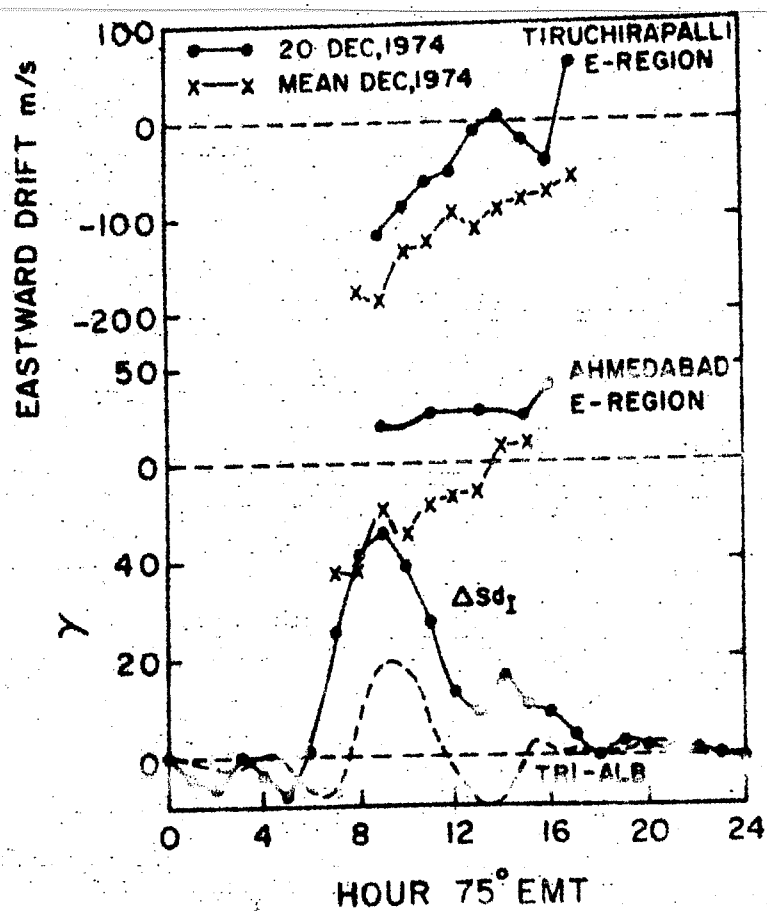


Fig.4.12 - Same as Fig.4.11 on 20 Dec. 1974.

CHAPTER - V

SPACED RECEIVER EXPERIMENT

5.1 Introduction

A well known method of studying the ionospheric irregularities is from the phenomenon of scintillation produced when radio waves from a radio star or a satellite (with radio beacon) traverse the medium containing irregularities. This phenomenon occurs in a number of media starting from lower atmosphere to as remote a medium as intergalactic space. Table 1 (compiled by Dr.S.N. Bhandari, Physical Research Laboratory, Ahmedabad) gives a brief account of this phenomenon in the universe. Scintillation has been a powerful tool for the measurement of irregularity heights, motions, as well as for the detailed study of the properties of irregularities. Satellites in particular allow spatial coverage which is otherwise difficult or even impossible to achieve with other techniques.

5.2 Radio Star Scintillation

The radio star scintillation was first discovered by Hey et al. (1946) as the variable component of radio emission from the constellation of cygnus.

Once the phenomenon of ionospheric scintillation by radio stars was discovered, many research workers (Little and Maxwell 1952

UNIVERSAL OCCURRENCE OF SCINTILLATION PHENOMENA

PHENOMENON	MEDIUM RESPONSIBLE AND ITS AVERAGE DISTANCE FROM THE EARTH	AVERAGE CHARACTERISTICS					TIME SCALE OF OBSERVED INTENSITY FLUCTUATIONS	UNIT ON ANGULAR SIZE θ_c OF SOURCES FOR APPRECIABLE SCINTILLATION
		IRREGULARITY SIZES	ELECTRON DENSITY N_0	FLUCTUATION IN N_0 ΔN_0	SPEED OF IRRADIANTES			
twinkling of stars	ATMOSPHERIC NEUTRAL DENSITY FLUCTUATIONS $\sim 0-5$ km	~ 5 cm - 1 m	-	-	~ 10 m s $^{-1}$		~ 0.2 s	STELLAR OBJECTS AT OPTICAL WAVELENGTHS $\theta_c \lesssim 5''$
IONOSPHERIC SCINTILLATION (IS)	IONOSPHERE $\sim 100-400$ km	$\sim 0.1-10$ km	$\sim 10^{6-7}$ el cm $^{-3}$	$\sim 10^{4-5}$ el cm $^{-3}$	$50-100$ m s $^{-1}$		$\sim 2-100$ s	ARTIFICIAL SATELLITES AND ASTRONOMICAL RADIO SOURCES (e.g. CAS-A, YAU-A) $\theta_c \lesssim 10''$
INTERPLANETARY SCINTILLATION (IPS)	SOLAR WIND INTERPLANETARY MEDIUM ~ 1 A.U. (1 A.U. = 1.5×10^8 km)	~ 100 km	$10-100$ el cm $^{-3}$	$0.1-1.0$ el cm $^{-3}$	$300-1000$ km s $^{-1}$		$\sim 0.1-2$ s	COMPACT EXTRAGALACTIC RADIO SOURCES (RADIO GALAXIES & QSOs) $\theta_c \lesssim 1''$
INTERSTELLAR SCINTILLATION (ISS)	INTERSTELLAR MEDIUM ≥ 100 pc (1 pc = 3×10^4 km)	$\sim 10^{6-8}$ km	$10^{-1}-10^{-2}$ el cm $^{-3}$	$10^{-4}-10^{-5}$ el cm $^{-3}$	$\sim 10^2$ km s $^{-1}$		$\sim 10-200$ min	PULSARS AND HIGHLY COMPACT RADIO SOURCES $\theta_c \lesssim 10^{-4}''$ etc
INTERGALACTIC SCINTILLATION (IGS)	INTERGALACTIC MEDIUM $\geq 10^4$ kpc	$\sim 10^{10}$ km	$\sim 10^{-5}$ el cm $^{-3}$	$\sim 10^{-8}$ el cm $^{-3}$	$\sim 10^{2-3}$ km s $^{-1}$		$\sim 0.1-1$ year	EXTREMELY COMPACT AND VARIABLE EXTRAGALACTIC RADIO SOURCES (e.g. QSOs) $\theta_c < 10^{-5}''$ etc

Wright et al. 1956, Wild and Roberts 1956, Dagh 1957, 1957a, Briggs 1958, Koster 1958, Koster and Wright 1960, Koster 1963, Briggs 1964, Basu et al. 1964, Aarons and Allen 1966, Briggs 1966 etc.) utilised this technique to study the ionospheric irregularities and compared their properties with other geophysical parameters like geomagnetic index, solar activity etc.

Similarly plasma density irregularities in the interplanetary medium associated with solar wind produce rapid (faster than about a second) fluctuation in the intensity of radio sources possessing angular diameter less than about 1". These fluctuations are referred to as interplanetary scintillation (IPS) in order to distinguish these from analogous phenomena occurring in the ionosphere and the interstellar medium. The characteristics of the observed IPS depend on the spatial structure and dynamics of the interplanetary plasma as well as on the angular size of the radio source being observed. However, with a satisfactory knowledge of interplanetary medium, interplanetary scintillation data can be interpreted to yield useful information on the structure of sources and vice versa. Thus observations are useful to study the structure of plasma density fluctuations in the interplanetary and inter-stellar space and of galactic and extragalactic radio sources.

5.3 Satellite Scintillation

Early studies of the ionospheric scintillation using radio signals from the radio stars showed that it is basically a night-time phenomenon and that it is associated with spread-F observed in the ionograms (Wild and Roberts 1956, Koster 1958, Booker 1958, Bhargava 1964).

The advent of the beacon signals aboard the artificial satellite provided the opportunities for global studies of the ionospheric scintillations. Both the signals from orbiting satellites like Explorer 22 and Explorer 27 as well as geostationary satellites like Intelsat IIF2, Intelsat IIF3 and ATS-3 have been widely used for ionospheric scintillation studies.

Most of the ionospheric scintillation studies using beacons from geostationary satellites were carried out at high and middle latitudes. Only a few studies for equatorial latitudes are available for Legon (dip 9°S) (Koster 1972) and Huancayo (dip 2°N) (Mullen 1973). Recently in the Indian zone for Ootacamund (dip 4°N) (Rastogi et al. 1977) scintillation study was carried out using ATS-6 satellite:

Global morphological study of the occurrence of scintillation has been carried out by Aarons et al. (1963)

and Aarons (1975). On an average there is an equatorial belt of 20° in width of high scintillation, then a region of weak scintillation in the middle latitudes and again ~~a high scintilla-~~tion region at high latitudes. Fig.5.1 shows global irregularities structure (after Aarons 1975) obtained using orbiting and geostationary satellites. It may be noted here that the density of hatching is proportional to the depth of fading in any region.

The equatorial night-time scintillation occurrence is maximum around midnight for any longitude and is mainly due to spread-F (Koster 1972, Mullen 1973, Chandra and Rastogi 1974). At high latitude some scintillations are observed during the daytime hours (Bolten et al. 1953, Duono 1956, Chivers and Greenhow 1959, Lyszka 1963, Munro 1966, Frihagen 1971, Mielson and Aarons 1974). McClure (1964) estimated the height of the irregularities responsible for the daytime scintillations to be embedded in the E-region. Association of the scintillations and Es patches has been noted at middle and low latitudes (Aarons and Whitney 1968, Rastogi and Iyer 1976, a). One of the most important aspects of the ionospheric scintillation is the frequency dependence of the amplitude fluctuation. This has been studied by the several workers viz. Hewish (1952) (frequency range) Chivers (1960) (frequency range), Aarons et al. (1967) (frequency range) and Deshpande et al. (1978).

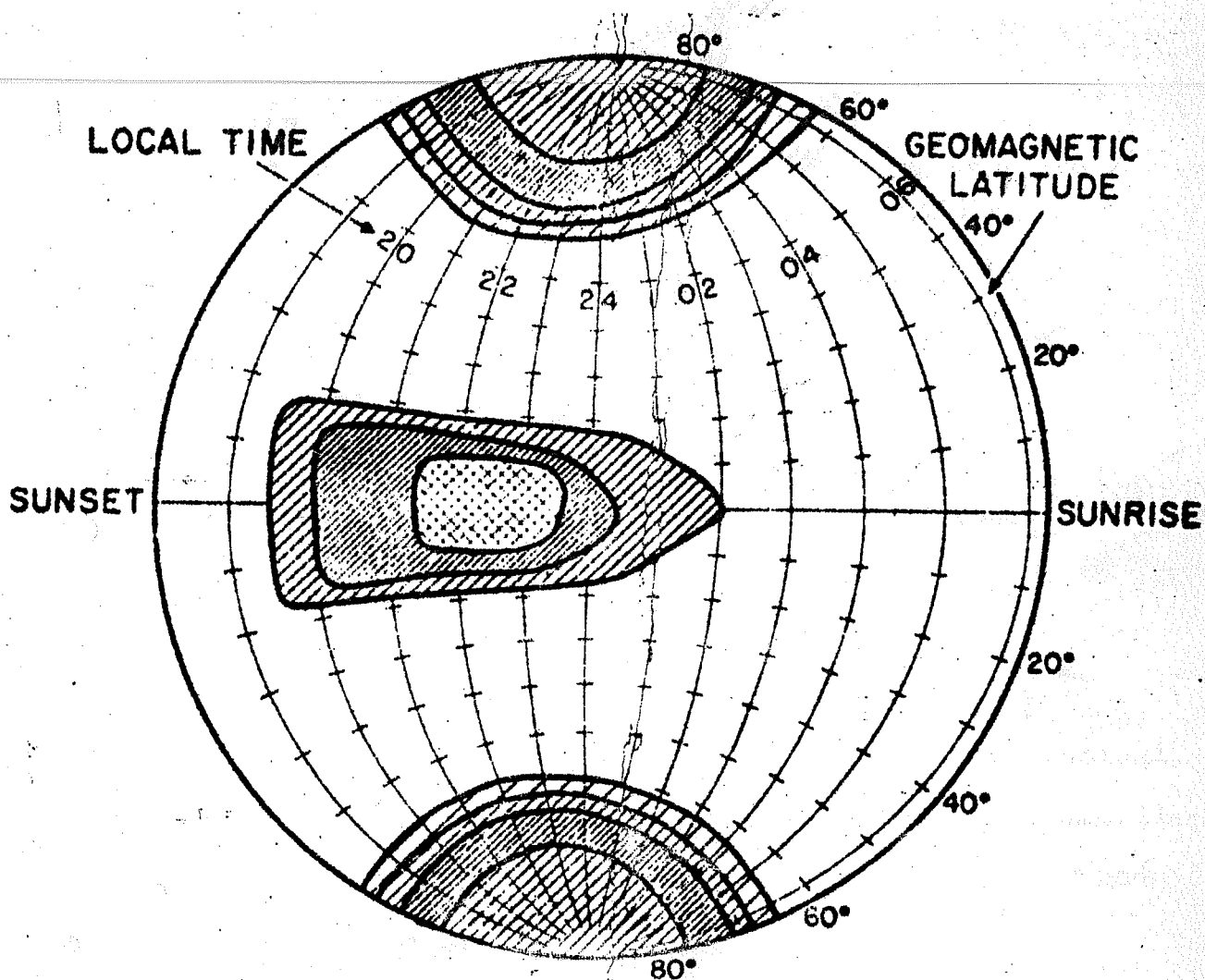


Fig.5.1 - A night-time occurrence of scintillation. Equatorial scintillation shows greater depth than scintillation at sub-auroral, auroral and polar latitudes (after Aarons, 1975).

During ATS-6 phase II, recordings of the amplitude and phase at 40, 140 and 360 MHz were made at Ootacamund(dip 4° N) in the Indian zone for one year (Sept. 1975 to Aug. 1976). Strong scintillations were observed during night-time associated with spread-F (Deshpande et al. 1977, Rastogi et al. 1977a, Vats et al. 1978). It was shown that strong scintillations during the night were associated with intense range spread, only moderate scintillations are associated with frequency spread (Chandra et al. 1979). In addition there were several day-time instances of strong scintillations primarily associated with the blanketing type of Es (Rastogi et al. 1977). Day-time scintillation instances are much more in the Indian zone than in the American zone at the equatorial locations. This is due to the fact that counter-electrojet events are much more in the Indian zone than in the American zone (Rastogi et al. 1979). Frequency dependence of the ionospheric scintillation was also studied for the discrete frequencies 40, 140 and 360 MHz (Deshpande et al. 1978).

To understand fully the irregularities causing scintillation it is necessary to study the nature and dynamics of the irregularities. This can be achieved by spaced receiver technique using satellite radio beacons. In addition, effectiveness of space diversity scheme to mitigate ionospheric scintillation effect on communication can also be studied. Such studies

near the equator are essential as the equatorial zone consists of intense irregularities. To study these irregularities a spaced receiver experiment using radio beacons (136 MHz) from ETS-2 satellite was set up at Tiruchirapalli (dip 4.8°N). In addition a spaced receiver drift experiment was conducted at 2.5 MHz and 5.0 MHz. Thus it was possible to compare the nature of the irregularities causing VHF and HF scintillation and to study the characteristics of irregularities having different scale size simultaneously. The sub-ionospheric coordinates for 350 km altitude for the ray-path from ETS-2 satellite at Tiruchirapalli are 84°E long., 10°N lat and 4.1° dip.

5.4 Experimental Set-up

The beacon signal (136.1123 MHz) radiated from the geostationary satellite ETS-2 is received by three crossed yagi antennae A_1 , A_2 and A_3 , situated at the vertices of a triangle as shown in Fig.5.2. The whole electronic set-up consists of three identical receivers. The block diagram is shown in Fig.5.3. The signals received on all the three antennae are amplified in the preamplifiers and brought to the recording room. These signals are amplified and mixed with the signal from the first common local oscillator. The mixer output at 10.7 MHz from all the three mixers are amplified and mixed with the signal from the second common local oscillator giving rise to second IF signal at 455 kHz. These outputs at 455 kHz are

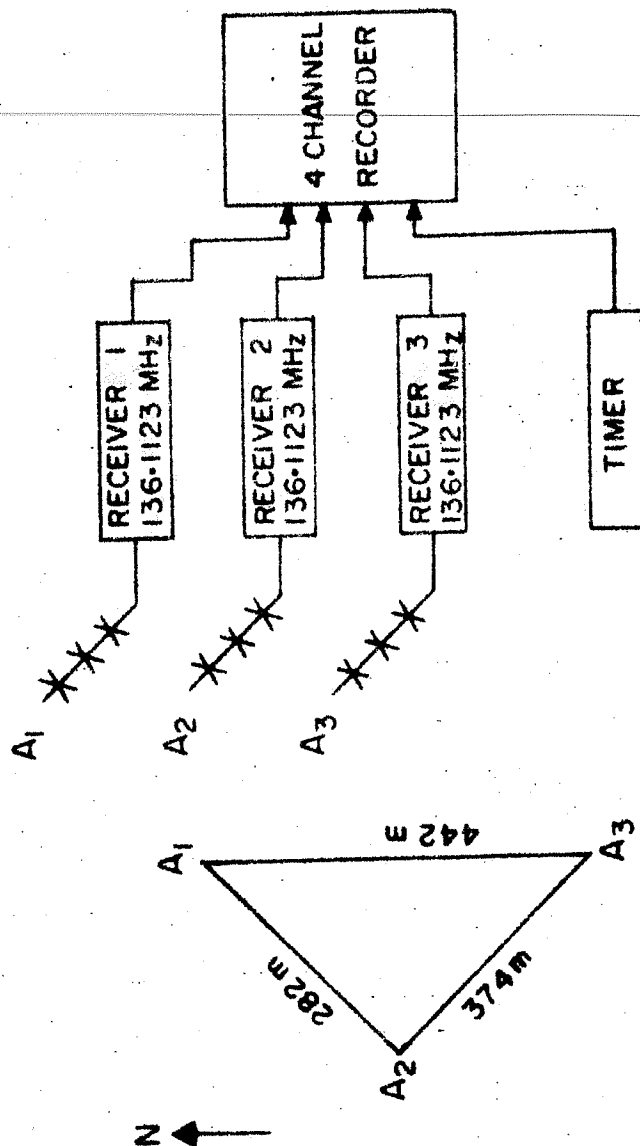


Fig.5.2 - Location of three receiving antenna A_1 , A_2 , A_3 at Tiruchirapalli.

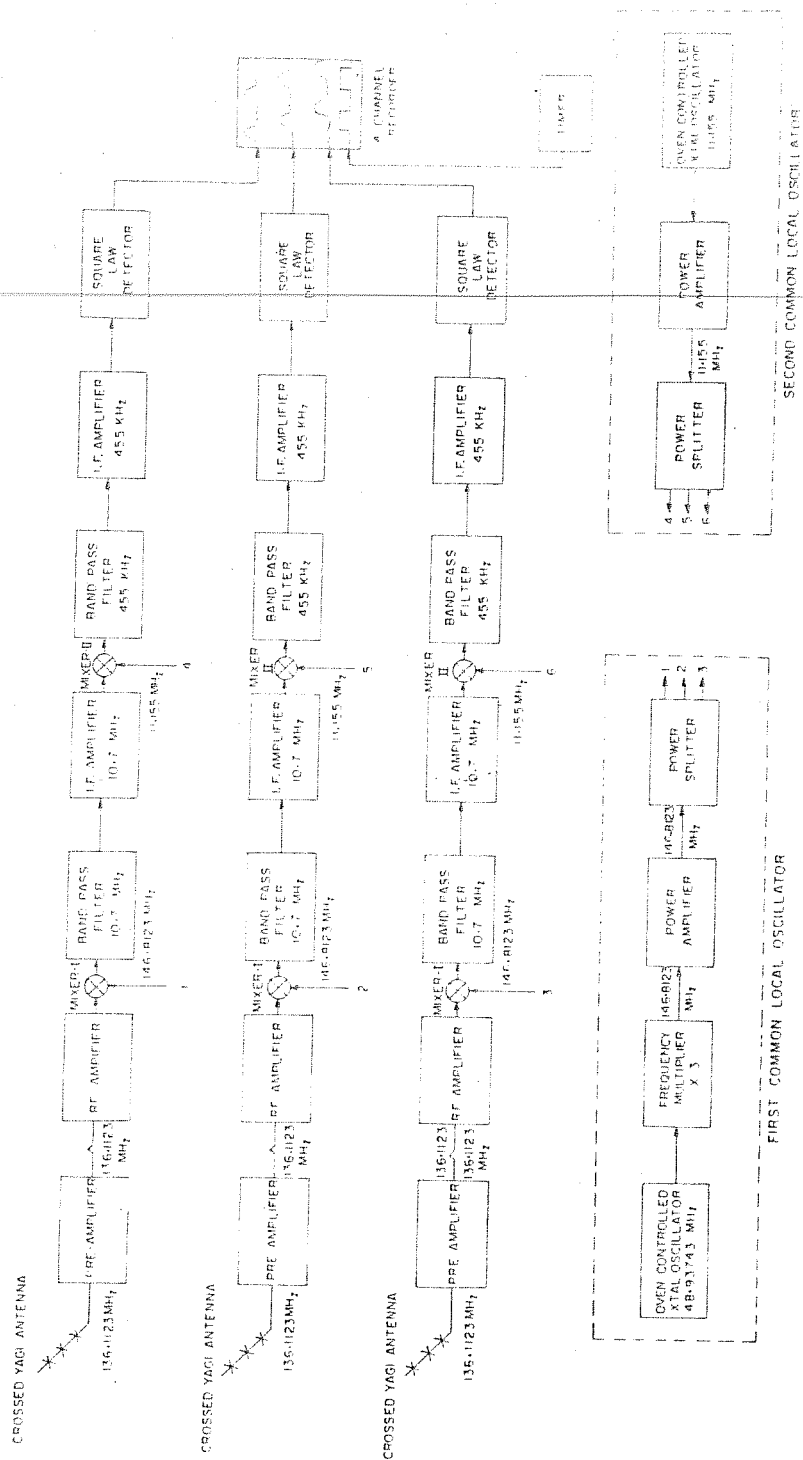


Fig.5.3 - Complete block diagram of receiving system.

amplified, detected and recorded on a fast response (60 Hz) chart recorder. The three receiver out-puts were recorded on three channels of the recorder and the fourth channel was used for time marking.

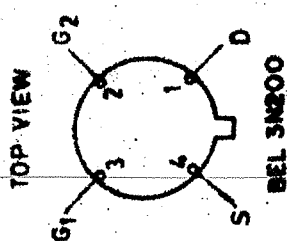
The special features of these receiving sets are that (i) local oscillator signals are derived from common crystal oscillators. This avoids the error of differential phase change in the records of the three receivers and (ii) these crystal oscillators are oven controlled and have short-term stability of the order of 1 part in 10^7 . As all the three receivers are identical we describe in some detail the various sub-systems of one of these receivers.

5.4.1 Receiving antenna

The antenna is a twelve element crossed yagi, with ~~one~~ driven element and eleven parasite elements. This has a measured gain of 8 dB relative to dipole antenna at the same frequency. Its output impedance is 50 Ohms. The driven element is connected to the 50 Ohms transmission line, via a 'T' match. The crossed yagi antenna has been used in circularly polarised mode, so as to avoid the effect of Faraday rotation of radio waves in the ionosphere.

5.4.2 Preamplifier

The signal received by crossed yagi antenna is amplified by a preamplifier. The preamplifier (Fig.5.4) consists of two stages,



	37 IN SWG ON	$\frac{3}{8}$ "	DIAMETER OR 1 CM D
L ₁	"	"	"
L ₂	"	"	"
L ₃	"	"	"
L ₄	"	"	"

—

has a measured gain of 35 dB. Its noise figure is less than 3 dB and 3 dB bandwidth is 1.5 MHz. The D.C. power to this amplifier is sent through the output cable with output signal riding over it thus avoiding additional cable for D.C. supply. The input and the output impedances are 50 Ohms. The signal from preamplifier is brought to the recording room and is again amplified by RF amplifier before feeding to the first converter.

5.4.3 First Converter

The amplified signal is converted down to 10.7 MHz by mixing with a first local oscillator signal at 146.3123 MHz. This is amplified in the 10.7 MHz IF amplifier as shown in Fig.5.5. The local oscillator signals for all these receivers are derived from a common crystal oscillator of 48.93743 MHz. The signal from this oscillator is tripled, amplified and power splitted as shown in Fig.5.6.

5.4.4 Second converter

The 10.7 MHz output signal of first converter is further mixed with the second crystal oscillator (local) signal at 11.155 MHz resulting in 455 kHz (2nd IF) signal. The signal at 455 kHz after second conversion is passed through a band pass filter (Piezo ceramic) in order to reduce the overall bandwidth of the receiving system. This helps in improving the signal to noise ratio. The circuit diagram for this converter stage (2nd mixer, filter and IF amplifier) is shown in Fig.5.7.

I. F. AMPLIFIER

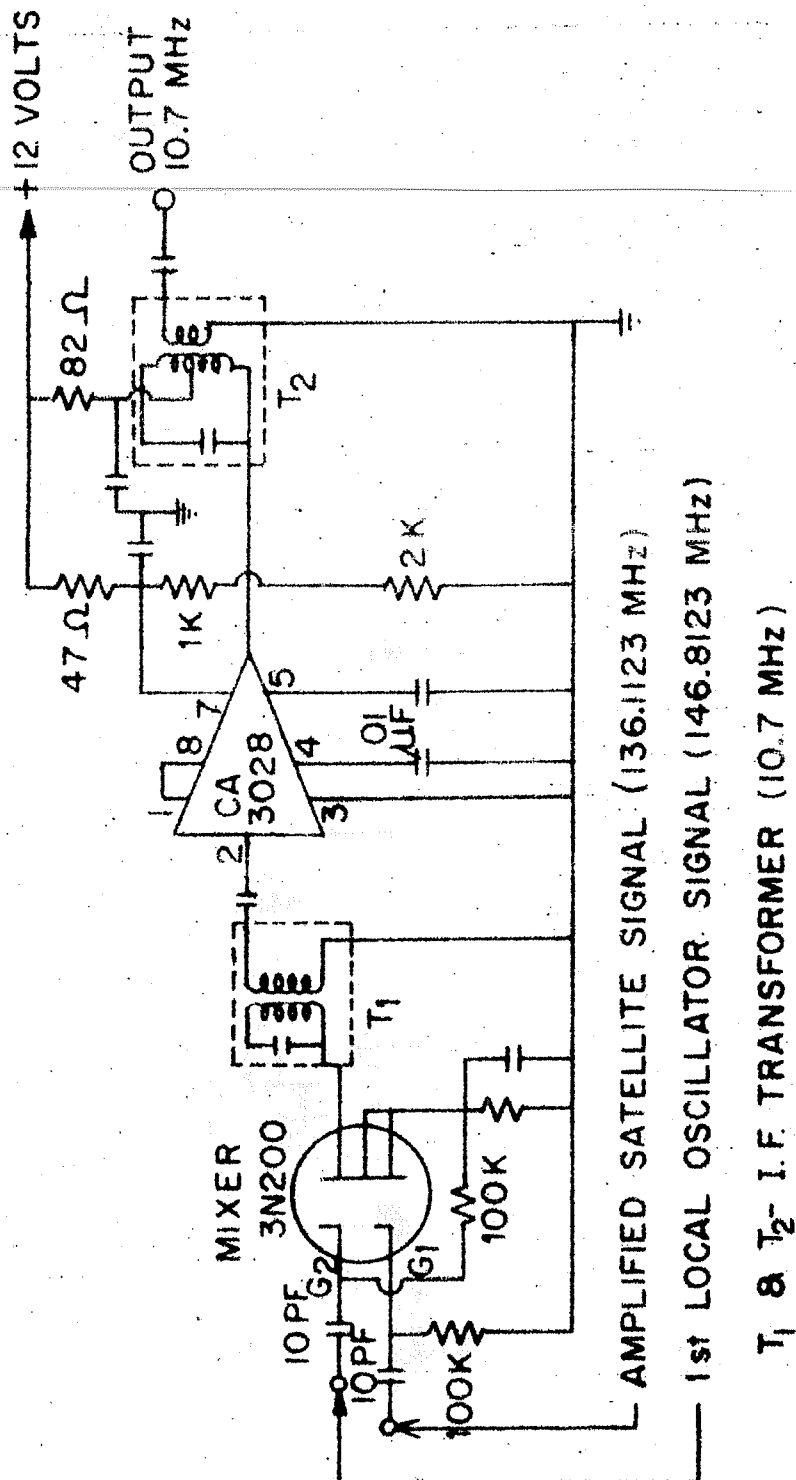


Fig.5.5 - Circuit diagram of mixer (first converter) filter and 10.7 MHz IF amplifier.

CRYSTAL OSCILLATOR

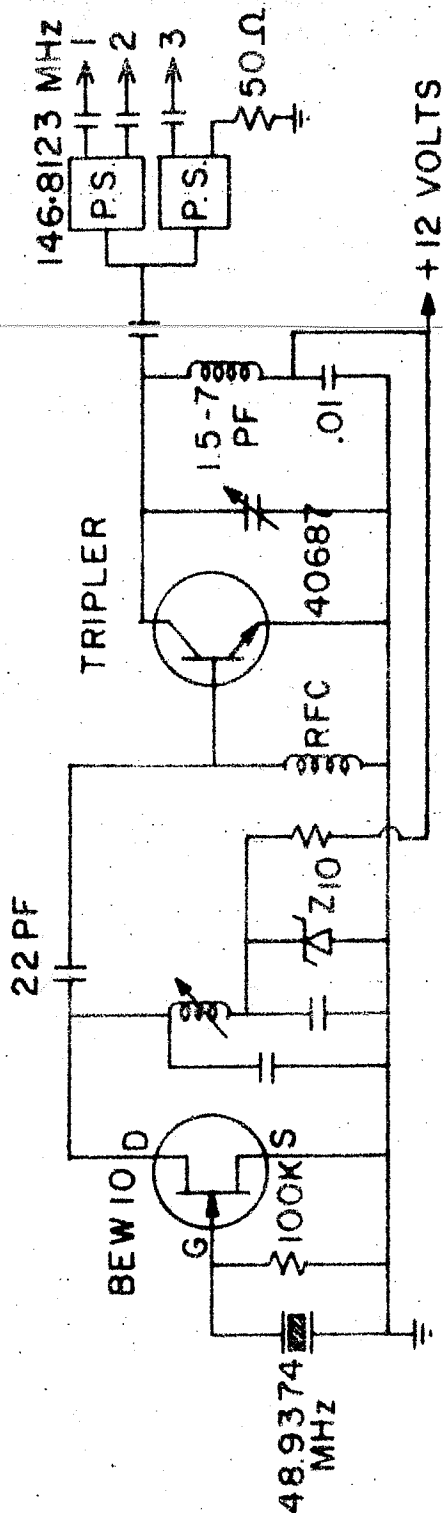


Fig.5.6 - Circuit diagram of common local oscillator at 146.8123 MHz.

I. F. AMPLIFIER 455 KHZ

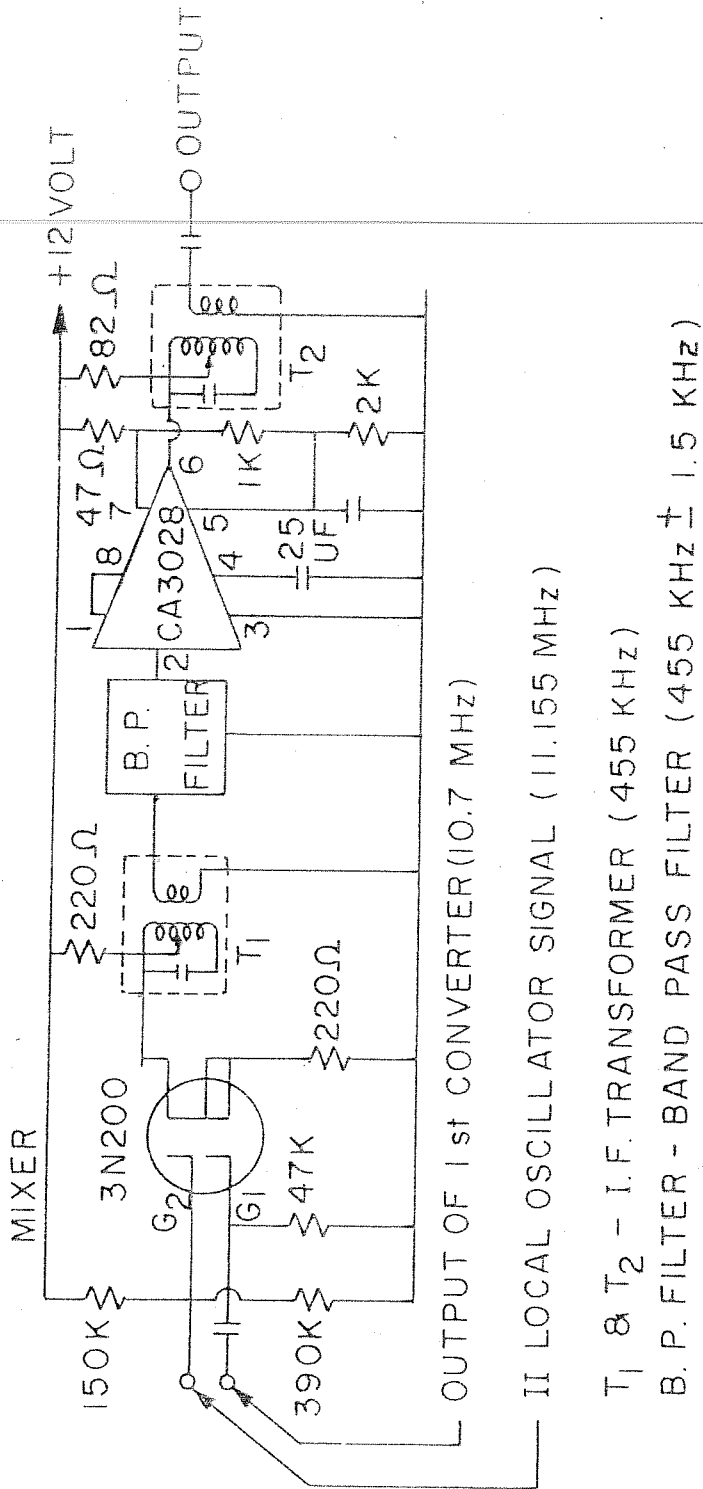


Fig.5.7 - Circuit diagram of mixer (second converter), filter and 455 kHz IF amplifier.

Like the first converter stage in this stage the local oscillator (Fig.5.8) is common for all the three receivers.

5.4.5 Detector

The doubly down converted and amplified signal is detected by a square law detector. In this I.C. MC 1596 which is double balanced modulator is used as a product detector with 455 kHz. IF signal is applied to both the inputs (Fig.5.9). The output is decoupled to bypass RF ripples. The detected balanced output is fed to an operational amplifier LM301 in differential mode and integrated (Fig.5.9). A 100 Ohm potentiometer is used as part of load of MC1596 to balance out the DC off-set in the system. Differential amplifier output is recorded on paper chart recorder. The voltage output of the detector is proportional to power or square of the amplitude of the received signal at the antenna. Thus recording in this system is linear for power of signal received.

To facilitate audio-monitoring of the satellite signal, a beat frequency detector (Fig.5.10) and a variable frequency oscillator (BFO) using a varicap diode, which generates signals of $455 \text{ kHz} \pm 5 \text{ kHz}$, has been incorporated in all the three receivers. The 455 kHz IF signal is mixed with BFO signal to produce a audio 0-5 kHz, thus indicating the presence of the satellite signal.

CRYSTAL OSCILLATOR

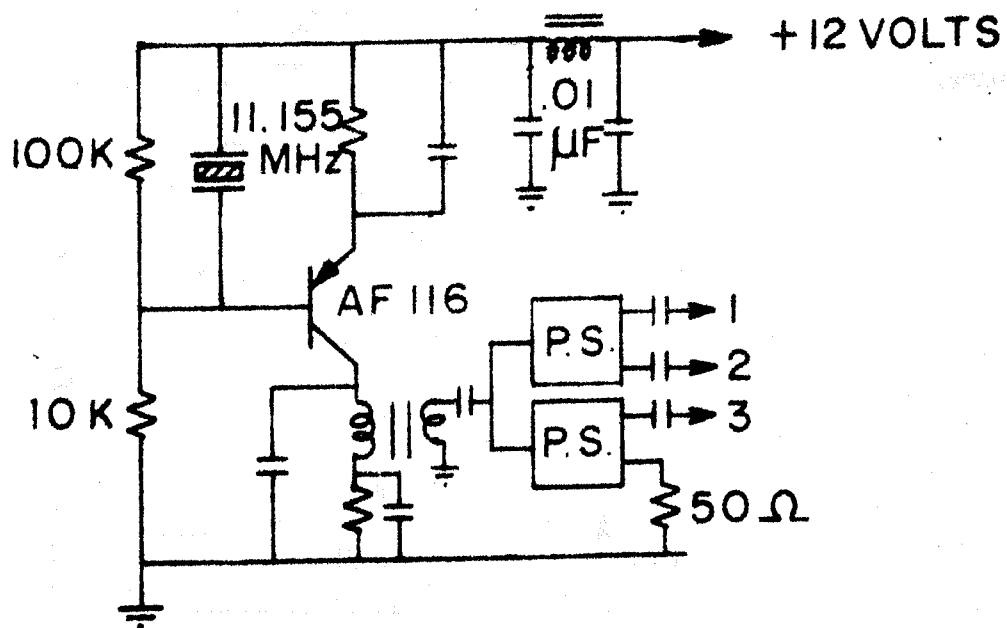


Fig.5.8 - Circuit diagram of common local oscillator at 11.155 MHz.

SQUARE LAW DETECTOR

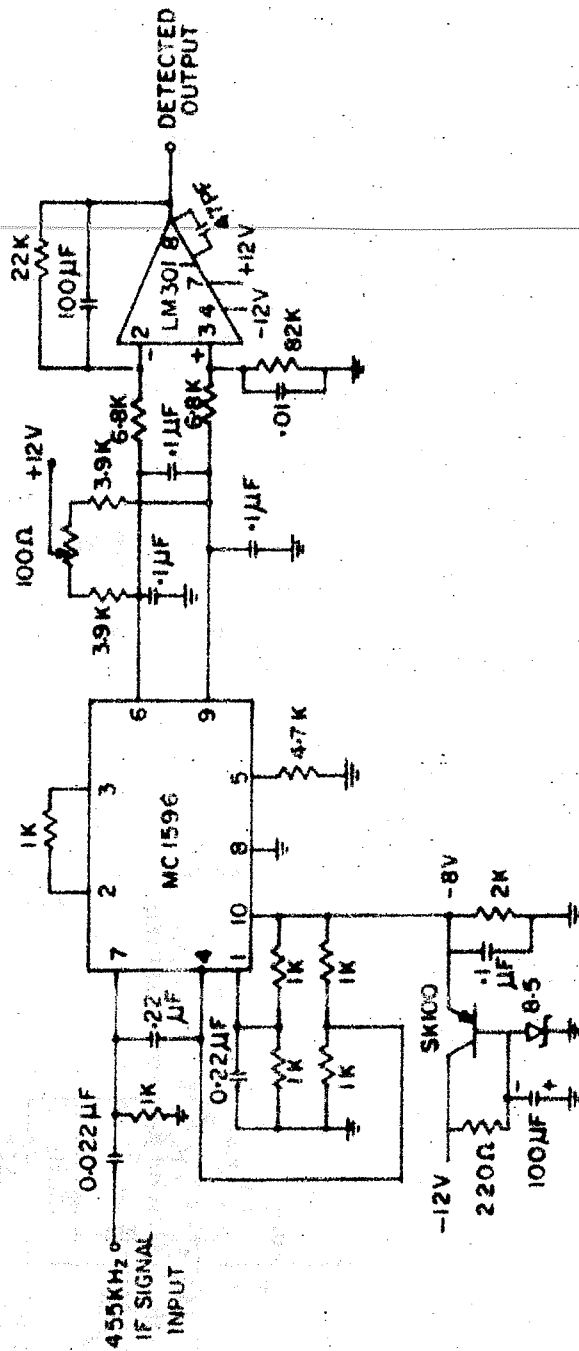
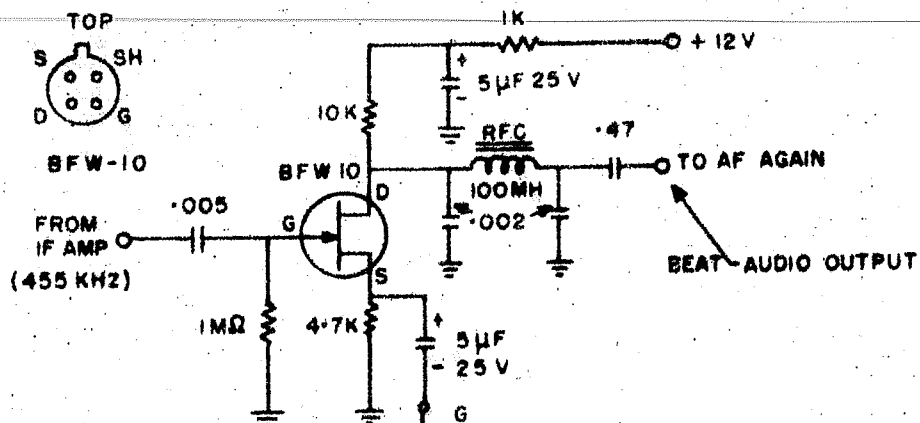


Fig.5.9 - Circuit diagram of square law detector and dc amplifier.

BEAT FREQUENCY DETECTOR



V F O (455 ± 5 KHz)

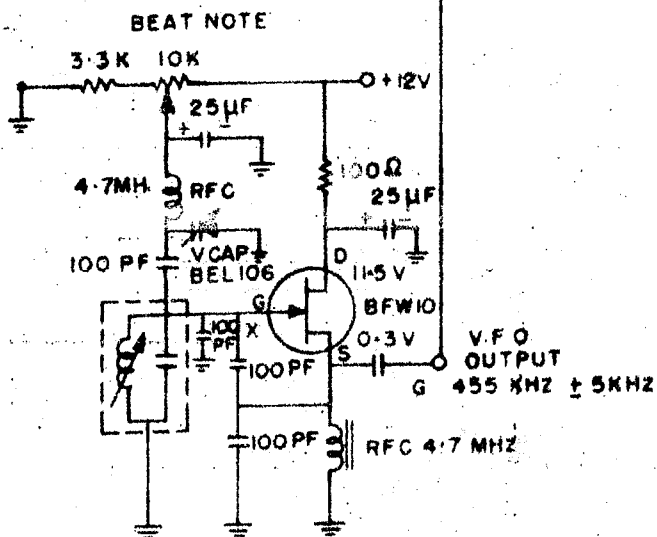


Fig.5.10 - Circuit diagram of beat frequency detector.

All the three receivers are narrow band super hetrodyne receivers. The overall characteristics of each of them are as follows:-

Input impedance	= 50 Ohms
Nominal frequency	= 136.1123 MHz
First IF	= 10.7 MHz
Second IF	= 455 kHz
Overall gain	= 140 dB
Overall bandwidth	± 1.5 kHz at -3 dB point
Threshold sensitivity by better than	-138 dbm
Image rejection	> 50 dB
Second IF bandwidth	= ± 1.5 kHz at -3dB point and ± 10 kHz at -60 dB point.

Preliminary results are presented in the following paragraphs. Fig.5.11 shows a sample amplitude ~~records~~ of 28th January 1978.

5.5 Scintillation Index

It is necessary to assign one index or few indices which can characterise the degree to which a signal is scintillating. The properties of such an index are (i) it should describe in full the characteristics of scintillation, (ii) it should have clear relation with the statistics of the scattered wave, (iii) at the same time it should be quickly calculable. All these requirements could possibly be fulfilled only by using two indices.

ETS-2 AMPLITUDE RECORDS (136 MHz) AT TIRUCHIRAPALLI
28 JAN. 1978 2330 HR 75° EMT

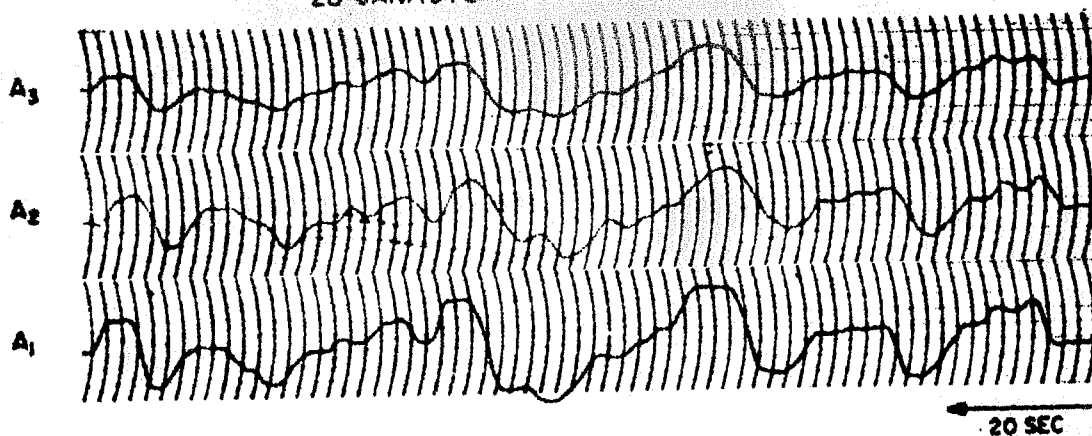


Fig.5.11 - Sample amplitude records (136 MHz) at
Tiruchirapalli on 28 January 1978
at 2330 hr 75° EMT.

One of them could be an exact index for investigating the characteristics of the irregularities, while the other should be an approximate index used for comparing the records from different observatories and especially for correlation with other geophysical phenomena. However, to ensure the reliability of this approximate index, there should be one to one relation between these two indices, so that the exact index could be estimated from the approximate index and vice versa (of course with some error). Exact or purely statistical indices were given by Briggs and Parkin (1963) as follows:

$$S_1 = \frac{1}{R} \left| \overline{(R - R)} \right| \quad (\text{normalised deviation of signal amplitude})$$

$$S_2 = \frac{1}{R} \left| \overline{(R - R)^2} \right|^{\frac{1}{2}} \quad (\text{normalised root mean square deviation of signal amplitude})$$

$$S_3 = \frac{1}{R^2} \left| \overline{(R^2 - R^2)} \right| \quad (\text{normalised deviation of signal power})$$

$$S_4 = \frac{1}{R^2} \left| \overline{(R^2 - R^2)^2} \right|^{\frac{1}{2}} \quad (\text{normalised root mean square deviation of signal power})$$

where R and R^2 are the instantaneous amplitude and power of the received signal, and the bar ($\overline{\quad}$) indicates the average. The advantage of these indices is that their quantitative values have a real physical meaning and provide information about the physical conditions of the region producing scintillation e.g.

size and strength of the irregularities (Briggs and Parkin 1963, Bischoff 1967, Vats and Deshpande 1979).

The calculation of the exact indices is almost impossible when the signal is recorded on the chart. To overcome these difficulties a number of indices which are termed as approximate indices are used. The most commonly used in the very early investigations is visual index. It only describes the sample visually by assigning a number ranging from 0 to 5. A more quantitative approximate index is the fluctuation rate or number of fade per unit time determined by counting all amplitude maximum and/or minimum in the sample.

The widely used approximate scintillation index (SI) (Whitney et al. 1969) that has been adopted by Air Force Geophysical Laboratory and the Joint Satellite Studies Group is:

$$SI = \frac{P_{\max} - P_{\min}}{P_{\max} + P_{\min}} \times 100 \quad (5.1)$$

This relationship was developed specifically for scaling from paper chart records of scintillation. Some of the research workers used this index without multiplying by 100. An 'arbitrary rate' is used for selection of P_{\max} and P_{\min} , P_{\max} is the power of the third peak down from the maximum excursion and P_{\min} is the power of the third level up from the minimum excursion. It is realised that this definition of scintillation index

offers little help towards understanding the relationship between properties of irregularities and their effects on radio wave propagation but it does result in a standard method of scaling which allows comparison of scintillation analysis between various experimenters.

5.6 Scintillation Observation at Tiruchirapalli

Scintillation index is calculated using equation (5.1) from the scintillation records. Fig.5.12 shows occurrence frequency of scintillation during night hours for the months April, June and December of the year 1978, which represents occurrence frequency of scintillation during equinoxes, summer and winter. For all the seasons the occurrence frequency of scintillation is maximum around mid-night hours. The maximum occurrence frequency is about 70% during equinoxes whereas it is about 40% during summer and winter seasons.

Fig.5.13 shows the mass plot of the scintillation index (at the top) and the drift velocity (at the bottom) as a function of local time for 6th to 10th February 1978. The drift velocities were calculated using time delay method. The scintillation index is ranging between 30% and 70%. The drift velocity is ranging between 100 m/s and 250 m/s. The drift direction is towards east.

ETS-2 TIRUCHIRAPALLI 1978

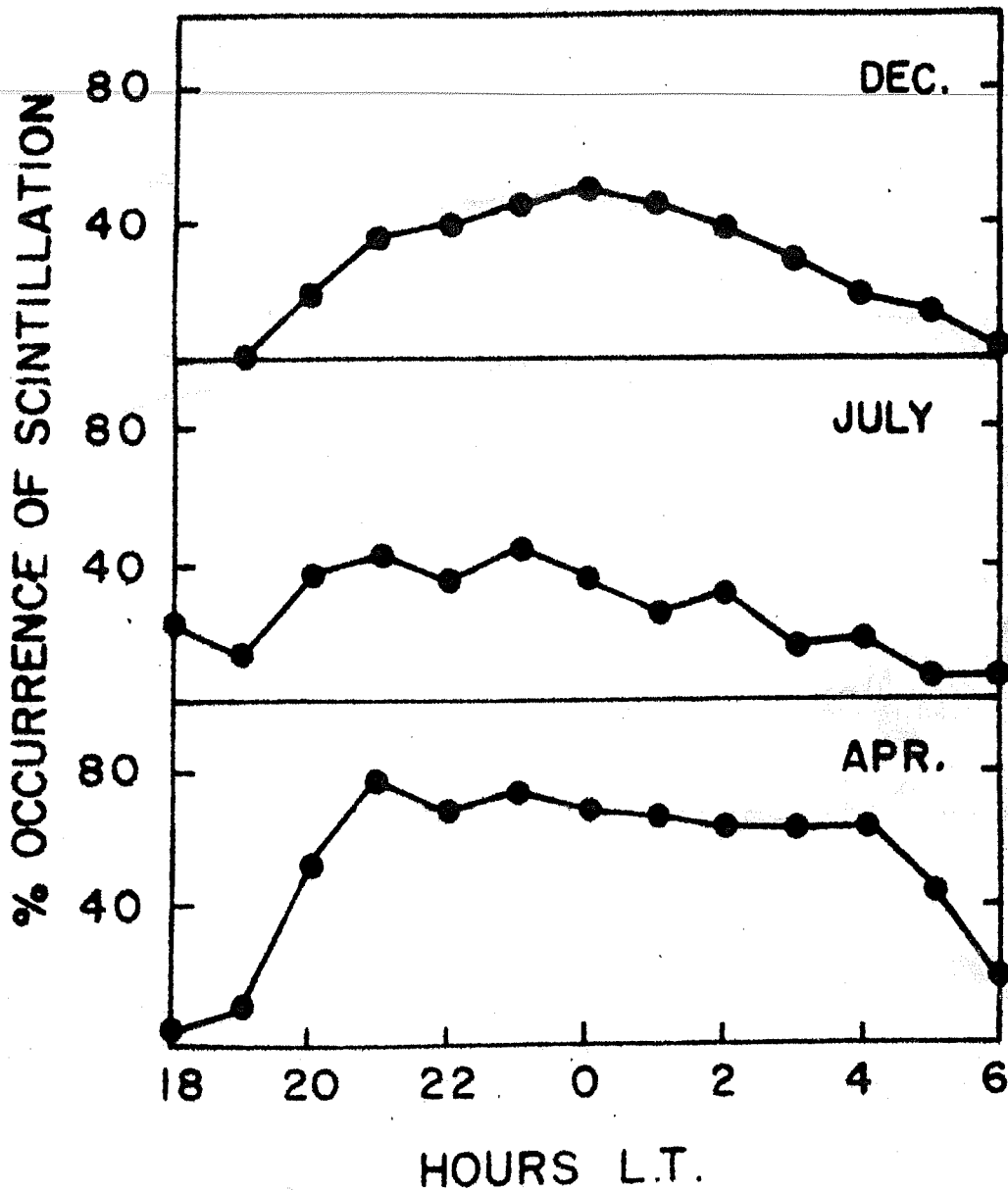


Fig.5.12 - Occurrence frequency of scintillation during night hours for the months of July, April and Dec. 1978.

TIRUCHIRAPALLI ETS - 2
(FEB, 1978)

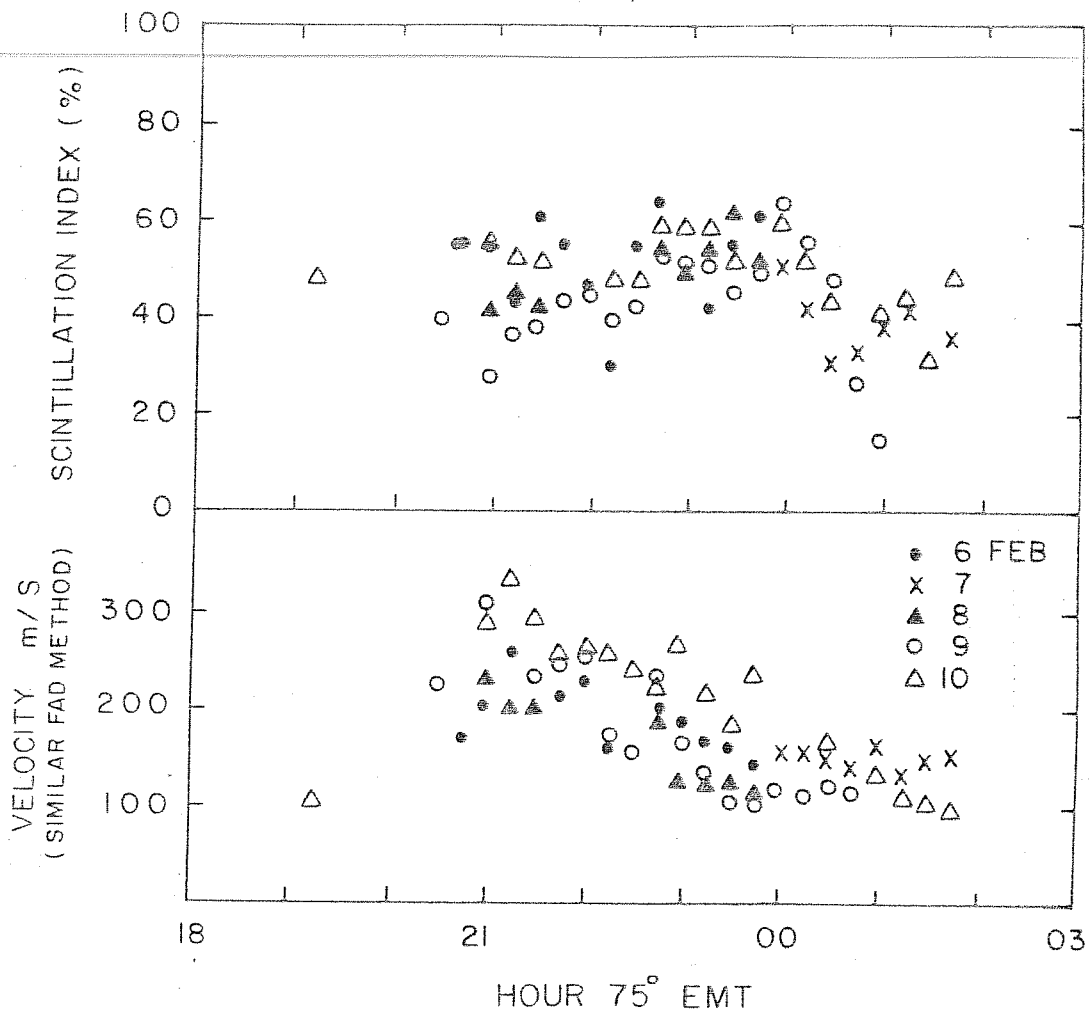


Fig.5.13 - Variation of scintillation index (at the top) and drift velocity (at the bottom) as a function of local time for 6th, 7th, 8th, 9th and 10th Feb. 1978.

5.7 Comparison of drift speeds and directions as obtained by spaced fading experiment and spaced scintillation experiments

In an attempt to compare drift speeds and directions as obtained by two different experiments (spaced fading experiment and spaced scintillation experiment) night-time F-region observations were conducted simultaneously.

The ground diffraction pattern in the spaced fading experiment (H.F. drifts) moves with a velocity twice that of the irregularities, whereas in the spaced scintillation experiment the speed at ground equal to the speed of the ionospheric irregularities. Here we have derived velocity from the time delay method which does not require knowledge of correlation function. Fig.5.14 is the mass plot of drift speeds obtained by the two techniques. The mass plot shows that the drift speeds obtained by spaced scintillation experiment are relatively higher than those obtained by fading experiment. Fig.5.15 (lower portion) shows the histogram of the percentage occurrence of ratios of the drift speeds obtained by these experiments. To check whether the drift speed obtained by spaced scintillation experiment is nearly double the drift speed obtained by spaced fading experiment, the histogram of percentage occurrence of ratios of the drift speed obtained by spaced scintillation experiment divided by two to drift speed obtained by spaced fading experiment is plotted (upper portion of Fig.5.15).

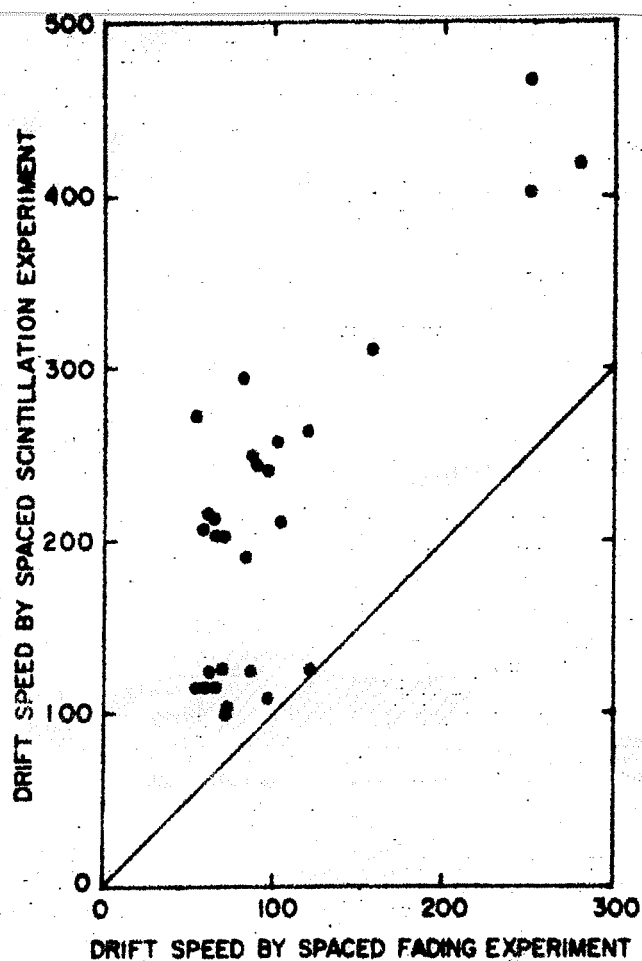


Fig.5.14 - Comparison of drift speed obtained by spaced fading experiment and by spaced scintillation experiment.

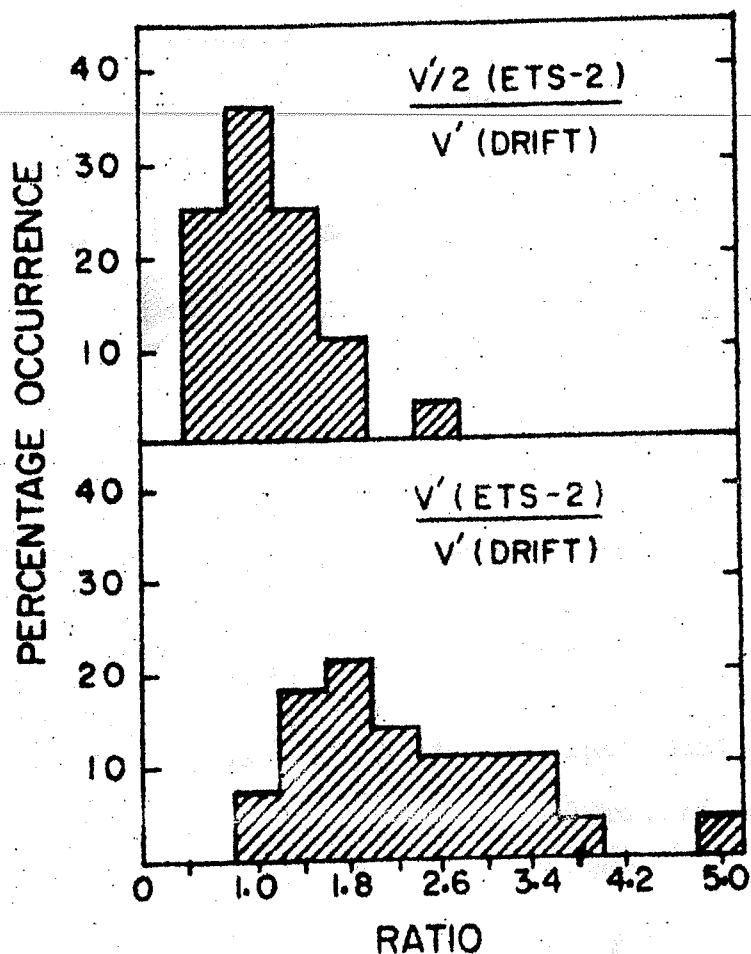


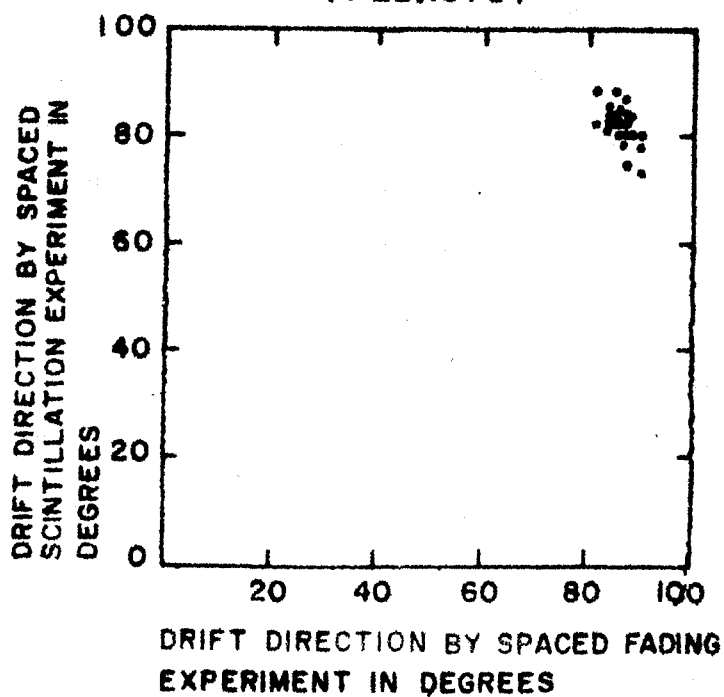
Fig.5.15 - Histogram of percentage occurrence of the ratio drift speed obtained by spaced fading experiment and spaced scintillation experiment.

Fig.5.16 shows drift directions of ionisation irregularities obtained by the two experiments which show good agreement with the direction being exactly eastward in both cases. The sub-ionospheric point of the ray-path is about 2° south of the station and hence measurements by these two experiments are not at the same location in the ionosphere. Chandra and Rastogi (1969) have shown the latitudinal variation of drift speed which shows large change close to the electrojet region which could be the reason for the difference observed in the velocities measured by two experiments. In addition to this, the spaced scintillation experiment measures the integrated effect over the entire F-region whereas spaced fading experiment gives the speed of the irregularities near the point of reflection. Another possibility of such difference can be due to the fact that we are observing different scale size of the irregularities in these two experiments.

5.8 Determination of the parameters of the irregularities by correlation analysis method

The scintillation records were digitized at an interval of 0.25 seconds which was found suitable for correlation analysis. The digitized values of the amplitudes were used in computing drift parameters using correlation analysis method. The drift parameters, apparent drift velocity (V_a), apparent drift direction (θ_a), true drift velocity (V), true drift direction (θ),

TIRUCHIRAPALLI
(FEB.1978)



5.16 - Comparison of drift directions obtained by spaced fading experiment and by spaced scintillation experiment.

characteristics velocity (V_c), major axis (a) and the minor axis (b) of the characteristic ellipse, the axial ratio r and the elongation of the ellipse (ψ) with respect to north were calculated for some records (see Table 5.2).

The true drift velocities and apparent drift velocities are not much different which indicates a small random velocity of irregularities. These results are in agreement with the drift observations using spaced receiver technique at H.F. (2.5 - 5.0 MHz) at the same station (Tiruchirapalli). The drift directions of true and apparent drift velocities are in good agreement. The irregularities are found to have an average (half-correlation) size of 400 to 500 metres in east-west direction and 2000 to 3000 metres in north-south direction. These results are in agreement with earlier observations of Koster (1966) in Ghana (Africa) employing similar technique.

5.9 Velocity spectrum and power spectrum by cross-spectral method

With this method of analysis one could find the amplitude and relative phases of the various Fourier components present in the records obtained from the three receivers. The phase shifts could then be converted into time shifts and using the aerial separation the velocity of motion of the individual Fourier component can be found out. If the components with different frequencies are moving with same velocity and there

Table 5.2

Date	Time	V_a M/s	ϕ_a	V M/s	ϕ	V_c M/s	Major axis a meters	Minor axis b meters	Axial ratio $\frac{a}{b}$	ψ
12-2-78	2230	53	91	45	91	27	2679	506	5.3	-1
12-2-78	2245	95	85	33 43	80	61	1713	433	4.0	10
12-2-78	2315	48	82	46	82	14	2281	256	8.8	8
12-2-78	2345	38	95	36	95	12	2325	333	7.0	-5
14-2-78	2115	77	85	65	88	28	2080	440	4.7	1

is no random motion, then the diffraction pattern would move steadily on the ground and all Fourier components derived from Fourier analysis of three fading records would have the same speed and fading directions.

Using cross-spectral analysis power, the drift velocity and directions were computed. Fig.5.17 shows the plots of velocities vs. fading frequency (in the middle), direction vs. fading frequencies (at the bottom) and relative power vs. fading frequencies (at the top). The velocity of the Fourier components is most of the time between 50 m/sec and 250 m/sec. Relative power (presented in arbitrary units) indicates the significance of that velocity component. The drift direction of all the component is found to be almost same for all components in all cases. This indicates that different Fourier components of drift velocity are having different magnitude, but they move in the same direction.

5.10 Probability distribution of amplitudes

As the word suggests the probability distribution provides information about the percentage occurrence of given amplitude range in specified time segments. Chytil (1967) theoretically showed that various amplitude distributions of VHF scintillation can be expressed by a general relation called as Nakagami-m distribution. In the case of weak scattering $m > 1$ and m distribution becomes Rice type, for $\frac{1}{2} < m < 1$ it becomes

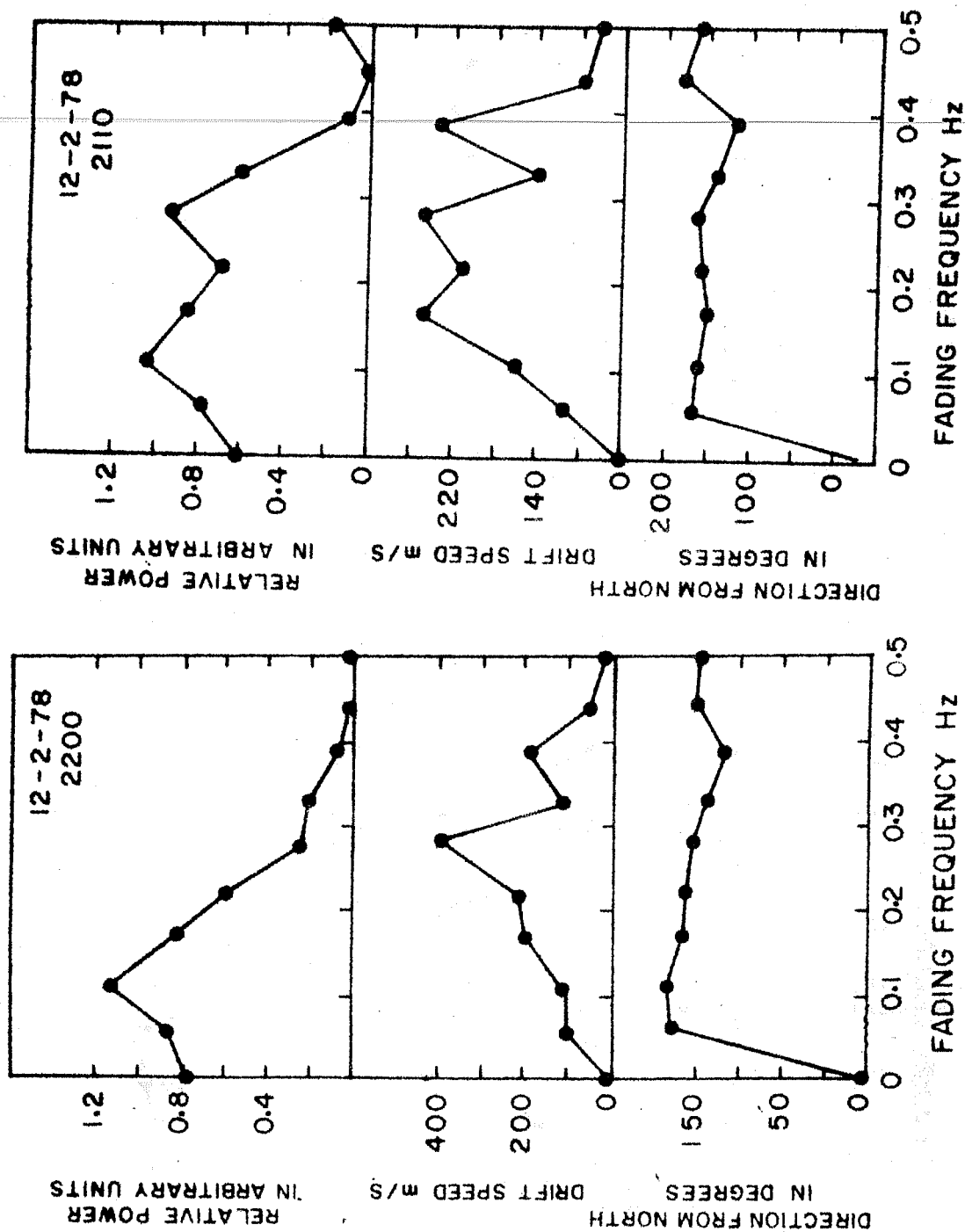


Fig.5.17 - Power, drift speed and direction plotted against fading frequency for a few P-region examples.

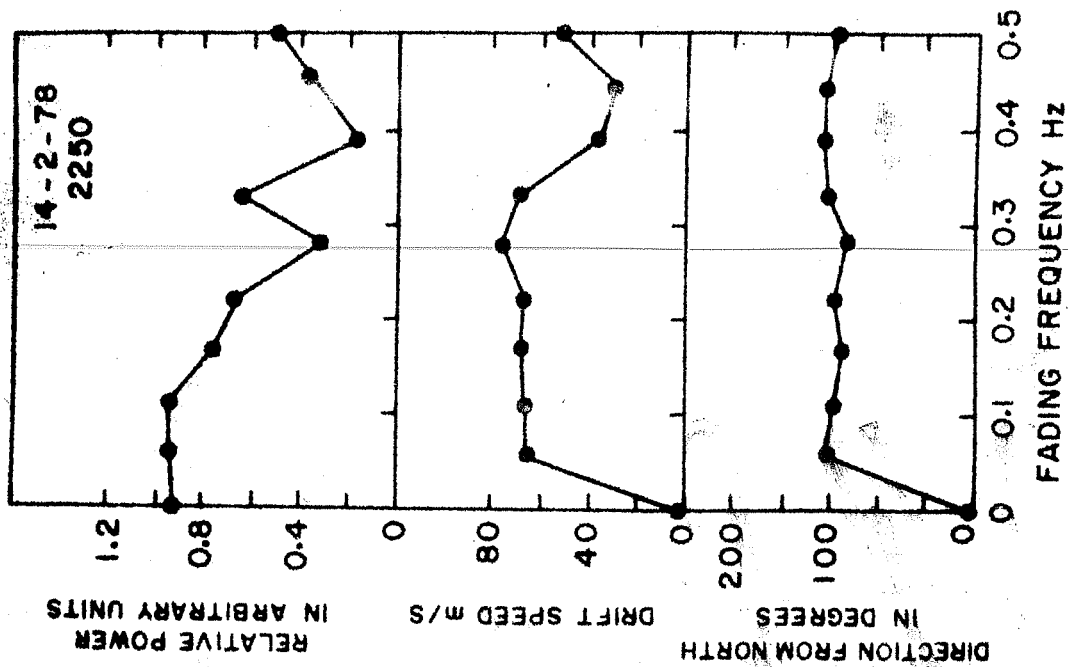
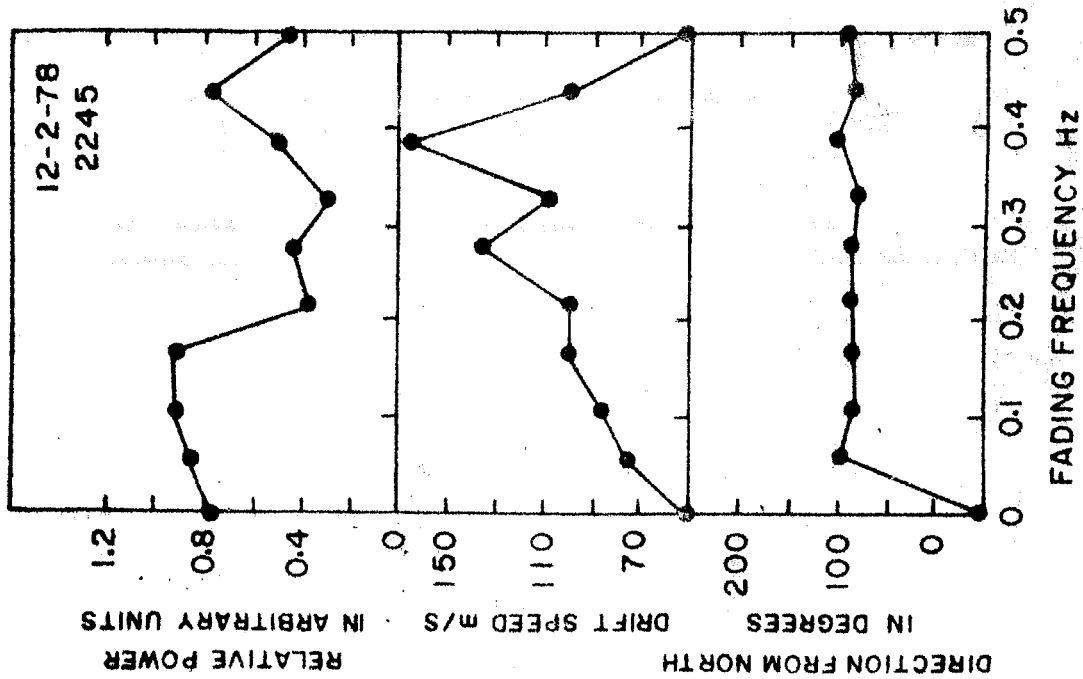


Fig.5.17 - Power, drift speed and direction plotted against fading frequency for a few F-region examples.

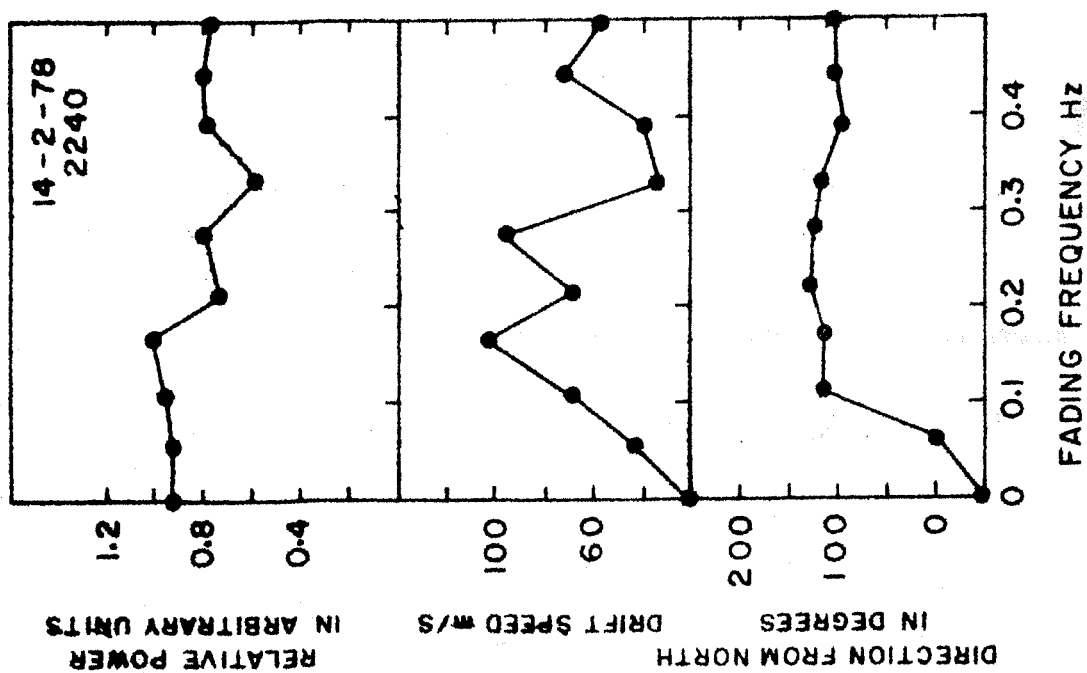


Fig.5.17 - Power, drift speed and direction plotted against fading frequency for a few P-region examples.

Hoyt distribution (or Nakagami q-distribution) for $m=1$ the Rayleigh distribution (strong scattering) and finally for $m=\frac{1}{2}$ it takes the form of one-sided Gaussian distribution (very strong scattering). The fact that the various amplitude distributions are functions of a single parameter m , it becomes very simple to determine the different conditions in the scattering region of the ionosphere. Nakagami- m distribution in the simpler form (Nakagami 1960) can be expressed as:

$$P(R) = 2(m/\Omega)^m \Gamma^{-1}(m) R^{2m-1} \exp(-mR^2/\Omega) \quad (5.2)$$

where $\Omega = \overline{R^2}$; $m = \overline{R^2}^2 / ((\overline{R^2} - \overline{R^2})^2)^{-1}$, only $m \geq \frac{1}{2}$;

R is the instantaneous amplitude and Γ is Gamma function.

The parameter $m = 1/S_4^2$ where S_4 is as defined earlier in 5.5.

Probability distribution of the record on 2nd February 1978 at 0225 hr is shown in the left portion of Fig. 5.18. Dashed line indicates theoretical probability distribution which agrees very well with experimental results. Root-mean square amplitude is 3.4. Here m value is 4.7 which shows weak scattering case.

5.11 Message Reliability

Message reliability analysis gives an estimate of the increase in fade margin which is required over the value specified by the cumulative amplitude probability distribution function (cdf) to obtain a given probability of receiving perfect

ETS-2 TIRUCHIRAPALLI
136 MHz
15-2-78 0225 HRS

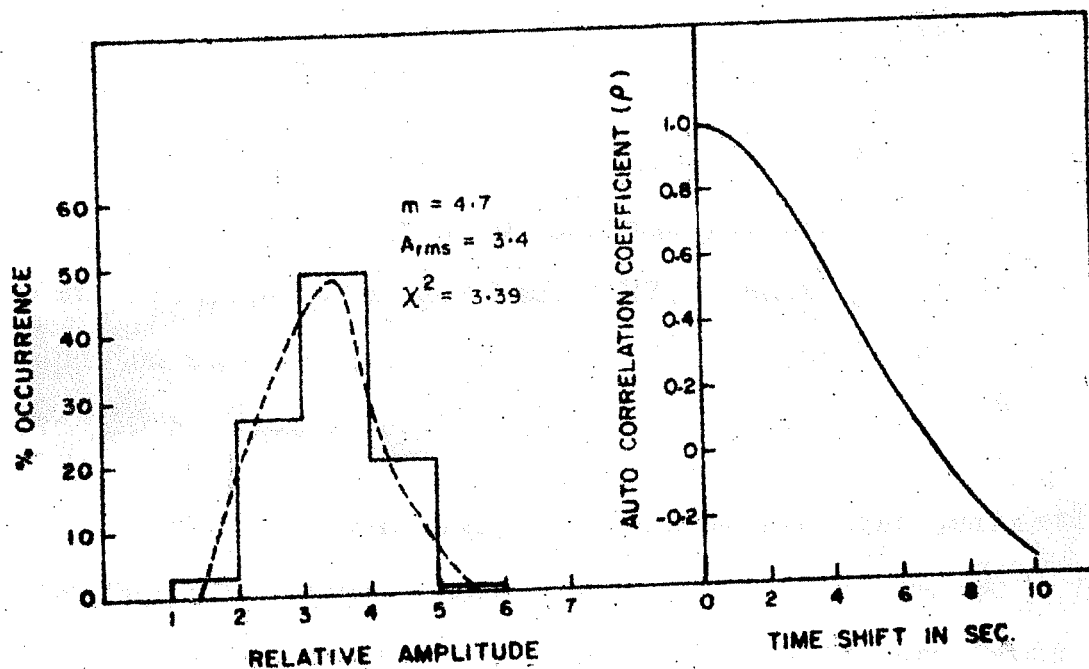


Fig.5.18 - Comparison of amplitude distribution with theoretical distribution (on the left). Typical auto-correlogram for night-time scintillation event on Feb.15, 1978 (on the right).

messages. Message reliability is measured by determining the number of time intervals or messages that completely fit within the signal enhancement or increases above specified calibration levels compared with the total possible number in a 5.0 minute period. Since the calibration levels are relative to the median level, these will represent various values of fade margin. As the time interval or message length approaches zero, the message reliability approaches the percentage given by the cdf at that level. Therefore cdf gives maximum possible value of message reliability (Whitney and Basu 1977). Whitney and Basu (1977) reported such investigations using amplitude recordings of 137 and 360 MHz at Huancayo, Peru.

In Fig.5.19 percentage of message received perfectly is shown as a function of message length on 15th February 1978 at 0225 hr LT for the fade margin -2 dB, -4 dB, -6dB, -8dB and -10dB at 136 MHz (recorded at Tiruchirapalli). It is seen that for the highest fade margin percentage of the perfect message received is about 50% for the message length of 50 sec and for the lowest fade margin it reaches 50% for message length of 10 sec and goes to zero for message length of 30 sec. Hence it is clear that as message length increases the message reliability reaches zero value.

ETS-2 TIRUCHIRAPALLI
136 MHz
15-2-78 0225 HRS

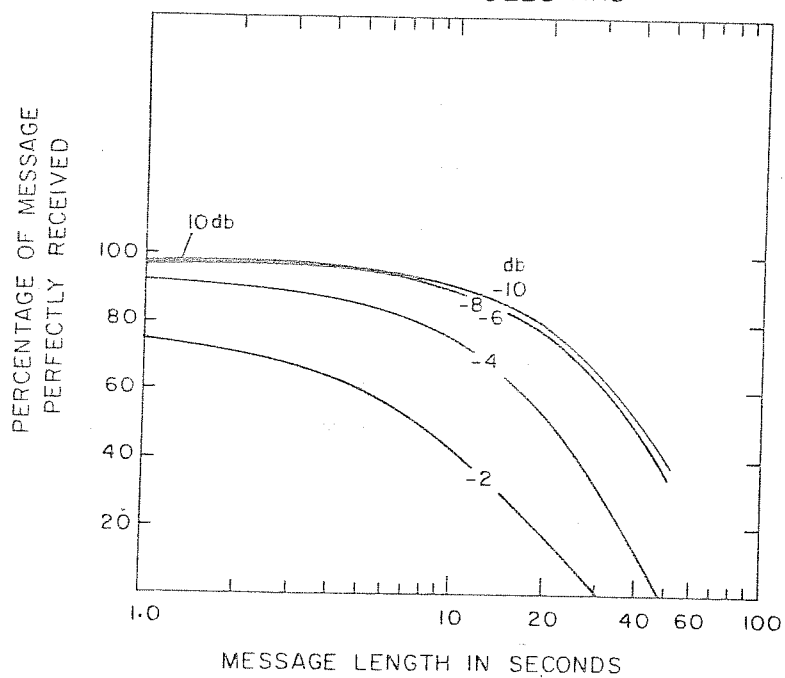


Fig.5.19 - Effect of scintillation on the reception of perfect messages of different message lengths for various fade margins (message reliability plots).

5.12 Auto-correlation of the received signal

The auto-correlation is the measure of comparison between the values of a function and the values of the same shifted function. It is especially useful in characterising the properties of irregular functions. The auto-correlation function is another way of inferring fading rate. It is the Fourier transform of the power spectrum and therefore has a width which is proportional to the bandwidth of the power spectrum.

Fig.5.18 (right portion) shows the autocorrelogram of 136 MHz at Tiruchirapalli on 15th February 1978 around 0225 hr LT.

The term auto-correlation time is defined as the time at which autocorrelation coefficient reduces to 0.5. If the scintillation is single scattering type the auto-correlation time is larger for the lower frequency and it is smaller for the higher frequency. This is due to the fact that the Fresnel dimension at the lower frequency is larger than that at higher frequency. In the case of multiple scattering type scintillation, the major scale of diffraction pattern is reduced by the factor of phase deviation and since the phase deviation increases faster with wave length than the Fresnel dimension, the larger Fresnel dimension at lower frequencies is more than off set by a factor of phase deviation (Yeh et al. 1975). Fig.5.18 (right portion) shows that the auto-correlation time is about 4 sec.

CHAPTER - VI

CONCLUSIONS AND SUGGESTIONS

The present investigations deal with the studies of movement and irregularities in the upper atmosphere (ionosphere). The study is based on (a) the results derived from the drift measurements at Ahmedabad during the period 1970-75 and from published drift data at Yamagawa and Sibilizmir, (b) the analysis of the geomagnetic H field data at Huancayo and at a chain of magnetic observatories at 74°E longitude and (c) the preliminary results of the spaced receiver scintillation experiment carried out at Tiruchirapalli (dip 4.8°N).

In this chapter the main conclusions of the present work have been summarised and also some suggestions for future work in this field, have been given.

The main conclusions are as follows:

(i) The circulation pattern at E-region altitude is of a global scale indicating zonal flow westward during winter and eastward during summer with change over during equinoxes (barring the equatorial latitudes where electric field determines the drift pattern).

(ii) The mean drift speeds at equatorial (Thumba), low-latitude (Ahmedabad) and at high-latitude (Sibilizmir) stations

are found to decrease with the increase in the solar activity.

(iii) A systematic change with latitude is observed in the magnetic activity effects in the mean drift speeds. Drift speeds are found to increase with increase in magnetic activity at high latitudes and decrease at the equator with a change over at about 40° dip. This is consistent with the idea of the imposition of electric fields of magnetospheric origin which is opposite to the S_q field at equator but in phase at the high latitudes.

(iv) Lunar tides in drifts at all stations show semimonthly oscillations with almost constant phase. The amplitude of semimonthly oscillations is found to increase in the equatorial region.

(v) Effects of the interplanetary magnetic field on drifts at Ahmedabad showed a decrease in the eastward component of drift with the increase in the northward component (B_z) of interplanetary magnetic field. However, increase in the eastward component is found with the increase in the B_y component of the interplanetary magnetic field.

(vi) The eastward component of the E-region drift at Ahmedabad during sporadic E is directed more towards east than for normal E-layer. Thus a consistent shift of the zonal component towards east is clear whenever Es is present.

(vii) Solar variations of geomagnetic H field at Huancayo showed time of maximum of diurnal and semidiurnal waves advance towards noon with the increase of average sunspot number. Amplitudes of diurnal and semidiurnal waves are found to increase linearly with the solar activity. Amplitudes of both the waves (diurnal and semidiurnal) are found to be seasonal dependent with peaks during equinoctial months. Comparison of these results with those at Trivandrum showed that the seasonal variation of the amplitudes is similar at two places but that of time of maximum is opposite in phase.

(viii) In the northern winter and equinoxes the H, and X and Y variations at low and middle latitudes have abnormally high amplitude on counter-electrojet days in the Indian region which gives indication that counter-electrojet could be related to intensification on certain days of normally weak winter hemisphere S_q current system in the Indian region.

(ix) During winter months there is marked change in the wind system at low latitudes (Ahmedabad) during counter-electrojet events. The zonal wind which is predominantly westward during winter changes to eastward during counter-electrojet events.

(x) Drift measurements using spaced scintillation experiment (F-region) in the equatorial region are found to be greater than the simultaneous drifts measured by HF fading experiment, the drift direction being same. The drifts measured by spaced

scintillation experiment are ranging between 100 m/s and 250 m/s. The occurrence frequency of scintillation is maximum during equinox. The scintillation is observed maximum around midnight hours.

Suggestions for Future Work

From the work reported in this thesis it is felt to have closer network of drift stations at low-latitudes, covering from dip equator to S_q focus. This will avail the opportunity for understanding the wind pattern in detail at low-latitudes during counter-electrojet events. This network will also avail the opportunity for the study of variations of S_q focus position with drift as there are two more magnetic observatories installed between Alibag and Sabhawala viz. at Ujjain and Jaipur.

A better global wind model can be built using extensive measurements at different latitudes on a global scale.

With spaced receiver technique employing partial reflections it is possible to have continuous measurements with good time resolution as well as with reasonable height resolution in the entire range of 60 to 110 km. This enables one to study height profiles of different components (viz. planetary, tidal and gravity waves) and their propagation characteristics.

REFERENCES

- | | | |
|----------------------------------|------|---|
| Aarons J. | 1973 | J. Geophys. Res., <u>78</u> , 7441. |
| Aarons J. | 1975 | Proc. on the Beacon Satellite investigations of the ionosphere structure and ATS-6 data, Nov. 1974, Moscow, <u>1</u> , 184. |
| Aarons J. and Allen R.S. | 1966 | Rad. Sci. <u>1</u> , 1180. |
| Aarons J. and Whitney H.E. | 1968 | Planet. Space Sci., <u>16</u> , 21. |
| Aarons J., et al. | 1963 | J. Geophys. Res., <u>68</u> , 3159. |
| Aarons J., et al. | 1967 | J. Geophys. Res., <u>72</u> , 2891. |
| Appleton E.V. and Barnett M.A.F. | 1925 | Nature (London), <u>115</u> , 333. |
| Baker W.G. and Matyn D.F. | 1953 | Phil. Trans. Roy. Soc. (London), <u>A246</u> , 281. |
| Balsley B.B. and Woodman R.F. | 1971 | World Data Center-A Report UGA-17. |
| Bartels J. and Johnston H.F. | 1940 | Terr. Magn. & Atmos. Electr. (USA), <u>45</u> , 269. |
| Basu S., et al. | 1964 | J. Atmos. Terr. Phys., <u>26</u> , 811. |
| Bhandari S.M. | 1978 | Ph.D. Thesis, Gujarat University, Ahmedabad. |
| Bhargava B.N. | 1964 | J. Inst. Telecom. Engrs., <u>10</u> , 404. |
| Bhargava B.N. and Sastri N.S. | 1977 | Ann. Geophys., <u>33</u> , 329-655. |
| Bischoff K. | 1967 | Geomag. and Aeron., <u>7</u> , 655. |

- | | | |
|-----------------------------------|------|--|
| Bolten J.G., et al. | 1953 | Aust. J. Phys., <u>6</u> , 434. |
| Booker H.G. | 1958 | Proc. IRE., <u>46</u> , 298. |
| Breit G. and
Tuve M.A. | 1926 | Nature (London), <u>116</u> , 357. |
| Briggs B.H. | 1958 | J. Atmos. Terr. Phys., <u>12</u> , 34. |
| Briggs B.H. | 1964 | J. Atmos. Terr. Phys., <u>26</u> , 1. |
| Briggs B.H. | 1966 | Rad. Sci., <u>1</u> , 1163. |
| Briggs B.H. and
Parkin I.A. | 1963 | J. Atmos. Terr. Phys., <u>25</u> , 339. |
| Briggs B.H. and
Spencer M. | 1954 | Rep. Prog. Phys., <u>17</u> , 245. |
| ✓ Briggs B.H., et al. | 1950 | Proc. Phys. Soc., <u>B63</u> , 106. |
| Chakrabarty S.K. and
Pratap R. | 1954 | J. Geophys. Res., <u>59</u> , 1. |
| Chandra H. | 1977 | Proc. Workshop on equatorial
electrojet and associated
phenomena, PRL, Ahmedabad
p.191. |
| Chandra H. and
Rastogi R.G. | 1969 | J. Atmos. Terr. Phys., <u>31</u> ,
1205. |
| Chandra H. and
Rastogi R.G. | 1974 | Curr. Sci., <u>43</u> , 567. |
| Chandra H., et al. | 1971 | Planet. Space Sci., <u>19</u> , 1497. |
| Chandra H., et al. | 1977 | Curr. Sci., <u>46</u> , 835. |
| Chandra H., et al. | 1979 | Ann. Geophys., <u>35</u> , 145. |
| Chapman J.H. | 1953 | Can. J. Phys., <u>31</u> , 120. |
| Chapman S. | 1919 | Phil. Trans. Roy. Soc. (London),
<u>A218</u> , 1. |
| Chapman S. | 1948 | Terr. Magn. Atmos. Elec., <u>53</u> ,
247. |

- | | | |
|-------------------------------------|-------|--|
| Chapman S. | 1951 | Arch. Meteorol. Geophys.,
Bioklimatal, <u>A4</u> , 368. |
| Chapman S. and
Raja Rao K.S. | 1965 | J. Atmos. Terr. Phys., <u>27</u> , 559. |
| Chapman S. and
Westfold K.C. | 1956 | J. Atmos. Terr. Phys., <u>8</u> , 1. |
| Chivers H.J.A. | 1960 | J. Atmos. Terr. Phys., <u>17</u> , 181. |
| Chivers H.J.A. and
Greenhow J.S. | 1959 | J. Atmos. Terr. Phys., <u>17</u> , 1. |
| Chytil B. | 1967 | Studia Geophys. et. Geod., <u>11</u> ,
221. |
| Crochet M., et al. | 1977 | J. Atmos. Terr. Phys., <u>39</u> , 463. |
| Currie R.G. | 1966 | J. Geophys. Res., <u>71</u> , 4579. |
| Dagg M. | 1957 | J. Atmos. Terr. Phys., <u>11</u> , 133. |
| Dagg M. | 1957a | J. Atmos. Terr. Phys., <u>11</u> , 139. |
| Deshpande M.R. and
Rastogi R.G. | 1966 | Ann. Geophys., <u>23</u> , 419. |
| Deshpande M.R., et al. | 1966 | Proc. IQSY Symp., New Delhi. |
| Deshpande M.R., et al. | 1977 | Nature, <u>267</u> , 599. |
| Deshpande M.R., et al. | 1978 | Proc. Ind. Acad. Sci., <u>A87</u> , 173. |
| Dueno B. | 1956 | J. Geophys. Res., <u>61</u> , 535. |
| Egedal J. | 1947 | Terr. Magn. Atmos. Elec., <u>52</u> , 449. |
| Egedal J. | 1948 | Nature (London), <u>161</u> , 443. |
| Elsasser W.M. | 1958 | Scientific American, <u>198</u> , 44. |

- | | | |
|-----------------------------------|-------|--|
| Fambitakoye O. and
Mayaud P.N. | 1976 | J. Atmos. Terr. Phys., <u>38</u> , 1. |
| Fambitakoye O. and
Mayaud P.N. | 1976a | J. Atmos. Terr. Phys., <u>38</u> , 19. |
| Fambitakoye O. and
Mayaud P.N. | 1976b | J. Atmos. Terr. Phys., <u>38</u> , 123. |
| Fambitakoye O., et al. | 1973 | J. Atmos. Terr. Phys., <u>35</u> , 1119 |
| Fambitakoye O., et al. | 1976 | J. Atmos. Terr. Phys., <u>38</u> , 113. |
| Felgate D.G., et al. | 1975 | Planet. Space Sci., <u>23</u> , 389. |
| Forbush S.E. and
Casavarde M. | 1961 | Carnegie Inst. (Washington)
Pub. 620, 140. |
| Frihagen J. | 1971 | J. Atmos. Terr. Phys., <u>33</u> , 21. |
| Galperin Yu. I., et al. | 1978 | J. Geophys. Res., <u>83</u> , 4265. |
| Goodman N.R., et al. | 1961 | Technometrics <u>3</u> , 245. |
| Gouin P. | 1962 | Nature (London), <u>193</u> , 1145. |
| Gouin P. and
Mayaud P.N. | 1967 | Ann. Geophys., <u>23</u> , 41. |
| Gouin P. and
Mayaud P.N. | 1969 | C.R. Acad. Sci., Paris, <u>268</u> ,
357. |
| Hewish A. | 1952 | Proc. R. Soc., London, <u>A214</u> ,
494. |
| Hey J.S., et al. | 1946 | Nature (London), <u>158</u> , 234. |
| Hines C.O. | 1960 | Can. J. Phys., <u>38</u> , 1441. |
| Hines C.O. | 1963 | Quart. J. Roy. Meteorol. Soc.,
<u>89</u> , 1. |
| Hines C.O. | 1965 | Rad. Sci., <u>69D</u> , 375. |
| Hutton, R. and
Oyinloye J.O. | 1970 | Ann. Geophys., <u>26</u> , 921. |
| James P.W. | 1962 | J. Atmos. Terr. Phys., <u>24</u> , 1962. |

- | | | |
|------------------------------------|-------|--|
| Kane R.P. | 1973 | PRL Report AER 73-08. |
| Kane R.P. | 1973a | J. Atmos. Terr. Phys., <u>35</u> , 1249. |
| Kane R.P. | 1978 | J. Geophys. Res., <u>83(A6)</u> , 2671. |
| Kaushika N.D. | 1969 | J. Atmos. Terr. Phys., <u>31</u> , 1127. |
| Kazimirosky E.S. | 1962 | Geomagn. Aeronomy, <u>2</u> , 897. |
| Kazimirosky E.S. | 1963 | Geomagn. Aeronomy, <u>3</u> , 380. |
| Kent G.S. and
Wright R.W.H. | 1968 | J. Atmos. Terr. Phys., <u>30</u> , 657. |
| Koster J.R. | 1958 | J. Atmos. Terr. Phys., <u>12</u> , 100. |
| Koster J.R. | 1963 | J. Geophys. Res., <u>68</u> , 2579. |
| Koster J.R. | 1966 | Ann. Geophys., <u>22</u> , 435. |
| Koster J.R. | 1972 | Planet. Space Sci., <u>20</u> , 1999. |
| Koster J.R. and
Wright R.W. | 1960 | J. Geophys. Res., <u>65</u> , 2303. |
| Krautkramer | 1950 | Archiv. Elekt. Upertragung, <u>4</u> ,
133. |
| Liszka L. | 1963 | Ark. Geofys., <u>4</u> , 211. |
| Little C.G. and
Maxwell A. | 1952 | J. Atmos. Terr. Phys., <u>2</u> , 356. |
| Lysenko I.A., et al. | 1972 | J. Atmos. Terr. Phys., <u>34</u> , 1435. |
| Marriot R.T., et al. | 1979 | J. Geomag. Geoelectr., <u>31</u> , 311. |
| Matsushita S. | 1968 | Geophys. J. Roy. Astronomical Soc
<u>15</u> , 105. |
| Matsushita S. | 1977 | J. Atmos. Terr. Phys., <u>39</u> , 1207. |
| Matsushita S. and
Balsley B.B. | 1972 | Planet. Space Sci., <u>20</u> , 1259. |
| Matsushita S. and
Campbell W.H. | 1967 | Physics of Geomagnetic
Phenomena, published by Academic
Press, Newyork and London,
<u>Vol.II</u> , p.939. |

- | | | |
|---|------|---|
| Mayaud P.N. | 1977 | J. Atmos. Terr. Phys., <u>39</u> , 1055. |
| McClure J.P. | 1964 | J. Geophys. Res., <u>69</u> , 2774. |
| McIntosh D.H. | 1959 | Phil. Trans. Roy. Soc., London, <u>A251</u> , 525. |
| McNish A.G. | 1937 | I.A.T.M.E. Bull., <u>10</u> , 271. |
| Misra R.K. | 1973 | Planet. Space Sci., <u>21</u> , 1109. |
| Mithilesh A., et al. | 1981 | Ind. J. Radio & Space Phys., <u>10</u> , 201. |
| ✓Mitra S.N. | 1949 | J. Instn. Elect. Engrs., <u>96(III)</u> , 441. |
| Mullen J.P. | 1973 | J. Atmos. Terr. Phys., <u>35</u> , 1187. |
| Munro G.H. | 1966 | Rad. Sci., <u>1</u> , 1186. |
| Nakagami M. | 1960 | Statistical methods of radio wave propagation, ed. Hoffman W.C., Pregmon Press London, p.3. |
| Nielson E. and
Aarons J. | 1974 | J. Atmos. Terr. Phys., <u>36</u> , 159. |
| Onwumechilli C.A. | 1967 | Physics of geomagnetic phenomena, ed. by Matsushita S. and Campbell W.H., Vol. <u>1</u> , p.425, Academic Press, New York and London. |
| Onwumechilli C.A. and
Akasofu S.I. | 1972 | J. Geomag. Geoelectr., <u>24</u> , 161. |
| Onwumechilli C.A. and
Alexander N.S. | 1959 | J. Atmos. Terr. Phys., <u>13</u> , 222. |
| Oyinloye J.O. and
Akinrimisi J. | 1976 | J. Atmos. Terr. Phys., <u>38</u> , 149. |
| Patel V.P., et al. | 1978 | Ind. J. Radio & Space Phys., <u>7</u> , 22. |
| Paulson M.R. and
Hopkins R.U.F. | 1973 | Defence Documentation Centre No.AD 910490C, Naval Electronic Lab. Center, San Diego, Cal California 92152. |

- | | | |
|-------------------------------------|-------|---|
| Pawsey J.L. | 1935 | Pro. Camb. Phil. Soc., <u>31</u> , 125. |
| Philips G.J. | 1952 | J. Atmos. Terr. Phys., <u>2</u> , 141. |
| Porath H., et al. | 1973 | Ground observations of the magnetic field of the electrojet with a large array of magnetometers, Paper presented at the First Llyod V. Berkner Symp. on irregularities in the equatorial ionosphere, Uni. of Texas at Dallas, Texas, May 14-17, 1973. |
| Pramanik S.K. and Hariharan P.S. | 1953 | Ind. J. Met. Geophys., <u>4</u> , 353. |
| Pramanik S.K. and Yegmanarayanan S. | 1952 | Ind. J. Met. Geophys., <u>3</u> , 212. |
| Pratap R. | 1957 | J. Geophys. Res., <u>62</u> , 581. |
| Price A.T. | 1963 | J. Geophys. Res., <u>68</u> , 2445. |
| Raghavarao R. | 1976 | Proc. Solar Planet. Phys. Symp., PRL, Ahmedabad, <u>1</u> , 273. ed. by Subramanian G. |
| Raghavarao R. and Anandarao B.G. | 1980 | Geophys. Res. Letts., <u>7(5)</u> , 351. |
| Ramanna K.V.V. and Rao B.R. | 1962 | J. Atmos. Terr. Phys., <u>24</u> , 220. |
| Rao G.L. | 1969 | Nature (London), <u>224</u> , 894. |
| Rastogi R.G. | 1963 | J. Atmos. Terr. Phys., <u>25</u> , 393. |
| Rastogi R.G. | 1965 | Ind. J. Met. Geophys., <u>16</u> , 385. |
| Rastogi R.G. | 1969 | J. Atmos. Terr. Phys., <u>15(3)</u> , 216. |
| Rastogi R.G. | 1971 | Planet. Space Sci., <u>19</u> , 371. |
| Rastogi R.G. | 1973 | Planet. Space Sci., <u>21</u> , 1355. |
| Rastogi R.G. | 1973a | J. Atmos. Terr. Phys., <u>35</u> , 329. |

- Rastogi R.G. 1974 J. Geophys. Res., 79, 1503.
- Rastogi R.G. 1974a J. Atmos. Terr. Phys., 36, 167.
- Rastogi R.G. 1975 Proc. Ind. Acad. Sci., 81, 80.
-
- Rastogi R.G. 1981 Ind. J. Radio & Space Phys., 10,
- Rastogi R.G. and Chandra H. 1974 J. Atmos. Terr. Phys., 39, 377.
- Rastogi R.G. and Iyer K.N. 1976 J. Geomag. & Geoelectr., 28, 461.
- Rastogi R.G. and Iyer K.N. 1976a Curr. Sci., 45, 685.
- Rastogi R.G. and Patel V.L. 1975 Proc. Ind. Acad. Sci., A82, 121.
- Rastogi R.G., et al. 1966 J. Atmos. Terr. Phys., 28, 137.
- Rastogi R.G., et al. 1968 J. Atmos. Terr. Phys., 30, 1547.
- Rastogi R.G., et al. 1971 Planet. Space Sci., 19, 1497.
- Rastogi R.G., et al. 1971a Nature (London), 233, 13.
- Rastogi R.G., et al. 1977 Ind. J. Radio & Space Phys., 6, 39.
- Rastogi R.G., et al. 1977a Pramana, 8(1), 1.
- Rastogi R.G., et al. 1978 Ind. J. Radio & Space Phys., 7, 6.
- Rastogi R.G., et al. 1979 Low Latitude Aeronomical Processes, COSPAR Symp. Series, 8, 201.
- Ratcliffe J.A. 1954 J. Atmos. Terr. Phys., 10, 161.
- Ratcliffe J.A. and Pawsey J.L. 1933 Proc. Camb. Phil. Soc., 29, 301.
- Richmond A.D. 1973 J. Atmos. Terr. Phys., 35, 1083.
- Richmond A.D. 1973a J. Atmos. Terr. Phys., 35, 1105.

- | | | |
|----------------------------------|------|---|
| Sastri N.S. and
Bhargava B.N. | 1980 | J. Geomag. Geoelectr., <u>32</u> , 333. |
| Sastri N.S. and
Jayakar R.W. | 1972 | Ann. Geophys., <u>28</u> , 589. |
| Schioldge J.A., et al. | 1973 | J. Atmos. Terr. Phys., <u>35</u> , 1045. |
| Schuster A. | 1889 | Phil. Trans. Roy. Soc. (London),
<u>A180</u> , 467. |
| Schuster A. | 1908 | Phil. Trans. Roy. Soc. (London),
<u>A208</u> , 163. |
| Skinner N.J., et al. | 1963 | Proc. Int. Conf. on Ionosphere,
ed. by Stickland A.C., p.301,
Phy. Soc. London. |
| Stewart and
Balfour | 1883 | Encyclopadea Britanica, 9th ed.,
p.36. |
| Stormer C. | 1932 | Geofys. Pubs. Oslo., <u>9</u> , 6. |
| Stormer C. | 1933 | Vid. Akd. Arch. M.N.M., No.2. |
| Stormer C. | 1935 | Nature (London), <u>135</u> , 103. |
| Stubbs T.J. | 1973 | J. Atmos. Terr. Phys., <u>35</u> , 909. |
| Sugiura M. and
Cain J.C. | 1966 | J. Geophys. Res., <u>71</u> , 1869. |
| Sugiura M. and
Chapman S. | 1960 | Abh. Akad. Wiss. Gottingen
Maths. Phys. Kl. Sonderheft, <u>4</u> , 1. |
| Sugiura M. and
Poros D.J. | 1971 | Goddard Space Flt. Center,
Pub. X-645-21-278 (July 1971). |
| Tabhagh J., et al. | 1977 | J. Atmos. Terr. Phys., <u>8</u> , 33. |
| Thiruvengadhan A. | 1954 | Ind. J. Met. Geophys., <u>5</u> , 267. |
| Vats H.O. and
Deshpande M.R. | 1980 | Proc. Ind. Acad. Sci. <u>89</u> , 137. |
| Vats Hari Om, et al. | 1978 | Nature (London), <u>272</u> , 345. |
| Vestine E.H. | 1954 | J. Geophys. Res., <u>59</u> , 93. |

- Vincent R.A., et al. 1977 J. Atmos. Terr. Phys., 39, 813.
- Vyas G.D. and Chandra H. 1979 Low Latitude Aeronomical Processes, COSPAR Symp. Series, 8, 55.
- Vyas G.D., et al. 1978 Proc. Ind. Acad. Sci., 87A, 215.
- Vyas G.D., et al. 1981 Ind. J. Rad. & Space Phys., 10, 206.
- Whitney H.E. and Basu S. 1977 Rad. Sci., 12, 123.
- Whitney H.E., et al. 1969 Planet. Space Sci., 17, 1069.
- Wild J.P. and Roberts J.A. 1956 J. Atmos. Terr. Phys., 8, 55.
- Wright J.W., et al. 1976 J. Atmos. Terr. Phys., 38, 731.
- Wright R.W., et al. 1956 J. Atmos. Terr. Phys., 8, 240.
- Yeh K.C., et al. 1975 Rad. Sci., 10, 97.

1005 2441